The effects of vegetation on riverbank stability in the Ayeyarwady River

D. F. van Duijn

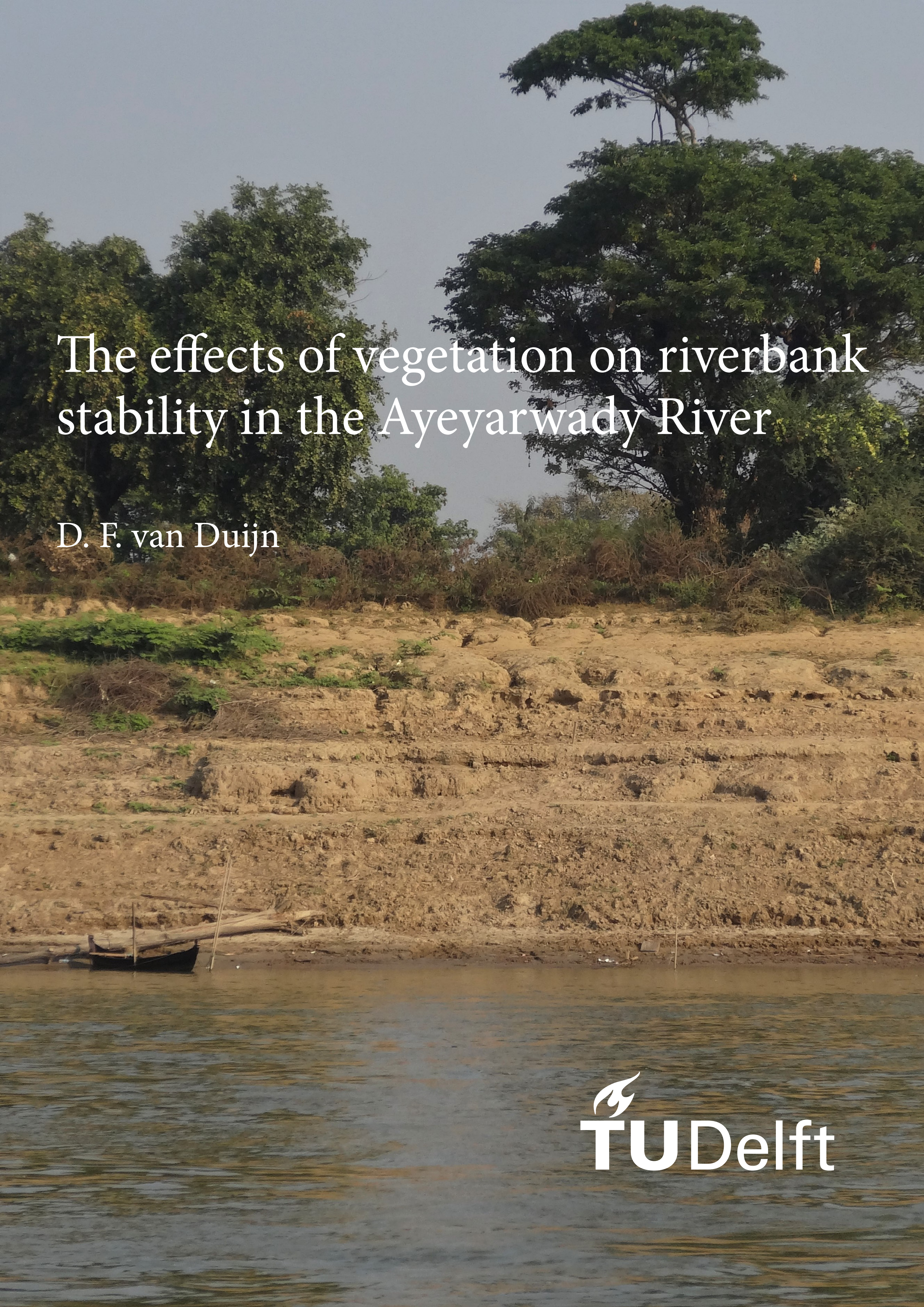

TU Delft

Delft University of Technology

Faculty of Civil Engineering and Geosciences

The effects of vegetation on riverbank stability in the Ayeyarwady River

The use of the Normalised Difference Vegetation Index as indicator for stabilising effects of vegetation by measuring bank retreat rates

By

Dirk Floris van Duijn

29-01-2018

Thesis committee:	Prof. dr. ir. W.S.J. Uijttewaal	TU Delft, Chair
	Dr. ir. M.M. Rutten	TU Delft
	Dr. ir. C.J. Sloff	TU Delft and Deltares

Preface

This thesis is the final result of the master program Hydraulic Engineering at the University of Technology of Delft. The research is part of the 'Partners voor Waterproject' initiative from the 'Rijksdienst voor Ondernemend Nederland' (VPdelta, 2017). It is part of a cooperation between the Myanmar and Dutch governments to manage water system strategies preventing future problems. In this cooperation, the TU Delft plays a role as well by promoting and stimulating Dutch innovations and start-ups in Myanmar. By exchanging knowledge and information, I, as representative of the TU Delft, tried to play a part in this collaboration and I am glad I got the chance to be part of this project.

My interests in river engineering, particularly the interaction of a river with its banks, forms the basis of this thesis subject. After the course 'Building with nature in hydraulic engineering', I recognised the importance of nature and realised the vital role vegetation could play in hydraulic phenomena. I wanted to learn more about this interaction between vegetation and river flow, and together with my supervisor Martine Rutten we combined my interests to one research subject. This thesis is about gaining insight into the effects of vegetation on riverbank stability in the Ayeyarwady river with remote sensing techniques.

I would like to express my gratitude towards my thesis committee, Prof. Wim Uijttewaal, Dr. Kees Sloff and Dr. Martine Rutten, who guided me towards this final product. Their knowledge and insightful comments on hydraulic engineering, remote sensing and research methods helped me to improve my understanding of the matter and my thesis report. Without them, I would not have been able to bring this graduation project towards a successful end.

I am grateful to all the people I got to work with during the fieldwork and met during my stay in Myanmar. The fieldwork team and the Myanmar students broadened my knowledge not only on river engineering but also enriched me with practical experience and quick-thinking skills. It was great to have the opportunity to work with and learn from you, whether it was about riverbanks, repairing a broken boat engine or just Myanmar culture, language and food. Each person enriched my stay and made it an unforgettable experience.

Last but not least I want to thank my parents, siblings, friends and girlfriend for their unending support during my student career and keeping their calm during my struggles to complete this thesis.

D.F. van Duijn
Valkenburg, January 2018

Summary

The Ayeyarwady River is the most important river in Myanmar, connecting the cities Mandalay and Yangon, making inland water transport economically attractive. People living near the river use the water for fishing, washing, and irrigation. The riverbanks are used for agricultural activities and living space. The Ayeyarwady River has a dynamic character, caused by the significant discharge difference between the dry and rainy season, and the related suspended sediment transport. Point bar formation in inner bends causes flow deflection towards the opposite riverbank. This causes local instability with as a result the banks to retreat. Vegetation contributes to the strength of riverbanks, by increasing the shear strength of the soil through roots and increasing hydraulic resistance, reducing flow velocities near the bank. However, to what extent the vegetation on the Ayeyarwady riverbanks contributes to this stability is debatable. Therefore it was the objective of this thesis to obtain a better understanding of the effects of vegetation on riverbank stability. By means of a fieldwork photo material of the river reach between Mandalay and Pakokku was collected, which was used for the NDVI validation. NDVI is the Normalised Difference Vegetation Index and is a remote sensing indicator for the 'greenness' of vegetation on satellite imagery. More vegetation means a higher NDVI value, hence it provides information about the livelihood of the vegetation present on the subsoil. In combination with determined bank retreat rates from a yearly comparison of satellite images in Google Earth, it was examined whether higher NDVI values, obtained with the Google Earth Engine, resulted in reduced bank retreat rates and therefore if NDVI can be used as a bank stability parameter.

Nine different areas where bank retreat was identified with the 'Aquamonitor' were analysed. The regions were both altogether and separately examined, but the graphs showed no definite answer of retreat rates being dependent on NDVI. Therefore, the results of the riverbank retreat analysis were categorised based on location, erosion mechanism, the slope of the riverbank and riverbank vegetation classes. The areas where fluvial entrainment was the primary erosion mechanism showed a clear division of results. When NDVI was smaller than 0.2, maximum bank retreat rates appeared to be 200 meters per year. When NDVI was higher than 0.2, bank retreat rates did not exceed 80 meters per year. On satellite images, vegetation was not observed in these areas, so the influence of vegetation remained questionable. In areas where mass failure caused bank retreat, no reduction in bank retreat was found. The results showed considerable scatter, although much more vegetation was present on these banks. Water level variability played a crucial role in the evaluation of the net effects of vegetation on riverbank stability. During low water, vegetation cannot provide the positive impacts, especially on steep river banks. Moreover, toe erosion causes banks to erode from underneath. In combination with mass failure the bank retreats, regardless of the amount of vegetation and, therefore, the value of the NDVI.

It is not possible to identify vegetation types from NDVI records only. Various vegetation species influence the hydrodynamic and morphological processes differently. NDVI also does not show which erosion mechanism takes place. This makes riverbank stability difficult to predict by using NDVI only, and therefore, NDVI does not seem to be an appropriate estimator for the additional effects of vegetation on riverbank stability. However, it can be used in combination with other remote sensing techniques to identify healthy vegetation areas and to make roughness estimations in river planform analyses. Moreover, it can help river engineers to implement nature-friendly river measures, and by a collaboration between researchers, engineers and Myanmar inhabitants, the Ayeyarwady River can establish a dynamically stable river planform.

Table of contents

List of figures vi

List of tables ix

List of abbreviations x

1. Introduction 1

1.1 Context 2

1.1.1 The Ayeyarwady River 2

1.1.2 Research area 3

1.2 Problem definition 5

1.3 Objective and research questions 7

1.4 Scope 7

2. Review of related literature 9

2.1 River planform 10

2.1.1 Bank erosion 10

2.1.2 Bank accretion 12

2.1.3 River planform analysis from remote sensing 13

2.2 Vegetation 15

2.2.1 Vegetation dynamics 16

2.2.2 Effects on hydrodynamics 16

2.2.3 Effects on morphodynamics 18

2.2.4 Effects on bank stability 19

2.2.5 Representation of vegetation in experiments and models 21

2.3 Normalised Difference Vegetation Index 23

3. Materials and Methods 26

3.1 Introduction 27

3.2 Research method 27

3.2.1 Software and applications 27

3.2.2 Plan of approach 28

3.3 Fieldwork 31

4. Results 33

4.1 General description of the general results 34

4.2 Results based on riverbank characteristics 36

5. Discussion 39

5.1 Bank retreat rates from satellite images 40

5.2 Effect of vegetation on erosion and bank stability 40

5.3 NDVI analysis 40

5.4 Bank retreat rates as a function of NDVI 41

6. Conclusion **43**
Recommendation 46
Bibliography **48**
Appendices **56**
Appendix A – Flow processes 56
A.1 Steady, uniform flow 56
A.2 Flow in a river channel 57
Appendix B – Determining bank retreat rates and NDVI of the Ayeyarwady river 58
Appendix C – Google Earth Engine script 76
Appendix D – NDVI validation with photo material 77

List of figures

Figure 1 A crew member on a large inland water transport vessel measuring the depth of the Ayeyarwady River with a measuring pole. The ever changing width and depth of the river are a large problem for inland water transport. 1
Figure 2 Map of Myanmar with the Ayeyarwady river flowing from North to South. 2
Figure 3 Local residents use the Ayeyarwady River for fishing and to earn money with selling their catch of the day. 3
Figure 4 Besides washing themselves, the women also wash their clothes and vegetables in the Ayeyarwady River. 3
Figure 5 The Ayeyarwady riverbanks are being used for multiple purposes, among others agriculture..3
Figure 6 Cattle grazing on the grass growing on the riverbanks. 3
Figure 7 Research area located in the central dry zone of Myanmar. The Ayeyarwady River is highlighted in blue. 4
Figure 8 Zoomed in on the Ayeyarwady river, where also the confluence with the Chindwin is shown..4
Figure 9 Typical vertical riverbank in the Ayeyarwady. The riverbanks overflow during high water. This bank is classified as a steep riverbank. 4
Figure 10 A nearly horizontal sand bar/ island in the middle of the Ayeyarwady river. This bank is classified as a flat riverbank with a mild slope. 4
Figure 11 The average monthly temperature (right, red) and rainfall (left, blue) in Myanmar from 1991-2015 (Climate Change Knowledge Portal, 2017). 5
Figure 12 People living on the riverbanks have easy moveable houses and can move their properties during high discharges and when the banks are retreating. 6
Figure 13 The larger villages need some protections works, like this wall in front of a road. The buildings are in this way protected against the high water levels. 6
Figure 14 Different types of vegetation are found on the Ayeyarwady River banks. Even a single tree can influence river processes. The role of vegetation on flow and river banks is being studied already for a long period. 9
Figure 15 (Theoretical) Shear failure mechanism where roots are not extended to the shear plane. Shear instability causes the riverbank to become steeper and prone to mass failure. 11
Figure 16 Shear plane failure is also evident in the Ayeyarwady river. The ridges on the bank indicate locations where shear failure has taken place. 11
Figure 17 Lawler's bank erosion mechanisms. Not represented is the effect of sub-aerial processes on erosion. The schematic resembles a typical Ayeyarwady riverbank, with high, steep edges. 12
Figure 18 River meandering process, where the deeper outer bend usually erodes and in the shallower inner bend a point bar forms. Figure retrieved from Crosato (2008). 12
Figure 19 Low water, Composite picture of February 2016. 15
Figure 20 High water, Composite picture of August 2016. 15
Figure 21 Low water, Composite picture of February 2017. 15
Figure 22 Relation between hydrodynamics, morphodynamics and vegetation. The interdependent relations make predictions of river planform development challenging. Figure retrieved from Baptist (2005). 16
Figure 23 Vegetation reduces the velocity, and thereby the bed shear stress. 'k' is the vegetation height, 'u(z)' is the velocity at a height above the bed 'z', 'h' is the water level. Figure retrieved from Baptist (2005). 17
Figure 24 Effect of flexibility on flow velocity. Figure retrieved from Dijkstra et al. (2006). 17
Figure 25 Difference in turbulence intensity of a bare river bed and a vegetated river bed. Also the streamwise velocity distribution is visible in this figure. Figure retrieved from Sukhodolov and Sukhodolova (2010). 17
Figure 26 Roots of vegetation are not able to strengthen the soil to prevent mass erosion. 19

Figure 27 Due to the plantings of emergent, woody vegetation in a straight channel (a), the flow is diverted around the vegetation and the river starts to meandering, including flow deflection and bank erosion, opposite of the vegetation locations (b). Then the point bars grow, inducing more opposite bank erosion, further enhancing river meandering (c). The black arrows represent flow velocities, the straight line is the channel after some time, the dashed line the original channel. Schematic retrieved from Bennett et al. (2008). 20
Figure 28 The different reflectance intensity for healthy and unhealthy vegetation and soil. The difference in reflection is small in the visible region but large in the NIR-region. By using this reflectance property of the material, it is possible to identify bare soil from vegetation. Schematic retrieved from PhysicsOpenLab (2017). 24
Figure 29 The Ayeyarwady River and Chindwin River confluence seen from above, courtesy of Floris Papenhuijzen. The Chindwin River merges from the lower right corner with the Ayeyarwady River, flowing from left to right. The confluence is marked by the colour difference between the rivers, caused by the sediment concentration difference. 26
Figure 30 Bank retreat (blue) and accretion (green) in the Ayeyarwady River made visible with the Aquamonitor. The image is the result of a comparison of a reach in the Ayeyarwady River between 2014 and 2016. 28
Figure 31 Summary of the plan of approach. 28
Figure 32 River reach around Mandalay. The five research areas are highlighted in red. 29
Figure 33 The Ayeyarwady river further downstream, with the other research areas (6-9). 29
Figure 34 An NDVI record retrieved with the GEE script. On the horizontal axis the date is presented; On the vertical axis the NDVI is presented. 30
Figure 35 Example of one of the fishing boats that were used during the fieldwork to perform experiments. 32
Figure 36 The locations of the collected photo material in the research area. 32
Figure 37 The Ayeyarwady River, seen from one of the boats used during the fieldwork. On the picture the Pakokku Bridge is also visible. The bridge has a length of 3.4 kilometres, the whole width of the river is hard to capture on a single picture. 33
Figure 38 Result of the bank retreat of all areas together, plotted against NDVI. 35
Figure 39 Total figure of erosion rates as a function of NDVI values. Each river section is represented by a different colour. 35
Figure 40 The average values of erosion rates per river section. 36
Figure 41 All bank retreat rates as function of NDVI, grouped per erosion mechanism. 37
Figure 42 The bank retreat rates filtered results of the points subjected to fluvial erosion. 37
Figure 43 All bank retreat rates as function of NDVI, grouped per riverbank slope. 38
Figure 44 Results classified into riverbank vegetation classes. 38
Figure 45 A picture of a steep riverbank in the Ayeyarwady River. The vegetation on the edge of the riverbank indicates that the riverbank is retreating rapidly and the farmer should take its crops from the land before it is lost in the river. 39
Figure 46 A (typical) NDVI record of an eroding riverbank, noticeable from the decreasing NDVI values during the dry season, and in January 2017 negative values. 41
Figure 47 Composite image of the Ayeyarwady river from August 2015, indicating cloud cover during the rainy season. 41
Figure 48 Two fishers hauling in their catch from the Ayeyarwady River. Also for them a stable river is desirable. 43

Figure A1 Uniform flow in a schematized river cross-section. Depicted is the logarithmic velocity profile, which can be described by Chézy's law. 57

Figure B1 River reach around Mandalay (near area 1). The five research areas are highlighted in red. 58
Figure B2 The Ayeyarwady river further downstream, with the other research areas (6-9). 58
Figure B3 Area 1 - Comparison riverbanks 7 January 2014 with 11 January 2017. 60
Figure B4 Riverbank in area 3. Note the length of the vegetation with regard to the length of the human. 60
Figure B5 Grassy vegetation on this riverbank is not able to prevent toe erosion and mass failure. 60
Figure B6 Bank retreat rate as a function of the NDVI for area 1. 61
Figure B7 Area 2 - Comparison riverbanks 7 January 2014 with 20 December 2016. 62
Figure B8 Bank retreat rate as a function of the NDVI for area 2. 62
Figure B9 Area 3 - Comparison riverbanks 7 January 2014 with 11 January 2017. 64
Figure B10 Bank retreat rate as a function of the NDVI for area 3. 64
Figure B11 Area 4 - Comparison riverbanks 7 January 2014 with 11 January 2017. 65
Figure B12 Bank retreat rate as a function of the NDVI for area 4. 66
Figure B13 Area 5 – Comparison riverbanks 2 February 2014 with 11 January 2017. 67
Figure B14 Two different elevations in the Ayeyarwady river; a higher vegetated area and a lower unvegetated area. 67
Figure B15 Bank retreat rate as a function of the NDVI for area 5. 68
Figure B16 Area 6 – Comparison riverbanks of 15 February 2014 with 2 January 2017. 69
Figure B17 Bank retreat rate as a function of the NDVI for area 6. 70
Figure B18 Area 7 - Comparison riverbanks of 15 February 2014 with 2 January 2017. 71
Figure B19 Bank retreat rate as a function of the NDVI for area 7. 71
Figure B20 Area 8 - Comparison riverbanks of 15 February 2014 with 2 January 2017. 72
Figure B21 Bank retreat rate as a function of the NDVI for area 8. 73
Figure B22 Area 9 - Comparison riverbanks of 15 February 2014 with 2 January 2017. 74
Figure B23 Large amount of vegetation does not stop bank retreat of the riverbank. 74
Figure B24 The vegetation on top does not reach the toe of the bank, causing toe erosion to erode the riverbank. 74
Figure B25 Bank retreat rate as a function of the NDVI for area 9. 75
Figure B26 Result of the bank retreat of all areas together. 75

Figure D1 Riverbank at coordinates (21.8533; 95.9113), NDVI in February 2017 approximately 0.3. 77
Figure D2 Riverbank at coordinates (21.9322; 95.7136) NDVI in February 2017 approximately 0.5. 78
Figure D3 Riverbank at coordinates (21.9229; 95.8031), NDVI in February 2017 approximately 0.6. 78
Figure D4 Riverbank at coordinates (21.9122; 95.7569), NDVI in January 2017 approximately 0.57. 79
Figure D5 Riverbank at coordinates (21.7559; 95.4134), NDVI in January 2017 approximately 0.4. 79
Figure D6 This series of figures show how the placement of the geometry is essential for the correct NDVI. In the geometry, a large part of water contributes to a low NDVI. Riverbank at coordinates (95.7574; 21.9122). 80
Figure D7 A smaller part of water is present and is taken into account in the NDVI calculation, resulting in higher NDVI values compared to Figure D6. 80
Figure D8 No water is present in the calculation of the NDVI. The NDVI values raise. Trees are introduced as well, which are not in direct contact with water, resulting in an overestimation of the NDVI. 81
Figure D9 The influence of a different size of the geometry. In comparison with the figures above there is no influence of the trees, significantly reducing maximum NDVI values. The lower values are due to the overflowed riverbank during the rainy season. 81

List of tables

Table 1 Overview of different river planform studies....14
Table 2 Different types of resolutions....15
Table 3 Positive effects of vegetation on hydrodynamic processes....18
Table 4 Negative effects of vegetation on hydrodynamic processes....18
Table 5 Positive effects of vegetation on morphodynamic processes....18
Table 6 Negative effects of vegetation on morphodynamic processes....19
Table 7 Positive effects of vegetation on bank stability....21
Table 8 Negative effects of vegetation on bank stability....21
Table 9 Manning coefficients for different types of vegetation, dependent on season and water level. Table modified from Phillips and Tadayon (2006)....22
Table 10 Nikuradse roughness coefficients. Table modified from Baptist (2005)....22
Table 11 Drag coefficients for different types of vegetation. In this table 'k' is the vegetation height, '1/a' vegetation density, 'd_s' the stem diameter, and 'C_d' the drag coefficient. Table modified from Van Velzen et al. (2003)....22
Table 12 Ranges of NDVI values of different subsoils. Table modified from Bertoldi et al. (2011)....24
Table 13 Table of the yearly-averaged bank retreat rates....30
Table 14 Information of the data of the satellite imagery, the number of coordinates per area and the date of NDVI values retrieved....31
Table 15 Riverbanks classified according to the amount and state of vegetation....34
Table 16 Summary of the riverbank and erosion mechanism per area in the Ayeyarwady River....34

Table B1 Table with information of the data of the satellite imagery, the number of coordinates per area and the date of NDVI values retrieved....59
Table B2 Characteristics of area 1....59
Table B3 Characteristics of area 2....61
Table B4 Characteristics of area 3....63
Table B5 Characteristics of area 4....65
Table B6 Characteristics of area 5....66
Table B7 Characteristics of area 6....68
Table B8 Characteristics of area 7....70
Table B9 Characteristics of area 8....72
Table B10 Characteristics of area 9....73

List of abbreviations

Abbreviation	Definition
AVHRR	Advanced Very High Resolution Radiometers
DWIR	Directorate of Water Resources and Improvement of River Systems
GEE	Google Earth Engine
LAI	Leaf Area Index
NDVI	Normalised Difference Vegetation Index
NIR	Near-Infrared Light
NOAA	National Oceanic and Atmospheric Administration
RVC	Riverbank Vegetation Class
USGS	United States Geological Survey
VI	Vegetation Index
VIS	Visible light

I

Introduction

"Like a river that does not know where it is flowing, I took a wrong turn and I just kept going." – Bruce Springsteen

Figure 1 A crew member on a large inland water transport vessel measuring the depth of the Ayeyarwady River with a measuring pole. The ever changing width and depth of the river are a large problem for inland water transport.

In this chapter, the context of this thesis report is presented. The complex state of the Ayeyarwady River is described, as well as the problems that people living around the Ayeyarwady River have to cope with. Some background information is given and the research questions are presented. The structure of this report is also included in this chapter.

1.1 Context

1.1.1 The Ayeyarwady River

The Ayeyarwady River is one of the four most important rivers in Myanmar, others being the Chindwin, the Salween and the Sittaung. With a length of approximately 2.170 km, a total drainage area of about 411.000 km^2 and an average discharge of 13.000 m^3/s, this river is the most important transport corridor in Myanmar. Starting in the glaciers of Tibet, the Ayeyarwady River flows from north to south into the Andaman Sea. The Ayeyarwady River connects large cities like Mandalay, Bagan and Yangon, shown in Figure 2, and is located in the central-dry zone of Myanmar. In the fast developing country of Myanmar transport by boats is one of the quickest ways of travel over long distances. Underdeveloped roads and railways are the main reasons road- and railway transport are not yet competitive with inland water transport. The value of the Ayeyarwady River is further emphasised by people living around the river, who use it for fishing (Figure 3), washing and doing laundry (Figure 4) and agricultural lands. People grow crops (Figure 5) and let their cattle graze along the river boundaries (Figure 6), marking the economic value of the river for the local inhabitants.

Figure 2 Map of Myanmar with the Ayeyarwady river flowing from North to South.

Figure 3 Local residents use the Ayeyarwady River for fishing and to earn money with selling their catch of the day.

Figure 4 Besides washing themselves, the women also wash their clothes and vegetables in the Ayeyarwady River.

Figure 5 The Ayeyarwady riverbanks are being used for multiple purposes, among others agriculture.

Figure 6 Cattle grazing on the grass growing on the riverbanks.

1.1.2 Research area

The specific region of interest is the reach of the Ayeyarwady River located between Mandalay and Pakokku, see Figure 7 and Figure 8, where a more detailed satellite image of the research area is shown. Also, the confluence of the Ayeyarwady River (East River) and the Chindwin River (West River) is shown, marked by the black star. The Chindwin River is also an important transport corridor. The reason for the extended research area is that this research is part of other studies, among others the determination of the dispersion in the Ayeyarwady River (Bakker, 2017) and the mixing of the Chindwin River with the Ayeyarwady River (Bogaard et al., 2017). The different studies could be combined into one week of experimenting on the Ayeyarwady River and Chindwin River.

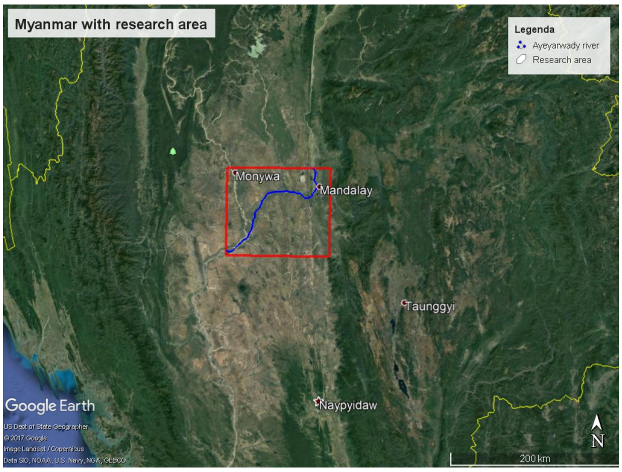

Figure 7 Research area located in the central dry zone of Myanmar. The Ayeyarwady River is highlighted in blue.

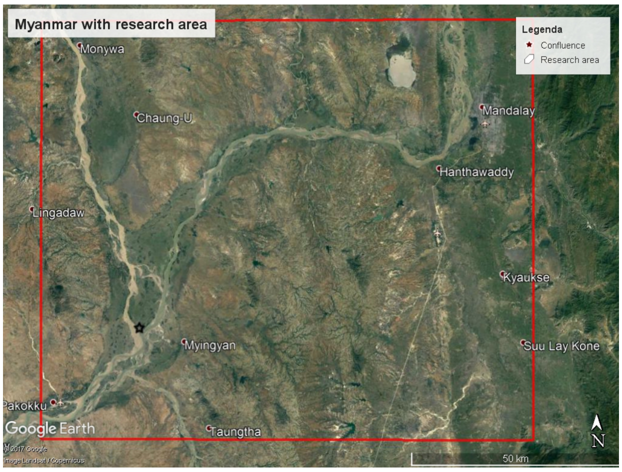

Figure 8 Zoomed in on the Ayeyarwady river, where also the confluence with the Chindwin is shown.

Not visible in the figures above, but the Ayeyarwady is characterised by a braided pattern, where bars and islands are present in the river. Point and mid-channel bars appear in the wider river reaches, since flow velocities are locally lower for sediment to settle. In some parts of the river, the river is enclosed by mountain ridges, for example near Mandalay (Ligthart, 2017). Typical for braided rivers is the abundance of small-sized sediments and the large suspended sediment transport.

In Figure 9 and Figure 10 some pictures of typical river features of the Ayeyarwady are shown, taken during the fieldwork. In Figure 9 a nearly vertical riverbank is shown, which in this thesis is defined as a ‘steep’ bank. When looking at the steep riverbank, it is possible to identify different types of soil, indicated by the difference in colour. In the top layer, mostly sand is present, whereas in the lower layers clay prevails. In the sandy layer, the erosion occurred more gradual what resulted in a more even layer, whereas in the clayey layer, humps of the bank are eroded as a whole which can be seen from the angular parts. In Figure 10 a flat bank is visible, which is further referred to as a ‘mild’ or ‘gentle’ sloped riverbank. It is necessary to keep the different types of banks in mind since there is a clear difference in erosion mechanisms.

Figure 9 Typical vertical riverbank in the Ayeyarwady. The riverbanks overflow during high water. This bank is classified as a steep riverbank.

Figure 10 A nearly horizontal sand bar/ island in the middle of the Ayeyarwady river. This bank is classified as a flat riverbank with a mild slope.

1.2 Problem definition

The Ayeyarwady river is classified as a braided river, meaning that the river consists of channels separated by bars and islands (Schumm and Khan, 1972). As a result of the braided pattern, river water is diverted by the bars towards the banks, causing significant pressure on the riverbank. This force of the water causes the banks to retreat. Especially during floods, large portions of land are abraded, bringing more sediments into the river system. This surplus of sediment will create (point) bars at other locations, inducing erosion further downstream and the processes are repeated. This is the ever-changing nature of rivers, and the Ayeyarwady River is no exception. The fine soil material present in the central dry zone of Myanmar makes the Ayeyarwady one of the most rapidly changing rivers in the world. To illustrate the rapid river planform changes an estimate with satellite images shows a channel shift of 1.3 kilometres within seven years. Erosion rates of 150 meter per year are not exceptional. From the same pictures, it is visible that some villages had to be relocated.

Highly fluctuating flow conditions make it even more difficult to predict the course of the river, causing troubles for waterway transportation. This difference in discharge over the year is caused by the monsoon climate of Myanmar. In Figure 11 it can be seen that there is a considerable variation in rainfall between the rainy season and dry season in Myanmar. During the rainy season (May to October), the discharge can be as large as ten times the discharge during the dry season (November to March), and water levels differ up to twelve meters (van der Velden, 2015; Commandeur, 2014). Besides the risk of running aground during low water, the high flow velocities during high water levels can make sailing problematic. Moreover, different discharge levels contribute to channel formation in various ways (Nanson and Hickin, 1983; Ferguson, 1987; Church, 1992). Riverbanks continuously change their planform under (natural) dynamic hydrologic conditions, since a change in discharge alters the river morphology. Since monthly rainfall varies around yearly averages, frequency, duration and intensity vary remarkably, and river morphology changes drastically during a single season (Schumm and Lichty, 1963).

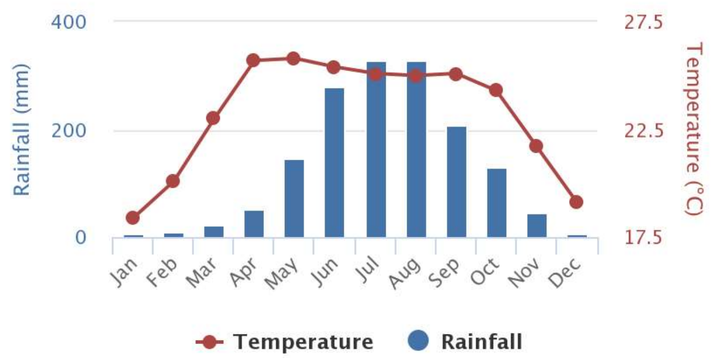

Figure 11 The average monthly temperature (right, red) and rainfall (left, blue) in Myanmar from 1991-2015 (Climate Change Knowledge Portal, 2017).

Erosion and bank retreat occur during floods, making rivers wider and deeper. The higher velocity is capable of transporting more sediment, causing bank instability and making riverbanks prone to erosion. Moreover, the size of the sediments in and around the Ayeyarwady River is small, resulting in significant sediment transport rates. The Ayeyarwady River transports an estimated volume of 364 ± 60 megatons suspended sediment load, which is the fifth-largest suspended sediment load compared to other rivers over the world (Robinson et al., 2007). Sedimentation results during low flows, when velocities are lower, making it possible for sediments to settle on the bed and floodplains.

Riverbank erosion and sedimentation occur in every type of river and is a natural mechanism that is the result of a morphological imbalance. Most rivers have a healthy amount of erosion. However, the rapid and continuously changing Ayeyarwady River planform is a cause for concern. Villages are forced to move when erosion of the riverbanks threatens their living- or agricultural land, for example, shown in Figure 12. Where the river grows wider, sandbars arise which cause hampering for inland water transport and chances of running aground increase. In order to prevent riverbank erosion, bank protection works, shown in Figure 13, are measures that are often thought of by river managers. Though right solutions, they are expensive and because of the length of the Ayeyarwady River overambitious. Moreover, completely shutting down the exchange of sediments with riverbanks disrupts the sediment balance and morphological equilibrium. Finally, riverbank structures often only address fluvial erosion, whereas mass failure also often occurs in the Ayeyarwady River. Such structures do not counteract this erosion mechanism.

Figure 12 People living on the riverbanks have easy moveable houses and can move their properties during high discharges and when the banks are retreating.

Figure 13 The larger villages need some protections works, like this wall in front of a road. The buildings are in this way protected against the high water levels.

Another control influencing river morphodynamics is the presence of vegetation on riverbanks (Gray and Sotir, 1996) because vegetation creates additional protection for the soil by providing more resistance against the flow (Lowrance et al., 1988). The resistance against the flow causes lower flow velocities and hence less bank erosion (Elliot, 2000); therefore the bank is considered more stable. Dependent on the properties of vegetation (e.g. species, density, length, submerged length, flexibility etc.) the stabilising effect on riverbanks is different (Thorne, 1990; McKenney et al., 1995). This makes it very difficult to assess riverbank stability and the role of vegetation in this (Hickin, 1984; Nanson et al., 1995).

Since hydraulic and morphological data and knowledge about vegetation types of the Ayeyarwady River are very scarce, other techniques should be reviewed to get more insight in this dynamic behaviour of the river and the influence that vegetation imposes. A combination of remote sensing data and ground observations could create insight into the overall effect of vegetation on riverbank stability. A measure to quantify vegetation on satellite images is the Normalised Difference Vegetation Index (NDVI). NDVI is a vegetation index which reveals whether land contains vegetation or not. A validation of these NDVI records assesses whether vegetation fits NDVI records and if NDVI can be used as an indicator of the state of the vegetation on the riverbanks. Photo material collected during a fieldwork performs as a benchmark. Bank retreat rates express the stability of riverbanks. If vegetation functions like an additional defence against erosion, riverbanks with more vegetation should retreat less. Therefore, if healthier vegetation relates to a higher NDVI signal, bank retreat rates should decrease with higher NDVI. The retreat rates are compared with NDVI records, and the results could provide insight into the overall stabilising effects of vegetation.

1.3 Objective and research questions

The purpose of this thesis is to get more insight into the use of the normalised difference vegetation index in river planform studies. It is investigated whether this indicator expresses the effects that vegetation imposes on riverbank stability. The research method is applied as a case study on the Ayeyarwady River since this river has a large variety of vegetation species and the river is not as fixed as most rivers. The central question of this thesis research is:

How is the Normalised Difference Vegetation Index related to the stabilising effects of vegetation on riverbanks?

The following sub-questions will help to find an answer to the main question:

1. What are the effects of vegetation on bank retreat rates and stability of riverbanks?
2. Is the NDVI representative for the vegetation on riverbanks?
3. How are bank retreat rates and NDVI related?
4. Can NDVI be expressed as a hydraulic resistance parameter?

1.4 Scope

The Ayeyarwady River in Myanmar is a rapidly changing river, and its planform is hard to predict. Therefore in chapter 2, an analysis of the processes determining river planform has been made. Riverbank erosion and accretion have been discussed. Also, remote sensing techniques that are being used in river planform analyses are reviewed to get a better understanding of the driving mechanisms of a natural river. Due to the economic state of Myanmar, the Ayeyarwady riverbanks are hardly touched upon by human interventions. Because of this, the river flows naturally through the landscape and processes occur as nature imposes them. A natural based solution to prevent the rapid change could therefore work. The interaction between hydrodynamics, morphodynamics and vegetation is complicated and the mechanisms are described in paragraph 2.2. The various processes when water is flowing over soil and vegetation have been reviewed. It is shown that the relationship is not straightforward and different authors have different opinions about positive and negative effects. After an analysis of the various processes, it is possible to state that vegetation stabilises riverbanks and that riverbanks without vegetation are more vulnerable to erosion. It also showed that vegetation could initiate river meandering and therefore induce opposite bank erosion. The beneficial effects of the presence of vegetation on a riverbank can consequently work contradictory for other locations. In the Ayeyarwady River, the balance between positive and negative impacts of vegetation is further complicated by the water level variability. During low water, the vegetation is not in contact with water to provide beneficial effects. Therefore, the negative effects dominate the positive. However, to determine the impact of vegetation more precisely remote sensing can provide a solution. This has been discussed in paragraph 2.3. Possibilities to identify vegetation have been presented. NDVI is a standard remote sensing parameter that can show where (healthy) vegetation is present. NDVI is used as the vegetation indicator because it can be used on a large scale quickly and is being recorded already for a long time. If the NDVI can be the first indicator for riverbank stability, it could provide a way to identify (un)stable riverbanks with remote sensing and show locations where erosion prevention measures are necessary. Furthermore, the coupling between NDVI and roughness coefficients have been investigated. Since vegetation is represented by roughness coefficients in numerical models, it is tried to find a relation between NDVI values and roughness parameters. If there is a relation, NDVI could be used as a quick indicator to represent vegetation in numerical and computer models or as a more founded estimate when other roughness data is lacking. Hydraulic roughness in models and field studies was discussed in paragraph 2.2.5.

Materials and methods are discussed in chapter 3. In this chapter is explained how the research is conducted and with what materials. After a short introduction in paragraph 3.1, the research method is discussed in paragraph 3.2. A description of used software and applications, such as of the Aquamonitor, Google Earth and Google Earth Engine, is given. A plan of approach is presented on how these tools have been used to compare riverbank retreat rates with NDVI records. Finally, in paragraph 3.3 the conditions during the fieldwork are summarised.

In chapter 4 the results of the research are given. The nine different research areas can be found separately in Appendix B. A summary of the results of the bank retreat rates as a function of the NDVI values are presented in this chapter. The overall figures, separated in different characteristic properties, can be found here as well.

In chapter 5, the results obtained from the analysis of bank retreat rates and NDVI records are being discussed, as well as assumptions that were made and problems that were encountered. The determination of the bank retreat rates is discussed in section 5.1. The effects of vegetation on the bank retreat rates are then discussed in section 5.2. In section 5.3, the NDVI analysis is treated and in section 5.4 a discussion on the relation between erosion rates and NDVI is presented.

Finally, in Chapter 6 the research question is answered, after the answers to the sub-questions have been presented. Also, a recommendation is given. In this recommendation, some suggestions for follow-up research are given. To complete the story, an advice is given to three specific stakeholders on how to use the results of this study.

II

Review of related literature

"The more that you read, the more things you will know. The more that you learn, the more places you'll go." – Dr. Seuss

Figure 14 Different types of vegetation are found on the Ayeyarwady River banks. Even a single tree can influence river processes. The role of vegetation on flow and river banks is being studied already for a long period.

This chapter reviews the relevant literature. In paragraph 2.1 river processes are studied, where the focus is on the interplay between erosion and accretion. These mechanisms are determinative for river planform. In paragraph 2.2 vegetation is broadly discussed, where positive and negative effects of vegetation on river planform are highlighted. In paragraph 2.3 knowledge about the Normalised Difference Vegetation Index is presented and how the NDVI is used in previous studies.

2.1 River planform

The appearance of a river is the result of the interaction between flowing water and the stability of the riverbanks. Changes in river planform can either result from human activities or natural causes. Human interventions that influence river planform are streambank protection works, river structures such as groins and dams, but one can also think of irrigation channels and dredging activities. Natural causes of changes in a river are a changing discharge, corresponding water level differences, river meandering and (point) bar development. Another factor that is influencing river planform is the soil the river is flowing over and through. A river flowing through a mountain has a distinct planform, and only small changes in lateral direction and bed slope occur due to the hard material. In areas where small-sized sediment is abundant, flow velocities do not need to be high to cause changes in river planform.

The resulting shape of a river channel is the result of a balance of two forces: the stabilising geological force, i.e. the gravity force of the weight of the soil, and the destabilising hydraulic force, i.e. the force induced by the flowing water. Where the forces are in balance, no morphological response is necessary to maintain a morphologic equilibrium, meaning the river planform remains stable. In the course of time, a river would tend to find an equilibrium state, where it can discharge all the water without needing to adapt its planform. Since the discharge is not constant in time, the river system is not in balance, and a river will continuously change its planform accordingly. The disequilibrium between the forces will either result in riverbank erosion or sedimentation.

2.1.1 Bank erosion

Erosion is the removal of sediments by the movement of water. Erosion occurs where the shear stress exerted by the water to the soil exceeds the critical value of the cohesive soil (Partheniades, 1965). For non-cohesive sediment, particle entrainment occurs when the dimensionless Shields parameter exceeds a critical value (Shields, 1936). Lawler (1992) names three mechanisms which are responsible for the destabilization of riverbanks. Firstly, sub-aerial processes are climate-related phenomena that reduce soil strength, for example, rainfall and freezing of the soil. Langedoen et al. (2009) found that the degree of saturation of soils significantly affects erosion rates of riverbanks. Especially (monsoon) rains cause high degrees of saturation and Pollen-Bankhead, and Simon (2010) named four mechanisms which causes a stable bank to become unstable during rainfall. First, infiltration of water adds weight to the soil. Secondly, when rain infiltrates the soil, decrease of matric suction causes weakening of the bank material. Thirdly, seepage causes a reduction of frictional strength. Finally, the water in the soil flows towards the channel, bringing small sediments as well, reducing the confining pressure, and resulting in an unstable riverbank. Moreover, rainfall can cause instability through the impact of rain droplets on the ground. The excessive rain degrades the soil due to the impact energy. Furthermore, during the dry season, the soil gets dry and therefore loses some of its cohesive properties, becoming more vulnerable to rainfall and fluvial entrainment. Fluvial entrainment is the second mechanism destabilising riverbanks and is the removal of soil particles from the riverbanks caused by the flow of water. Lastly, mass failure causes erosion when the weight of the soil is larger than the shear strength, causing a large block of soil to slide into the river. It often occurs on high and steep riverbanks (Osman and Thorne, 1988). Shear instability (Figure 15 and Figure 16) can be considered as a type of mass failure occurring on gentle slopes when a large part of the riverbank suddenly slides into the river. After the mild slope has become steep, mass failure, as is shown in Figure 17, is the main erosion mechanism.

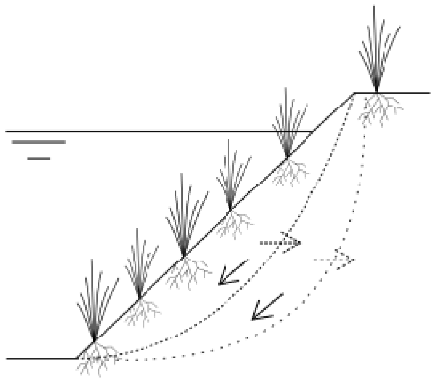

Figure 15 (Theoretical) Shear failure mechanism where roots are not extended to the shear plane. Shear instability causes the riverbank to become steeper and prone to mass failure.

Figure 16 Shear plane failure is also evident in the Ayeyarwady river. The ridges on the bank indicate locations where shear failure has taken place.

Fluvial entrainment and mass failure are schematized in Figure 17, both responsible for bank retreat. Thorne and Lewin (1979) observed bank erosion mechanisms in the river Severn (United Kingdom) and differentiated between fluvial entrainment and mass failure mechanisms. They found that bank retreat rates were more controlled by fluvial entrainment then by mass failure mechanisms. At high water levels, fluvial entrainment occurs at the top of the river bank, directly responsible for the bank retreat. During low water levels, fluvial entrainment wears away the vulnerable layer, after which mass failure causes the river bank to retreat. The Ayeyarwady River shows signs of all three mechanisms being present. Together the processes cause retreat of riverbanks when the bank becomes unstable to withstand the near bank flow strength (Ikeda et al., 1981).

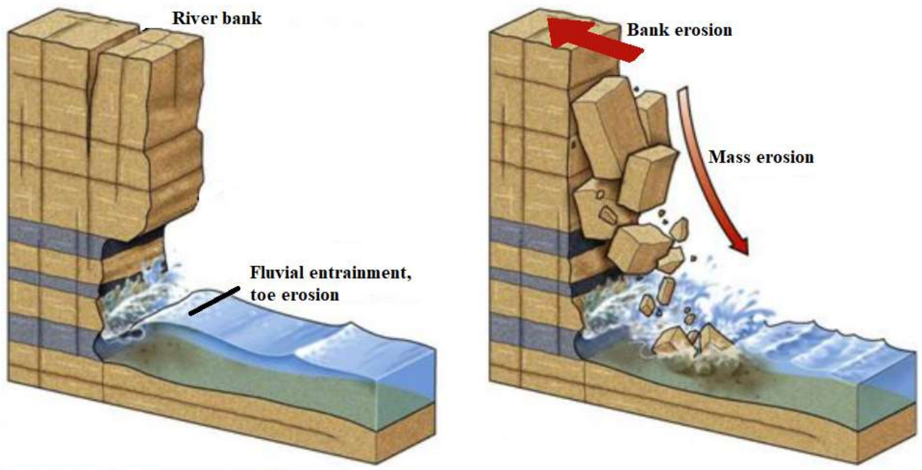

Figure 17 Lawler's bank erosion mechanisms. Not represented is the effect of sub-aerial processes on erosion. The schematic resembles a typical Ayeyarwady riverbank, with high, steep edges.

Crosato (2008) made a summary of all factors influencing bank erosion. Processes as opposite bank accretion (Dietrich and Smith, 1984; Mosselman et al., 2000), the presence and type of riparian vegetation (Macking, 1956; Wynn et al., 2004), groundwater flow (Darby and Thorne, 1996), pore water pressure (Dapporto et al., 2003) and the presence of floods (Carrol et al., 2004) are also influencing riverbank retreat rates. Flow processes, such as near bank flow and secondary flow, are also influencing riverbank erosion rates, and are further discussed in Appendix A.

2.1.2 Bank accretion

Riverbank accretion is defined as the progression of land supplied by sediment from upstream. According to Vargas Luna (2016) accretion is the result of the interaction between several factors. The most important factors are the sediment balance, the near-bank flow regime (Ikeda et al., 1981), riparian vegetation development (Hupp, 2000) and the compaction of near-bank deposits (Nanson, 1980). Accretion of land is the opposite of bank retreat, however, both processes are closely associated, since they form the basis for river meandering (Vargas Luna et al., 2012), shown in Figure 18. Due to river meandering, point bars are formed in the inner bend (cross-section A-A and C-C). The cause for this is a lower velocity near the inner bank, whereas in the outer bend a higher velocity prevails. In a river bend, the outer bend is therefore usually deeper.

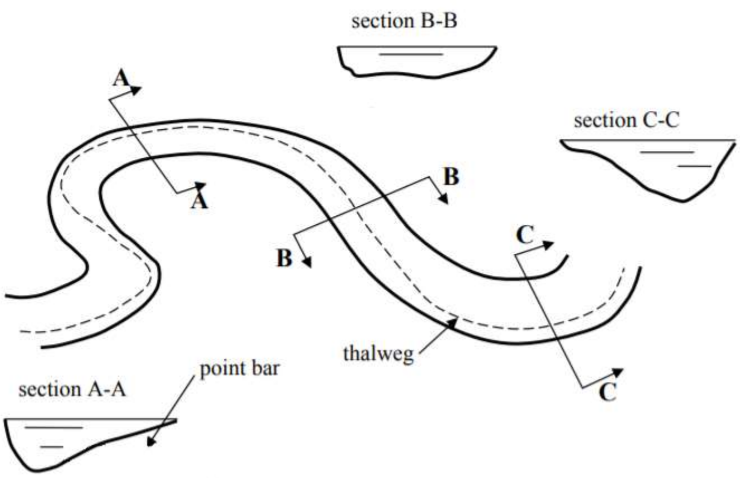

Figure 18 River meandering process, where the deeper outer bend usually erodes and in the shallower inner bend a point bar forms. Figure retrieved from Crosato (2008).

A point bar is a new part of land formed by sediment from upstream, building out layers of sediment that stack laterally against the inner bank of a bend (Nanson, 1980). Accretion of point bars can be responsible for opposite bank erosion by diverting flow towards the opposite bank, where it abrades the soil. Moreover, higher flow velocities tend to concentrate in the deeper parts of the cross-section (Dietrich and Smith, 1983). This mechanism enhances its development, where the outer bank is eroded further, and the inner bank can accrete more (Crosato, 2008).

The sediment accumulated on the point bar is generally fine, favouring vegetation development (Crosato, 2008; Camporeale et al., 2013). After vegetation has developed on the sandy point bar, plants can trap more sediment. In a positive feedback loop, the bar grows with more fine sediments and stronger vegetation, to become more stable and more frequently emerged (Corenblit et al., 2007). This causes the point bar eventually to become part of the stable riverbank. Hupp and Simon (1991) found that riparian vegetation growth and bank accretion occurred simultaneously and that accretion rates were greatest where vegetation density was highest. Other processes stimulating accretion are the abandonment of an anabranching channel (Schumm and Lichty, 1963) or the attachment of a (small) island to the riverbank due to silting up of the channel in between (Nadler and Schumm, 1981).

At present, little attention has been paid to river accretion in morphological models (Solari et al., 2015), even though this process is of vital importance for river planform. Most current process-based models only include erosion and assume river width to be constant. This would imply that the rate of erosion equals the rate of sedimentation in a river cross-section. Since the mechanisms behind erosion and sedimentation are different, this is not necessarily true. Moreover, erosion and sedimentation do not occur at the same time, since the hydrograph varies over a year and erosion usually occurs during high flow velocities and sedimentation during low flow velocities. Predicting riverbank accretion is essential for modelling river-width adjustment and river-planform changes (Crosato, 2008; Vargas-Luna, 2016).

2.1.3 River planform analysis from remote sensing

Development in river analyses is the use of remote sensing. Remote sensing is the science of obtaining information of the earth and its processes from a distant location. By using remote sensing data, it is possible to study river evolution on a large scale. River features such as (point) bars, braiding or meandering patterns and vegetation patterns can easily be identified and provide information for river management projects. Also, potential sites for future field studies can be assessed rapidly. In Table 1 an overview is given of different research topics that have made use of remote sensing. Also, each area and the time frame over which the research is conducted is shown, as well as the satellite data used for the purpose. It shows that a large variety of satellite data is available and can be used for various research fields. An agency that provides free satellite data is the United States Geological Survey (USGS) which provides worldly, up-to-date imagery and reliable information to analyse biological, geological-, geographical and hydrological processes. With developing technology and increasing satellite missions, more accurate and renewed data is obtainable on a large scale.

Table 1 Overview of different river planform studies.

Author	Topic	Research area	Satellite data	Time frame
Hickin (1974)	Channel migration by identifying micro-environments in meandering rivers	Beatton river, Canada	Aerial photographs	Unknown
Lewin (1976)	Point bar formation in meander development	Ystwyth river, Wales	Field observations and photographs	1969-1970
Kummu et al. (2008)	Riverbank changes as function of river width	Mekong river, Thailand	Aerial photographs, field survey, SPOT5	1961-1992; 1992-2005
Boruah et al. (2008)	Changes in flow patterns, vegetated islands and sand bar	Brahmaputra river, India	Indian Remote Sensing satellite imagery	1990-2002
Bertoldi et al. (2011)	Changes in vegetation density on riverbanks	Tagliamento river, Italy	ASTER	2004-2009
Maurya and Yadav (2016)	Evaluation of river course changes, focussing on meandering	Ranganga river, India	Landsat MSS, TM, ETM+, LISS-III	1972-2013

Two examples from Table 1 are further highlighted. Boruah et al. (2008) did a study to planform changes of the Brahmaputra river and showed an accuracy of 85% regarding mapping river water, sandbars and riparian vegetation. With that accuracy they stated the importance of satellite remote sensing on a large scale, yielding more information than fieldwork-based studies. Bertoldi et al. (2011) showed the usefulness of ASTER data to investigate changes in vegetation density between 2004 and 2009 along the Tagliamento river in Italy, by comparing reflectance of the earth's surface in that reach. They showed the importance of ASTER data when investigating fluvial processes, which is hardly possible with using standard aerial photographs.

Lawler (1993) made a review of remote sensing techniques and concluded satellite images to be the most popular approach to study lateral channel movement. Aerial- and satellite imagery are frequently used to measure bank retreat rates and the resulting channel migration by comparing riverbank locations at various intervals. It should be noted that the river course must be analysed during comparable conditions (e.g. same water levels, discharge, same month) and at regular intervals. Lawler (1993) named six problems that are difficult to avoid when using satellite images, namely (1) the assumption of linearity of channel change in time, (2) error in data sources, (3) confusion over map revision, (4) change in channel definitions over time, (5) misleading information and (6) contradictory evidence. With advancements in data storage and processing, most of these difficulties, such as errors, map revision and the misleading information on maps, are being avoided. When other hydrological data is lacking, attention should be paid to the usability of the satellite images. For example, after a period of rainfall, the water level is higher, and a riverbank could appear to be eroded. However, the riverbank is (temporary) submerged, and the bank will reappear when the water level drops. This phenomenon is not 'visible' for a satellite because it can only see the earth's surface. This is shown in Figure 19 - Figure 21, where a reach in the Ayeyarwady River is shown with low, high and low water levels respectively in a period of one year. One could say that in Figure 20 there was significant erosion on both riverbanks, but when looking at Figure 21, when the water level drops to the level before high water, little change is visible when compared to Figure 19. A recently developed tool called 'Aquamonitor' shows the change of surface from water to land and vice versa and filters out the changes in water-land boundaries due to effects such as water level variability with a technique called change detection. With this tool, it is possible to identify hotspots for erosion or sedimentation. More details about Aquamonitor are given in chapter 3.

Figure 19 Low water, Composite picture of February 2016.

Figure 20 High water, Composite picture of August 2016.

Figure 21 Low water, Composite picture of February 2017.

Images retrieved from Google Earth Engine; Code: https://code.earthengine.google.com/ac4afe469047822c635f92c885afeefd

Another remark is to be made about the different types of resolution. There are four types of resolution when using satellite images, namely spatial, spectral, temporal and radiometric resolution, summarized in Table 2.

Table 2 Different types of resolutions.

Resolution	Definition
Spatial	Represents the size of the surface area being measured (i.e. cell size).
Spectral	The range of wavelengths of the electromagnetic spectrum that is being measured.
Temporal	Determined by the interval between satellite images.
Radiometric	Describes the ability to distinguish (slight) differences in radiation energy.

The different resolutions are relatable, for example, opting for an increase in radiometric resolution would mean a loss in spectral resolution. Therefore, for each study, it is necessary to make a trade-off between the different resolutions (Alavipanah et al., 2008). Barsi et al. (2014) have summarised which satellite information is useful and what spectral bands are best to use for different kinds of studies.

2.2 Vegetation

Vegetation plays a vital role in the stability of riverbanks and the water flow (Vargas Luna 2016). Vegetation alters hydraulic roughness of the bed, and as a result flow patterns adjust. In turn, this also changes sediment transport rates. Baptist (2005) summarised the relationship between the hydrodynamics, morphodynamics and vegetation dynamics as shown in Figure 22. In paragraph 2.1 the morphodynamics and the bank stability were discussed, and in Appendix A the hydrodynamics were reviewed. In this paragraph, the interdependent relations between hydrodynamics, morphodynamics and vegetation are further analysed. At the end of each section, a summary table of the effects is presented.

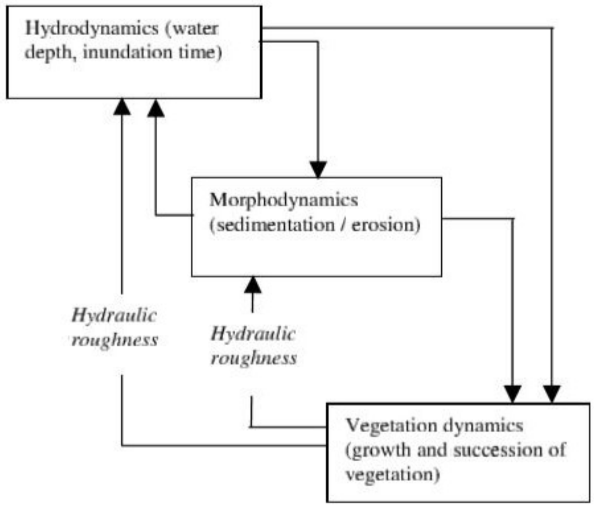

Figure 22 Relation between hydrodynamics, morphodynamics and vegetation. The interdependent relations make predictions of river planform development challenging. Figure retrieved from Baptist (2005).

2.2.1 Vegetation dynamics

Riparian vegetation is more and more recognised as a river system engineer (Tal et al., 2004). However, the extent of its effect depends on the vegetation characteristics. Density, age, diameter, stiffness and height are few of the properties that vary in time and space, even within the vegetation itself. Furthermore, there is a difference between emergent and submerged plants, that influence water flows differently. Seasons, variations in climatic and environmental conditions and land use will further affect the development of riparian vegetation (Simon et al., 2004), and therefore in the effects on hydrodynamic and geomorphological processes (Kirkby, 1995).

During low flow stages, inner bends become colonised by pioneer vegetation, initiating a (point) bar. Since the soil becomes hydraulically rougher, flow velocities near the bed are reduced, and vegetation can trap more sediment, thereby growing horizontally and vertically. At first, the bar floods completely, but after a couple of floods, the frequency of flooding decreases (Hupp and Osterkamp, 1996). Eventually, the (point) bar develops as a stable riverbank (Hickin, 1984), or even an island in a braided river system (Gurnell and Petts, 2002). This shows that vegetation controls its development, by reducing flow velocities and trapping sediment within vegetation patches. In this way, it creates favourable conditions to expand and thrive (Hupp, 2000). In contrast, removal of riparian vegetation leads to a smoother river bed with higher flow velocities and therefore larger erosion rates.

2.2.2 Effects on hydrodynamics

The characteristics of the flow are changed when water encounters vegetation. Vegetation increases hydraulic resistance by increasing drag and reducing flow velocity near the river bed and banks (Thorne, 1990). Bennett et al. (2002) observed flow deceleration in a flume experiment with in-stream vegetation and found similar results. The reduction in flow velocity is schematized in Figure 23. In the case of a river bed with submerged vegetation, the distribution of flow velocity shows two distinctive layers. In the lower layer, from the bed to the vegetation canopy, the velocity is considerably reduced. This holds for both flexible (Nepf and Vivoni, 2000) and rigid vegetation (Lopez and Garcia, 2001).

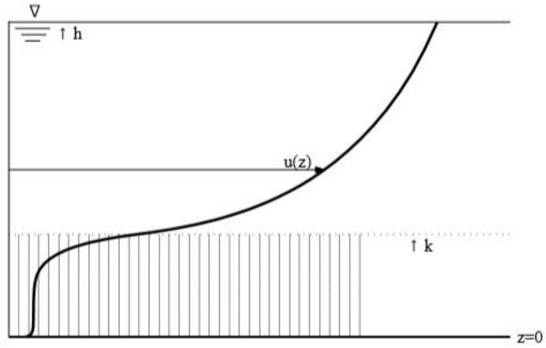

Figure 23 Vegetation reduces the velocity, and thereby the bed shear stress. 'k' is the vegetation height, 'u(z)' is the velocity at a height above the bed 'z', 'h' is the water level. Figure retrieved from Baptist (2005).

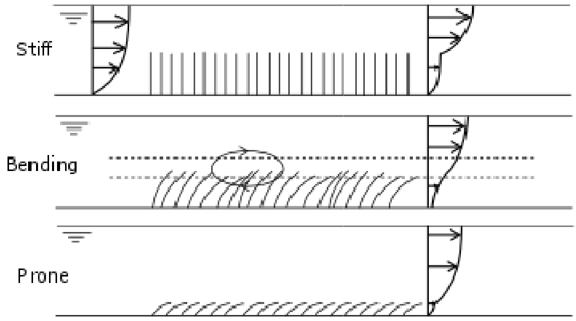

Figure 24 Effect of flexibility on flow velocity. Figure retrieved from Dijkstra et al. (2006).

In the layer above the submerged vegetation, a logarithmic velocity profile will develop as with regular flow. However, depending on the flow velocity and the flexibility of the vegetation, plants tend to bend with the flow, shown in Figure 24. This reduces the active area of the vegetation and therefore reduces the additional drag exerted by the vegetation on the current (Nepf and Vivoni, 2000; Dijkstra et al., 2006).

Baptist (2003) showed with flume experiments that because of the reduction in flow velocity, the bed shear stress is reduced by 80% when vegetation is present in comparison with beds without vegetation. It should be mentioned that this value is not applicable to all rivers, since it is dependent on local conditions, and the value is based on a numerical 1DV-model. Close to the bed, turbulence is damped by plant stems and leaves, leading to a reduction of bed shear stress, as is shown in Figure 25. In this figure from Sukhodolov and Sukhodolova (2010) it can be seen that on a bare river bed, turbulence intensity is maximum near the bed. When water flows over a vegetated bed, turbulence intensity near the bed is nearly zero. The peak intensity is moved to the top and sides of vegetation patches, where velocity differences are highest (Nepf, 1999). Lokin (2017) stated that the density of vegetation is of importance for the reduction in turbulence, where turbulence is damped more in dense vegetation than in sparse vegetation.

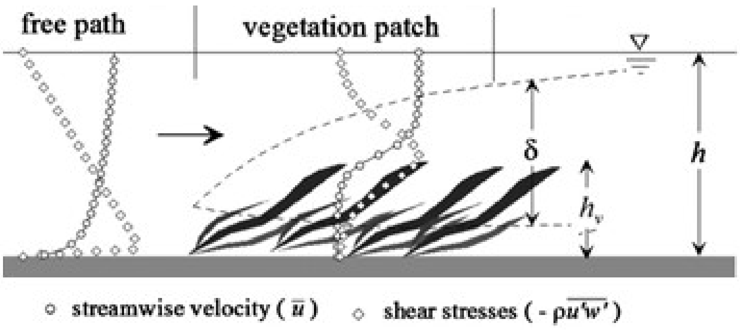

Figure 25 Difference in turbulence intensity of a bare river bed and a vegetated river bed. Also the streamwise velocity distribution is visible in this figure. Figure retrieved from Sukhodolov and Sukhodolova (2010).

The presence of vegetation in a river obstructs the flow of water and reduces the conveyance capacity (Kouwen and Unny, 1973). Moreover, due to the increased resistance, the flow is deflected into the main channel where vegetation is absent (Thorne 1990). At those unvegetated areas, flow velocities are increased. Similar, Rominger et al. (2010) investigated in an outdoor stream laboratory the influence of vegetation located on the inner bend on secondary currents in river bends. They found an increase of secondary current velocities of 50% in the main channel. In Table 3 and in Table 4 respectively the positive and negative effects of vegetation on hydrodynamic processes as described in this section are summarised.

Table 3 Positive effects of vegetation on hydrodynamic processes.

Positive effect of vegetation	Author(s)
Increase in hydraulic roughness	Thorne (1990)
Reduction of flow velocities	Thorne (1990); Bennett et al. (2002)
Decrease bed shear stress	Thorne (1990); Baptist (2003)
Reduction of turbulence inside vegetation	Nepf (1999); Lokin (2017)

Table 4 Negative effects of vegetation on hydrodynamic processes.

Negative effect of vegetation	Author(s)
Reduction of conveyance capacity, increase in water level	Kouwen and Unny (1973)
Increased turbulence near vegetation edges	Nepf (1999)
Flow deflection into main channel	Thorne (1990)
Increase in secondary current	Rominger et al. (2010)

2.2.3 Effects on morphodynamics

Due to the presence of vegetation, hydraulic roughness is locally increased, resulting in decreased flow velocity and the associated reduction of the bed shear stress. Therefore suspended sediment transport rates are reduced (Bennett et al., 2008), and sedimentation rates inside vegetated areas increase (Wu and He, 2009). Lowrance et al. (1988) described the effect of vegetation on erosion and sedimentation rates and found that vegetation acts as an efficient sediment trap. They researched the South-eastern coastal plain, USA, and found erosion and sedimentation rates of about 63 and 256 milligrams per hectare per year respectively in a forest river.

As was discussed in the previous section, the increase in hydraulic roughness decreases turbulence intensity near the bed in a vegetated patch. The stirring up of the sediment and consequent transport by flow is thereby reduced (López and García, 2001). However, due to flow diversion, fluvial entrainment is now concentrated near the vegetation edges, where turbulence intensity is increased (Bouma et al., 2007; Lokin, 2017). In Table 5 and Table 6 respectively the positive and negative effects of vegetation on morphodynamic processes as described above are summarised.

Table 5 Positive effects of vegetation on morphodynamic processes.

Positive effect of vegetation	Author(s)
Decreased sediment transport rate	Bennett et al. (2008)
Pick up capacity flow reduced	López and García (2001)
Increased sedimentation inside vegetation	Lowrance et al. (1988); Wu and He (2009)
Restrain soil particles	Gray and Leiser (1982)

Table 6 Negative effects of vegetation on morphodynamic processes.

Negative effect of vegetation	Author(s)
Increased erosion near vegetation edges	Bouma et al. (2007); Lokin (2017)
Cut-off sediment supply from secondary current towards inner bend	Rominger et al. (2010)

2.2.4 Effects on bank stability

In addition to the effects of modifying the flow fields and acting as a sediment trap, vegetation patches increase the stability of riverbanks. (Thorne, 1990; Simon, 1999). Pollen-Bankhead and Simon (2010) examined both beneficial and detrimental effects of vegetation on streambank stability. They stated that in general positive effects are predominate so that comparable banks with vegetation erode more slowly than banks without vegetation. Moreover, sites along rivers where vegetation was removed have shown accelerated erosion and increased bank instability (Gray and Sotir, 1996). The stabilisation is provided in two ways, namely via increasing flow resistance and via soil stabilisation through roots. Typical parameters that determine this additional strength provided by roots are root density, root strength, number of roots and root diameter (Pollen-Bankhead and Simon, 2009).

Vegetation stabilises riverbanks via their root system by anchoring through the soil and confining the earth across weak and unstable zones (Zeimer and Swanston, 1977; Gray and Leiser, 1982). Soil has a high compression strength, however low tensile strength. The combination of soil and roots makes a robust composite material that has higher resistance to mass failure. Abernethy and Rutherford (2000) used the physically based slope stability model 'GWEDGEM' to assess the changes in geotechnical properties along the Latrobe River. The model indicated an increase of the factor of safety against mass failure and shear instability with 60% due to the addition of roots. However, shear failure will still occur when the depth of the failure plane exceeds the rooting depth (Figure 26) (Abernethy and Rutherford, 1998). O'Loughlin and Ziemer (1982) estimated an additional shear strength of 1 to 20 kPa provided by the roots of small vegetation. More massive trees showed a tensile strength between 10 MPa and 60 MPa.

Figure 26 Roots of vegetation are not able to strengthen the soil to prevent mass erosion.

The spatial density and configuration of roots increase soil strength by providing shear strength to the soil. Simon and Collison (2002) researched the root system of vegetation and found that vegetation with multiple smaller roots has a more beneficial effect on soil stability than vegetation with a few large roots (e.g. trees). They stated that root area is more important than root strength.

Smith (1976) concluded that banks of the Saskatchewan river with vegetation were up to 20.000 times more resistant to erosion than similar banks without vegetation after he compared erosion rates of a riverbank with up to 16 to 18 percent of roots volume with a non-vegetated riverbank. Pollen-Bankhead and Simon (2010) showed a (non-linear) decrease of erosion volumes with increasing grass root volumes per unit volume of soil. Moreover, the eroded volume of banks with highest root densities was 10% less compared to riverbanks without roots.

Vegetation can also have negative effects on bank stability, for example by adding more weight, making the bank more prone to mass failure (Simon and Collison, 2002). However, additional surcharge also increases the normal stresses within the soil and therefore the shear strength. Dabney et al. (1997) state about this that grass and smaller vegetation has the most beneficial effect, because of the little surcharge and extensive root networks. However, the net results depend mainly on the erosion mechanism. An example of this is visible in Figure 26, where the vegetation on top of the riverbank is not protecting against toe erosion due to the flow of water at this water level. This will cause the riverbank to erode, and when the mass above becomes too heavy, mass failure will cause the bank to retreat.

Another negative aspect is stated by Howard (1984). Plants on bars cause flow deflection towards the opposite bank, the so-called 'bar push effect', which makes the opposing bank more vulnerable to erosion. Enhanced erosion rates due to this resultant redirection of the flow towards the opposite bank were found by Simon et al. (2004). This process was investigated in a flume with planted woody vegetation by Bennett et al. (2008), schematized in Figure 27.

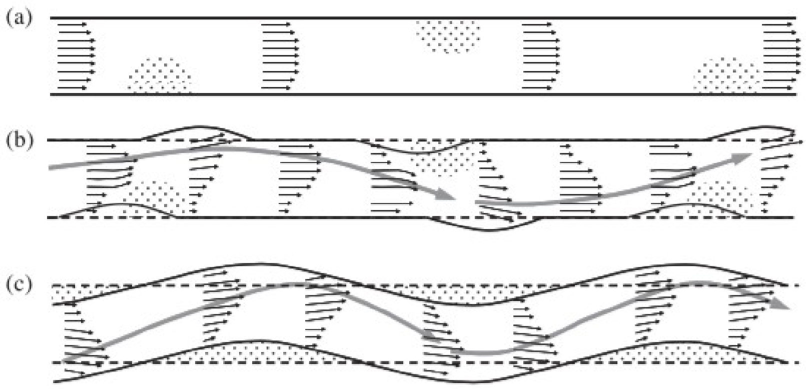

Figure 27 Due to the plantings of emergent, woody vegetation in a straight channel (a), the flow is diverted around the vegetation and the river starts to meandering, including flow deflection and bank erosion, opposite of the vegetation locations (b). Then the point bars grow, inducing more opposite bank erosion, further enhancing river meandering (c). The black arrows represent flow velocities, the straight line is the channel after some time, the dashed line the original channel. Schematic retrieved from Bennett et al. (2008).

Rominger et al. (2010) performed a study about the effect of vegetation on the secondary current. They found an increase of the depth-averaged centrifugal force, which drives the secondary flow, of about 30% because of flow diversion due to the presence of vegetation on the inner bend. Due to this increase, the erosion rate of the outer bend increased as well. In Table 7 and Table 8 respectively the positive and negative effects of vegetation on bank stability as described above are summarised.

Table 7 Positive effects of vegetation on bank stability.

Positive effect of vegetation	Author(s)
Decreased bank erosion rates	Pollen-Bankhead and Simon (2010); Gray and Sotir (1996)
Soil anchoring	Zeimer and Swanston (1977); Gray and Leiser (1982)
Increase resistance against shear failure	Abernethy and Rutherford (2000)
Increase shear strength	O'Loughlin and Ziemer (1982)

Table 8 Negative effects of vegetation on bank stability.

Negative effect of vegetation	Author(s)
Additional surcharge	Simon and Collison (2002)
Bar-push effect	Howard (1984)
Opposite bank erosion	Bennett et al. (2008); Rominger et al. (2010)

2.2.5 Representation of vegetation in experiments and models

In present studies, it is tried more and more to realistically model vegetation in numerical- and computer models (Wu et al., 2005; Van De Wiel and Darby, 2007). Also, laboratory tests (Kouwen et al., 1969; Wu et al., 1999) and (field) experiments (Darby, 1999) are performed to comprehend the functioning of vegetation in rivers better. Field research provides answers how processes occur in a natural environment. For example, Temmerman et al. (2005) investigated the impact of vegetation on flow routing and sedimentation patterns in a tidal marsh in the Scheldt estuary. They showed with their 3-dimensional hydrodynamic and sediment transport model that vegetation on higher marsh platforms deflected the flow into the unvegetated tidal channels, causing velocity pulses with accompanying increased erosion rates in the channels. If vegetation was removed, water flowed just as smoothly over the elevated bars than through the tidal channels, and no velocity pulses were found.

That is why a lot of research has been done to roughness coefficients of vegetation. The resistance predictors of Manning-Strickler, Chezy, and Nikuradze are most common. Crosato (2008) used a Chezy coefficient 25 $m^{1/2}/s$ to model overbank and floodplain flows covered with vegetation. In comparison, a bare bed value of 47 $m^{1/2}/s$ was used for flow in the main channel. Fathi-Moghadam et al. (2011) expressed vegetation in terms of Manning's roughness coefficient by using artificial plastic plants in a 4-meter long flume. The results showed an increase in Manning coefficient as vegetation density increased, where the coefficient decreased with increasing flow depth and velocity, confirming Cowan's procedure (Cowan, 1956). Cowan's method for estimating the Manning coefficient uses separate contributions dependent on local conditions, which together sum up to a total value for Manning's roughness coefficient. Another Manning coefficient classification is given in Table 9, where the Manning coefficient is dependent on different types of vegetation, season and water level. In Table 10 the Nikuradse roughness coefficients according to Baptist (2005) are presented.

Table 9 Manning coefficients for different types of vegetation, dependent on season and water level. Table modified from Phillips and Tadayon (2006).

Vegetation species	Manning's roughness		
	Minimum	Normal	Maximum
Short grass	0.025	0.030	0.035
High grass	0.030	0.035	0.050
Mature field of crops	0.030	0.040	0.050
Scattered shrubs	0.035	0.050	0.070
Light shrubs and trees in winter	0.035	0.050	0.060
Dense shrubs and trees in summer	0.070	0.100	0.160
Cleared land with tree stumps	0.030	0.040	0.050
Same as above, but with heave growth of sprouts	0.050	0.060	0.080
A few down trees, little undergrowth, flood stage below branches	0.080	0.100	0.120
Same as above but with flood stage reaching branches	0.100	0.120	0.160
Dense willow trees, mesquite, salt cedar	0.110	0.150	0.200

Table 10 Nikuradse roughness coefficients. Table modified from Baptist (2005).

Ecotope	Nikuradse coefficient
Forest and shrub (hardwood and softwood)	10.0
Structure-rich herbaceous vegetation and reed	5.0
Open herbaceous vegetation	2.0
Structure-rich floodplain grassland	0.8
Floodplain grassland	0.5
Poor floodplain grassland	0.4
Bare substrate and production grassland	0.2

Table 11 Drag coefficients for different types of vegetation. In this table 'k' is the vegetation height, '1/a' vegetation density, 'd_s' the stem diameter, and 'C_d' the drag coefficient. Table modified from Van Velzen et al. (2003).

Vegetation type	k (m)	1/a (m^{-3})	d_s(m)	C_D (-)
Pioneer vegetation	0.15	50	0.003	1.8
Production grassland	0.06	150000	0.003	1.8
Natural grassland	0.15	4500	0.003	1.8
Thistle bushes	0.3	3000	0.003	1.8
Bushes	0.56	46	0.005	1.8
Reed bushes	2	40	0.004	1.8
Bramble bushes	0.5	112	0.005	1.8
Dune reed bushes	0.35	90	0.004	1.8
Reed	2.5	80	0.005	1.8
Reed grass	1	200	0.002	1.8
Reed-mace	1.5	20	0.0175	1.8
Pipe grass	0.5	300	0.004	1.8
Sedges	0.3	200	0.006	1.5
Young brushwood	3.5	19.6	0.011	1.5
Orchard	2.5	0.16	0.15	1.5

In simulation models, the effect of vegetation on flow is modelled as a group of vertical cylinders imposing additional drag in the momentum equation. The formulation of the drag force from Morison et al. (1950) is:

$$F_D(z) = \frac{1}{2} \cdot \rho_w \cdot C_D(z) \cdot a(z) \cdot u(z) \cdot |u(z)|$$

In which $F_D(z)$ is the drag force, depending on the height above the bed, ρ_w is the density of water, $C_D(z)$ the drag coefficient, represented by a roughness coefficient, and $u(z)$ the flow velocity above the bed. In Table 11 some values of different vegetation types are given that represent the increase in roughness. The total resistance is then the sum of the resistance provided by the (bare) bed and the additional drag force provided by vegetation. $a(z)$ is a vegetation density parameter, which can be defined as:

$$a(z) = n(z) \cdot d_s(z)$$

Where $n(z)$ is the number of stems per unit area and $d_s(z)$ the stem diameter. The drag coefficient represents the ability of vegetation to reduce the force of the flow on the bed by adding resistance (Bouma, 2010). The formulation is, for example, used by Temmerman et al. (2010), Bennett et al. (2008) and Barrios-Pina et al. (2014). The drag coefficient varies for different vegetation species, height, density, flexibility or stem diameter, as can be seen in Table 11, as well as hydrodynamic conditions, and is therefore subjected to extensive research (Nepf and Vivoni, 2000; Lopez and García, 2001; Uittenbogaard, 2003). What also can be noticed is the fact that despite the variability in species, density and vegetation height and diameter, the drag coefficient is not very variable. It is proven difficult to attach a roughness coefficient to vegetation types representing the effect it has on the hydrodynamic flow conditions. Jalonen et al. (2013) proved with direct drag force measurements that the leaf area index (LAI, which is a dimensionless number characterising the leaf area of species,) appeared to be a useful measure in estimating vegetative strength for hydraulic analyses. Other indicators describe the state of vegetation, and one of them is the normalised difference vegetation index (NDVI).

2.3 Normalised Difference Vegetation Index

Vegetation development can be monitored with remote sensing techniques. Satellites measure wavelengths of absorbed and reflected radiation from earth. The spectral reflectance provide information about the type of ground cover and is an unchanging property of a specific material, also called ‘spectral signature’. With algorithms, the signals can then be transformed into a vegetation index (VI), which is a measure for ‘vegetation greenness’ to quantify vegetation density, health and activity (Huete, 2015). Vegetation indices can be used for monitoring land cover and vegetation fluctuation all over the world and have a broad application range due to the simplicity of utilisation (Goward et al., 1991). Farmers, for example, can monitor the health of their crops and identify infested crops. Other cases are environmental and ecological studies (Pettorelli et al., 2005), hydrological studies (Su, 2000) and agriculture (Panda et al., 2010). General properties of vegetation can be assessed, including the leaf area index, percent green cover, chlorophyll content and (green) biomass. The applicability and differences between VIs have broadly been discussed by Baret and Guyot (1991) and Bannari et al. (1995). One of the most used vegetation indices to detect vegetation in remote sensing is the Normalised Difference Vegetation Index (NDVI). When analysed through time, NDVI indicates where vegetation is thriving or where it is under stress. This has provided a lot of insight in vegetation on national scales (Justice et al., 1985), environmental studies (Tucker and Sellers, 1986) and ecosystem productivity (Running, 1990).

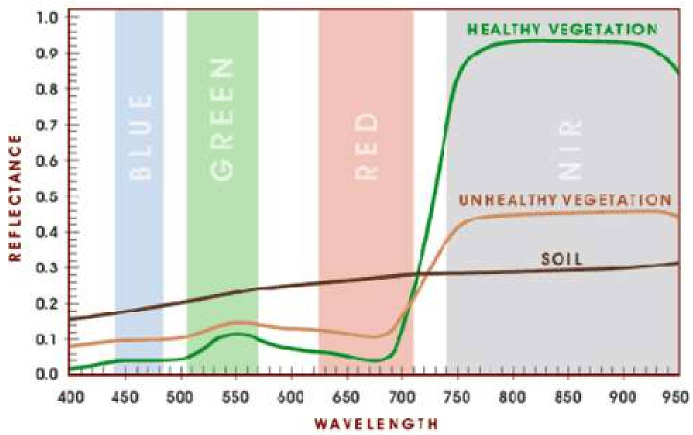

Figure 28 The different reflectance intensity for healthy and unhealthy vegetation and soil. The difference in reflection is small in the visible region but large in the NIR-region. By using this reflectance property of the material, it is possible to identify bare soil from vegetation. Schematic retrieved from PhysicsOpenLab (2017).

The green pigment in plant leaves, called chlorophyll, absorbs visible light (VIS), in the range of 0.6 – 0.7 µm, to photosynthesise. The cell structure of the leaves themselves reflects near-infrared light (NIR), in the range of 0.7 – 1.1 µm. This combination of absorption and reflection is a specific property of vegetation, shown in Figure 28. Therefore vegetation is easily distinguishable from inorganic material. The Advanced Very High-Resolution Radiometers (AVHRR), onboard the National Oceanic and Atmospheric Administration (NOAA) satellite information system records the reflectance of VIS and NIR of the earth. The AVHRR is a vital source of remote sensing data for already more than 20 years.

NDVI is calculated with the following formula:

$$NDVI = \frac{(NIR - VIS)}{(NIR + VIS)}$$

and has a value that ranges between -1.0 and 1.0. The different ranges of the NDVI depend on the subsoil and are presented in Table 12. In general, healthier vegetation reflects more NIR than unhealthy plants. In other words, the more significant the difference between NIR (reflected) and VIS (absorbed), the higher the NDVI. Negative values of NDVI correspond with urban areas and water, because of the very low reflectance in the NIR. Bertoldi et al. (2011) showed the accuracy and reliability of this classification system with low satellite resolution data to investigate vegetation dynamics along rivers. However, other classification systems exist, and distinct boundaries are difficult to define because of the vast differences in vegetation. Other popular vegetation indices in monitoring vegetation are RVI (Ration Vegetation Index) (Pearson and Miller, 1972), SAVI (Soil Adjusted Vegetation Index) (Huete, 1988) and EVI (Enhanced Vegetation Index) (Liu and Huete, 1995).

Table 12 Ranges of NDVI values of different subsoils. Table modified from Bertoldi et al. (2011).

Value	Indication
NDVI < 0	Water, snow, dead material, e.g. roads
$0 <$ NDVI < 0.3	Bare soil, sand, unhealthy vegetation
$0.3 <$ NDVI < 0.6	Small, healthy plant material, e.g. grass
NDVI > 0.6	Very healthy vegetation, e.g. shrubs and trees

A difficulty in using NDVI is the cloud cover disturbing the reflected radiation. Firstly, radiation from the sun towards the earth is reflected by clouds. Secondly, a part of the long wave radiation reflected from the earth's surface towards outer space (to be received by satellites) is absorbed by clouds as well (Graham, 1999). A part of that absorbed long wave radiation is then reemitted back to earth. Tang and Oki (2006) suggest using the NCI (Normalised Cloud Index) to obtain better estimates of the NDVI from images with cloud cover. Holben (1986), Verhoef et al. (1996) and Roerink et al. (2000) also provided methods to produce cloud-free NDVI results. Martinuzzi et al., (2007) analysed cloud removal from Landsat ETM+ datasets. Furthermore, other particles in the air, like aerosols and water vapour, cause distortions in the reflected radiation (Xie et al., 2008). Via compositing and mosaicking, a large part of cloud cover can be removed, and the influence of clouds can be reduced (Tang and Oki, 2006; Compositing and mosaicking, 2016).

Though NDVI seems to be an appropriate indicator and has certain advantages, it also has several limitations:

- Satellite accuracy is still not accurate enough to retract information at the scale of for example a tree. The smallest resolution is 15 meter, the most common is 30 meter, both exceeding the size of the tree (Barsi et al., 2014).
- Vegetation of different species can produce similar spectral signals as other vegetation groups and are problematic to distinguish. Also, same vegetation groups can generate different spectral signals, further complicating interpretation (Jung et al., 2006). It can help to define for each research a local-based NDVI classification to better describe the complexity between different vegetation groups within a research area (Xie et al. 2008).
- NDVI becomes 'saturated' when the biomass is exceptionally high. This can be the case in rainforests and jungles. This means that when the amount of vegetation approaches maximum NDVI values, the increase in NDVI gets smaller and smaller (Normalised Difference Vegetation Index, 2013).
- Other vegetation indices, e.g. SARVI and GEMI, reduce negative influences from soil- and atmospheric effects (Pinty and Verstraete, 1992), but give up on accuracy and are more sensitive to topographic effects, such as variable slopes (Qi et al., 1994).

Goward et al. (1991) measured deviations of 50% in NDVI values between satellite records and ground measurements when these issues are not taken into account. When measures, such as maximum-value composite images to remove errors caused by clouds Holben (1986), are considered, deviations could decrease to approximately 10%. However, despite the limitations of the NDVI, it remains an appropriate indicator for rapid assessment to use in vegetation monitoring on a large scale.

III

Materials and Methods

"I have never tried that before, so I think I should definitely be able to do that." – Astrid Lindgren

Figure 29 The Ayeyarwady River and Chindwin River confluence seen from above, courtesy of Floris Papenhuijzen. The Chindwin River merges from the lower right corner with the Ayeyarwady River, flowing from left to right. The confluence is marked by the colour difference between the rivers, caused by the sediment concentration difference.

In this chapter is explained how the research is conducted and with what materials. After a short introduction in paragraph 3.1, the research method is discussed in paragraph 3.2. A description of the Aquamonitor, Google Earth and Google Earth Engine is given. These tools have been used in this study to compare riverbank retreat rates with NDVI records. Finally, in paragraph 3.3 the conditions during the fieldwork are summarised.

3.1 Introduction

Little hydraulic and soil data is available on the Ayeyarwady River. Because of the modest economic state of the country, no extensive records for discharges, water levels or soil characteristics exist. Moreover, the river system is changing continuously, therefore, the data acquired in recent years have no significant value to apply, for example, in numerical models. To acquire usable and up-to-date data remote sensing can provide a solution since developments in space industry make it possible to freely obtain satellite images on a large scale at any time. Large datasets are available and remote sensing techniques have already been used for a long period. However, remote sensing cannot give all the answers, especially when more detailed information is needed to get a better view of local conditions. Hence, also a fieldwork has been conducted, to obtain additional information and to make photo material for further processing.

The research comprises all different riverbanks with vegetation; The NDVI records retrieved were chosen to be leading. This means that no distinction was made between steep and gentle banks, locations of erosion, erosion mechanism, etcetera. The focus is on places of bank retreat independent of bank characteristics. Also, all sorts of vegetation types are examined since it is interesting to investigate if specific vegetation types have characteristic control on riverbank stability. As was discussed in section 2.3, NDVI is a measure of the livelihood of vegetation, without being able to distinguish different kinds of vegetation. In this research, no distinction is made beforehand, although it is well understood that various vegetation types have a distinct influence on flow, morphology and bank stability. In chapter 4, the results have been analysed by categorising the results into smaller groups. By categorising, interesting observations were made.

3.2 Research method

3.2.1 Software and applications

The first step is to identify locations where bank retreat is evident. A recently developed tool by Deltares called 'Aquamonitor' can spot and mark those places (Donchyts et al., 2016). The Aquamonitor is an internet application that based on satellite imagery from different years shows areas of land that have been turned into water, indicated with a blue colour, and vice versa of water that has been turned into land, shown in green. With the Aquamonitor it is possible to monitor land surface changes with a spatial resolution of 30 meters. The Aquamonitor gives the first impression of land cover changes on a local, regional, as well as on an (inter)national scale, whether it occurs naturally (for example a meandering process) or it is the result of human interventions (e.g. a dam) (Deltares, 2016). An example of the Aquamonitor is given in Figure 30. The remote sensing images used by the Aquamonitor are made available by NASA and the United States Geological Survey (USGS) via the Landsat mission and the Shuttle Radar Topography Mission (SRTM) (Cardno, 2016), which has been collecting surface information for more than 30 years.

After local hotspots of erosion are identified, the following step is determining the bank retreat rates. This is also done with satellite images, more specifically with Google Earth. Beside satellite images, the Google Earth provides tools to measure distances, mark locations or make polygons. However, the most important reason to use Google Earth is the possibility to export information and data for further processing.

Figure 30 Bank retreat (blue) and accretion (green) in the Ayeyarwady River made visible with the Aquamonitor. The image is the result of a comparison of a reach in the Ayeyarwady River between 2014 and 2016.

Finally, the NDVI needs to be determined for the different areas coping with bank retreat. For this, the Google Earth Engine (GEE) is used. The ever-increasing growth of satellite data asked for a 'new' platform, where the large datasets can be analysed and processed. GEE provides this platform, where it has a large number of datasets publicly and freely available. This platform lets everyone who is interested make use of various datasets and use the computational power of the Google Cloud to analyse and process data, without the need to download the images. GEE forms the basis for the Aquamonitor, showing one of the possibilities of the GEE. Summarized, GEE provides access to satellite information in three ways. Firstly, the availability of satellite data and storage in the Google Cloud. Secondly, GEE provides the computational power and resources to process the data. Thirdly, GEE provides a large analytical toolset to compile an end product (Google Earth Engine Developer's guide, 2017).

3.2.2 Plan of approach

The plan of approach is summarised in Figure 31. This figure shows the different steps of the riverbank analysis and are further elaborated. The results of this research method are given in Appendix B.

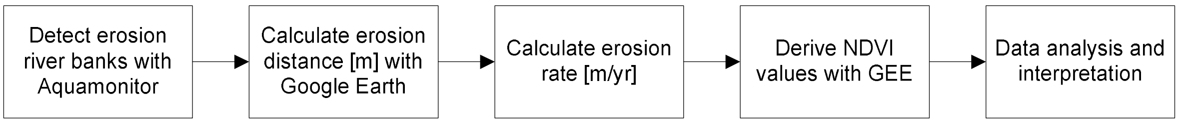

Figure 31 Summary of the plan of approach.

First, the areas of bank retreat were located. This was done by visual inspection of the Aquamonitor. The research area was found on the map, and with the toggle function, the years 2014 and 2017 were selected. The Aquamonitor shows the difference in planform of the Ayeyarwady River between 2014 and 2017. Figure 32 and Figure 33 show the nine regions of riverbank retreat and are numbered 1 till 9. Downstream of the Ayeyarwady – Chindwin confluence (not visible in the figures) no bank retreat areas were collected. This was done because downstream of the confluence, the reach is characterised by a tangled, braided river pattern with multiple bars and islands. It is decided to investigate initially the functioning of NDVI records in a more regular reach before it is applied to vigorously braiding rivers. In braiding rivers, various other effects, such as mixing effects, come into play and make processes in rivers even more complicated (Schuurman, 2015).

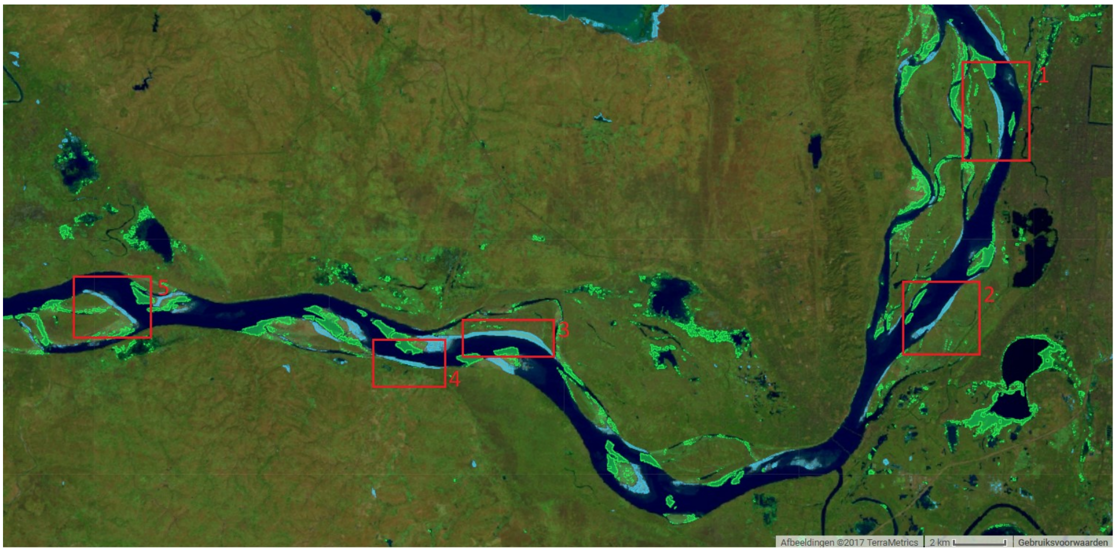

Figure 32 River reach around Mandalay. The five research areas are highlighted in red.

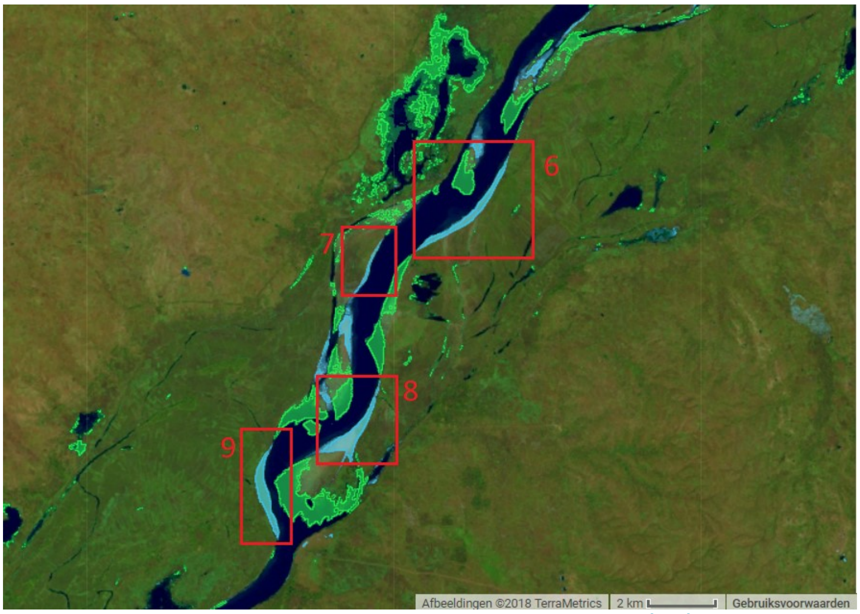

Figure 33 The Ayeyarwady river further downstream, with the other research areas (6-9).

Subsequently, the bank retreat rates were determined. The riverbanks were marked by using a 'path', which is a function in Google Earth. The path was made for two moments in time, namely in January 2014 and January 2017. The exact date of the year is dependent on the available satellite images of the area in Google Earth. The path was saved as a 'KML-file', which is a file used for geographic data, containing features such as coordinates. The riverbank coordinates of 2014 were then compared with the riverbank coordinates of 2017 by extracting the coordinates form both KML-files. However, the extracted coordinates are in degrees (longitude and latitude). To convert degrees into meters, the difference in degrees was multiplied by a factor 110.000. According to (Longitudestore, 2016), one degree is approximately equal to 110 kilometres, depending on the location on earth. The difference in meters between two coordinates is defined as the 'bank retreat distance'. The bank retreat distances were divided by a time unit, and a 'bank retreat rate' is obtained. An example of this is presented in Table 13, where 19 coordinates of area 7 are displayed.

Table 13 Table of the yearly-averaged bank retreat rates.

	Longitude	Latitude	Longitude	Latitude	Difference (m)	Bank retreat rate (m/yr)
	Coordinates 2014		Coordinates 2017			
7.1	95.4637593	21.8469108	95.4637593	21.8469108	0	0
7.2	95.4626927	21.8458372	95.4626927	21.8458372	0	0
7.3	95.4608553	21.8444245	95.4607488	21.8445928	21.9	7.3
7.4	95.4585270	21.8416163	95.4578020	21.8423699	115.0	38.3
7.5	95.4565995	21.8394298	95.4557790	21.8403177	133.0	44.3
7.6	95.4542489	21.8369493	95.4529608	21.8380071	183.4	61.1
7.7	95.4505931	21.8343132	95.4499243	21.8349906	104.7	34.9
7.8	95.4468400	21.8317547	95.4467692	21.8317986	9.2	3.1
7.9	95.4451986	21.8288553	95.4445416	21.8291435	78.9	26.3
7.10	95.4439634	21.8267260	95.4432235	21.8270707	89.8	29.9
7.11	95.4428005	21.8240762	95.4418598	21.8245488	115.8	38.6
7.12	95.4422892	21.8219693	95.4412356	21.8223249	122.3	40.8
7.13	95.4411095	21.8196287	95.4403498	21.8203387	114.4	38.1
7.14	95.4404318	21.8186992	95.4396313	21.8192690	108.1	36.0
7.15	95.4396860	21.8171508	95.4384500	21.8176886	148.3	49.4
7.16	95.4393186	21.8157589	95.4375096	21.8164442	212.8	70.9
7.17	95.4391280	21.8146467	95.4364629	21.8151534	298.4	99.5
7.18	95.4388086	21.8131093	95.4354620	21.8137204	374.2	124.7
7.19	95.4390675	21.8112357	95.4352593	21.8113036	419.0	139.7

The final step is to determine the NDVI of the coordinates in 2014, to obtain an estimate of the state of the vegetation before the bank retreat. NDVI datasets were retrieved from composite NDVI time series of the 'Landsat 8 Surface Reflectance mission'. The details of this dataset can be retrieved from (USGS Landsat 8 Surface Reflectance, 2017). The Landsat 8 data is collected on a 16-day repeat cycle, which includes the NDVI records. The coordinates obtained for the bank retreat rate analysis were used again to calculate the NDVI around that point. The script used is presented in Appendix C. When using the GEE script, a polygon (further referred to as 'geometry') is introduced to mark the area over which the NDVI is to be determined. Over this area, the NDVI is calculated by averaging NDVI values over the geometry.

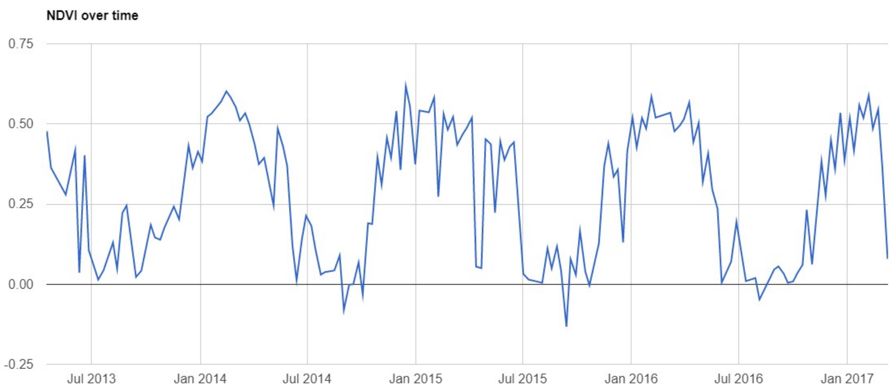

Figure 34 An NDVI record retrieved with the GEE script. On the horizontal axis the date is presented; On the vertical axis the NDVI is presented.

The script was run, which creates a graph showing the NDVI as a function of time of area marked by the geometry. An example of such an NDVI record is shown in Figure 34. Numeric values were obtained as well by extracting the values from the 'CSV-file'. After a coordinate was processed by the script, a new coordinate was introduced into the script. This process was repeated till all the coordinates of the nine different riverbanks were processed, a total of 126 points. A summary of the data and the number of coordinates per riverbank is given in Table 14.

Table 14 Information of the data of the satellite imagery, the number of coordinates per area and the date of NDVI values retrieved.

Area	Date of original riverbank	Compared with riverbank at	Number of coordinates	Date of NDVI
1	07/01/2014	11/01/2017	11	13/01/2014
2	07/01/2014	20/12/2016	17	13/01/2014
3	07/01/2014	11/01/2017	8	13/01/2014
4	07/01/2014	11/01/2017	10	13/01/2014
5	02/02/2014	11/01/2017	13	13/01/2014
6	15/02/2014	02/01/2017	19	13/01/2014
7	15/02/2014	02/01/2017	19	13/01/2014
8	15/02/2014	02/01/2017	12	13/01/2014
9	15/02/2014	22/01/2017	17	13/01/2014

3.3 Fieldwork

This thesis is part of a large-scale research to gain more insight into the Ayeyarwady River. It was decided to perform a fieldwork and combine the different studies into one week of testing and experiments. The fieldwork took place from 30 January till 3 February 2017, so during the dry season. This week was chosen because of sailing safety, and it provided favourable conditions. Especially the calm water conditions (i.e. low flow velocities and water levels) contributed to the execution of the experiments. As was already shown in Figure 7, the river reach between starting point Mandalay and end point Pakokku is the area of the fieldwork. This extensive region upstream of the confluence was sailed by small fishing boats, shown in Figure 35, on which various experiments could be performed, among others the collection of photo material. The photo material is collected in the first place to visualise the effects of vegetation on riverbank stability and to make comparisons between collected NDVI data and the observed vegetation. The validation of this comparison is done in Appendix D. This method showed unforeseen problems that decreased accuracy. The critical issue was the placement and the size of the geometry. This broadly discussed in Appendix D as well.

Figure 35 Example of one of the fishing boats that were used during the fieldwork to perform experiments.

Summarised, the validation of the NDVI records comprises the following steps:

1. Localisation of the riverbank. Characteristics of different riverbanks were photographed during the fieldwork. The GPS information was stored together with the picture, so the coordinates of the picture could be extracted. The locations of the collected photo material are depicted in Figure 36. In total 295 photos were made, of which 72 photos were used for this research.
2. Determination of the NDVI values. For this the GEE script of Appendix C was used. The coordinates obtained in step 1 were used as input for the point of which the NDVI was to be determined. The geometry placed around this point would give the NDVI values over that area.
3. Comparison of various riverbanks. The final step involved the comparison of different riverbanks with different amount and types of vegetation with one another, to validate whether a riverbank with denser vegetation resulted in a higher NDVI.

Figure 36 The locations of the collected photo material in the research area.

IV

Results

"You cannot beat a river into submission; you have to surrender to its current and use its power as your own." – Tilda Swinton

Figure 37 The Ayeyarwady River, seen from one of the boats used during the fieldwork. On the picture the Pakokku Bridge is also visible. The bridge has a length of 3.4 kilometres, the whole width of the river is hard to capture on a single picture.

Nine different areas are analysed and the results of the bank retreat rates as a function of the NDVI values are presented in this chapter. A more detailed description is presented in Appendix B, where each area is treated separately. This chapter presents the findings and compares results in terms of different characteristic features, such as erosion mechanism, location and vegetation type.

4.1 General description of the general results

For each of the nine areas, the bank retreat rates were determined, as well as the NDVI values at those locations. Similarities and differences between regions, riverbanks, erosion mechanisms and NDVI records are presented in this chapter. A riverbank classification was made with riverbank vegetation classes (RVC, Table 15) to narrow the results even more. A summary of the properties of the nine different areas is given in Table 16.

Table 15 Riverbanks classified according to the amount and state of vegetation.

RVC	Definition
I	Sandy riverbank without vegetation
II	Riverbank with scarce vegetation, very light agriculture and some sandy areas, such as point bars are present.
III	Riverbank with light density vegetation, patches of grass, light bushes and agricultural lands.
IV	Riverbank with moderate vegetation, with patches of tall grass, bushes and numerous trees.
V	Riverbank with very dense vegetation, with large amounts of tall grass, bushes and trees.

Table 16 Summary of the riverbank and erosion mechanism per area in the Ayeyarwady River.

Area	Location	Type of bank	Erosion mechanism	Riverbank vegetation class
1	Inner bend	Steep	Mass failure	IV
2	Meandering section	Steep and flat	Fluvial entrainment	II
3	Outer bend	Steep	Mass failure	II
4	Outer bend	Steep	Mass failure	III
5	Head of large bar	Flat	Fluvial entrainment	I
6	Outer bend	Steep and flat	Mass failure	II
7	Outer bend	Flat	Fluvial entrainment	II
8	Outer bend	Flat	Fluvial entrainment	I
9	Outer bend	Steep	Mass failure	III

The main mechanism driving the erosion in the nine areas is the formation of point- and mid-channel bars that deflect flow towards the (opposite) retreating riverbank. Areas 3, 4, 6, 7, 8 and 9 were located in outer bends where point bars pushed the flow towards the bank. However, the properties of the riverbanks differed, which is also summarised in Table 16. It was noticed that the location and the slope of a bank are not correlated. Steep banks were found both in inner and outer bends. Moreover, outer bends showed steep and flat areas. The slope of a bank and the erosion mechanism were found to be correlated; At locations where toe erosion and mass failure were the main erosion mechanism, the riverbank was steep. Where fluvial entrainment was the main erosion mechanism, the bank was flat to mildly sloped. There seemed to be no correlation between riverbank vegetation classes and radii of curvature with the erosion mechanisms.

The overall results of the bank retreat analysis are shown in Figure 38. In this figure the NDVI is plotted on the horizontal axis. On the vertical axis the bank retreat rates are plotted. In this thesis bank retreat are assumed as positive values.

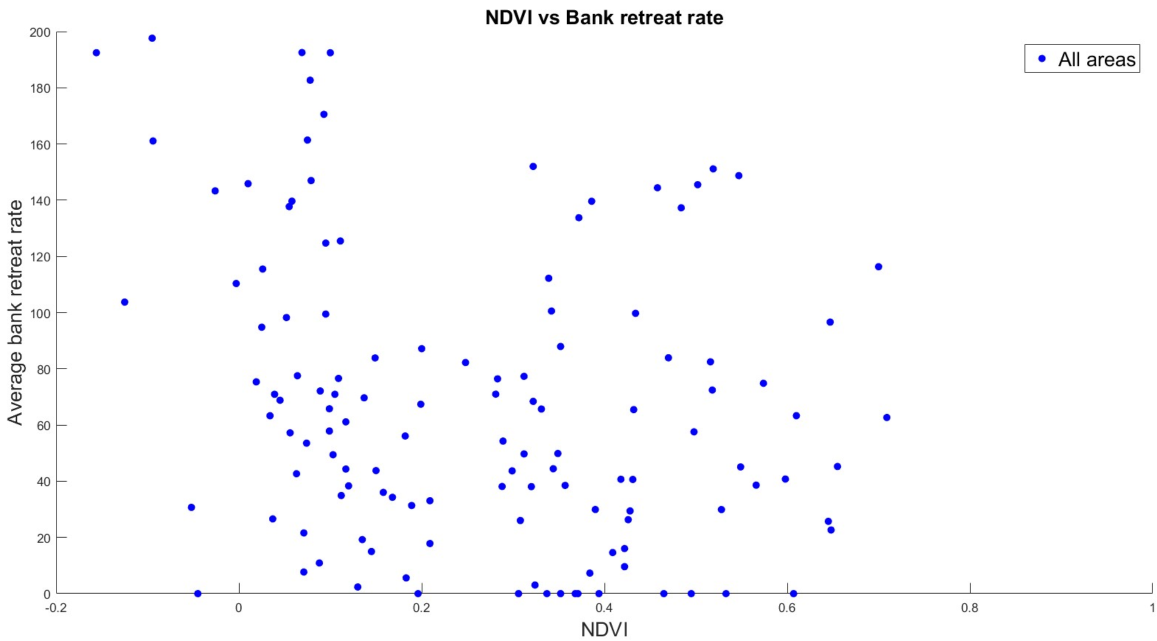

Figure 38 Result of the bank retreat of all areas together, plotted against NDVI.

The results were split up per area in Figure 39. There is a lot of scattering in the figure, and it is difficult to discern trends per area. Therefore the different areas are grouped, specified by erosion mechanism (Figure 41), slope of the riverbanks (Figure 43) and riverbank vegetation classes (Figure 44).

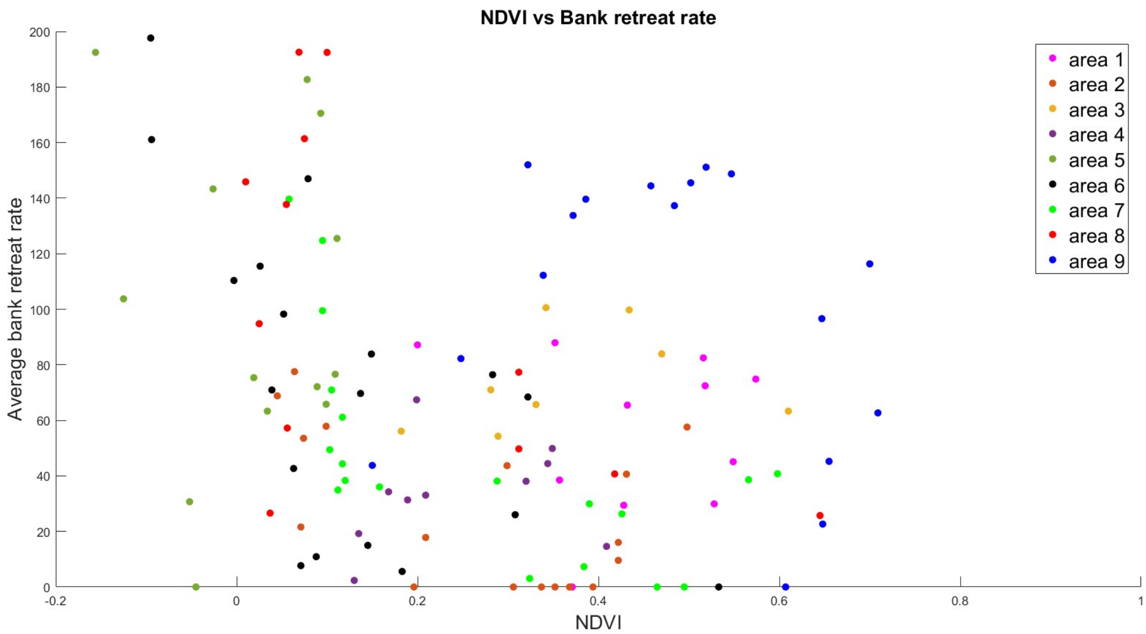

Figure 39 Total figure of erosion rates as a function of NDVI values. Each river section is represented by a different colour.

The average bank retreat rates as a function of reach-averaged NDVI per river section are visualised in Figure 40 as well, where also a large difference between the areas is visible. The areas where mass failure occurred (1, 3, 4, 6 and 9) are much scattered. The areas where mainly fluvial erosion occurred (2, 5, 7 and 8) show declining erosion rates with increasing NDVI values.

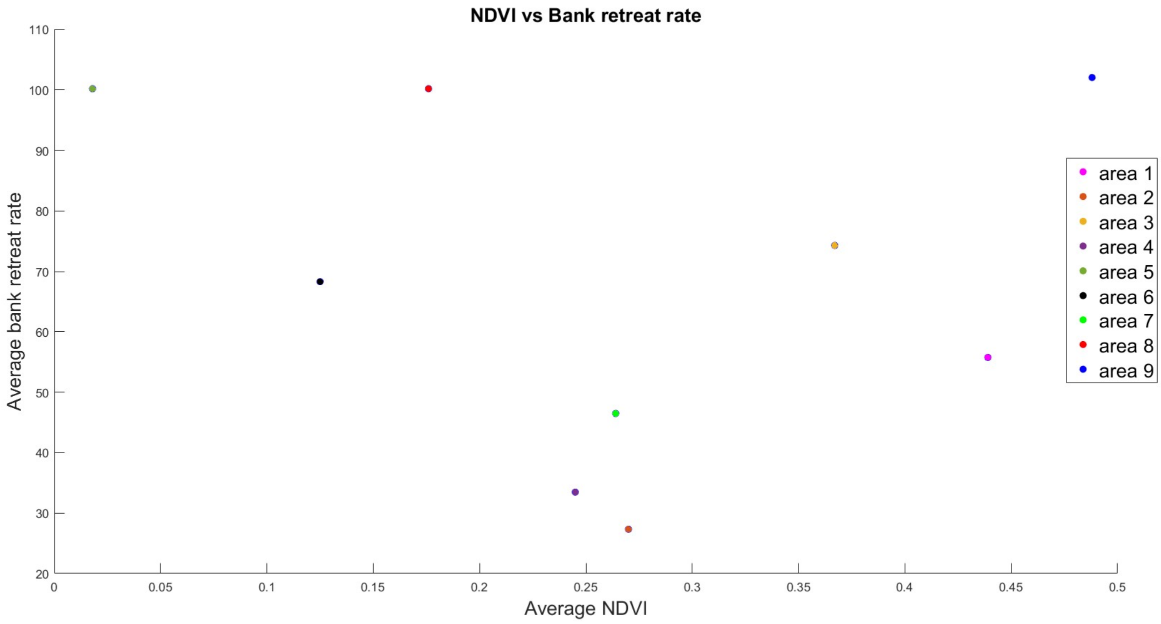

Figure 40 The average values of erosion rates per river section.

4.2 Results based on riverbank characteristics

When distinguishing between erosion mechanism, i.e. mass failure and fluvial entrainment, some trends point out. Firstly, the scatter observed in Figure 39 is mainly caused by the riverbanks subjected to mass failure, represented by the blue points in Figure 41. Secondly, the riverbanks subjected to fluvial entrainment can be divided into two regions based on bank retreat rates: (1) NDVI smaller than 0.2 and (2) NDVI larger than 0.2, see Figure 42. It was noted that there is a wide range in bank retreat rates in region 1, with maximum bank retreat rates of nearly 200 meters per year. In region 2 the maximum erosion rate is found to be 80 meters per year.

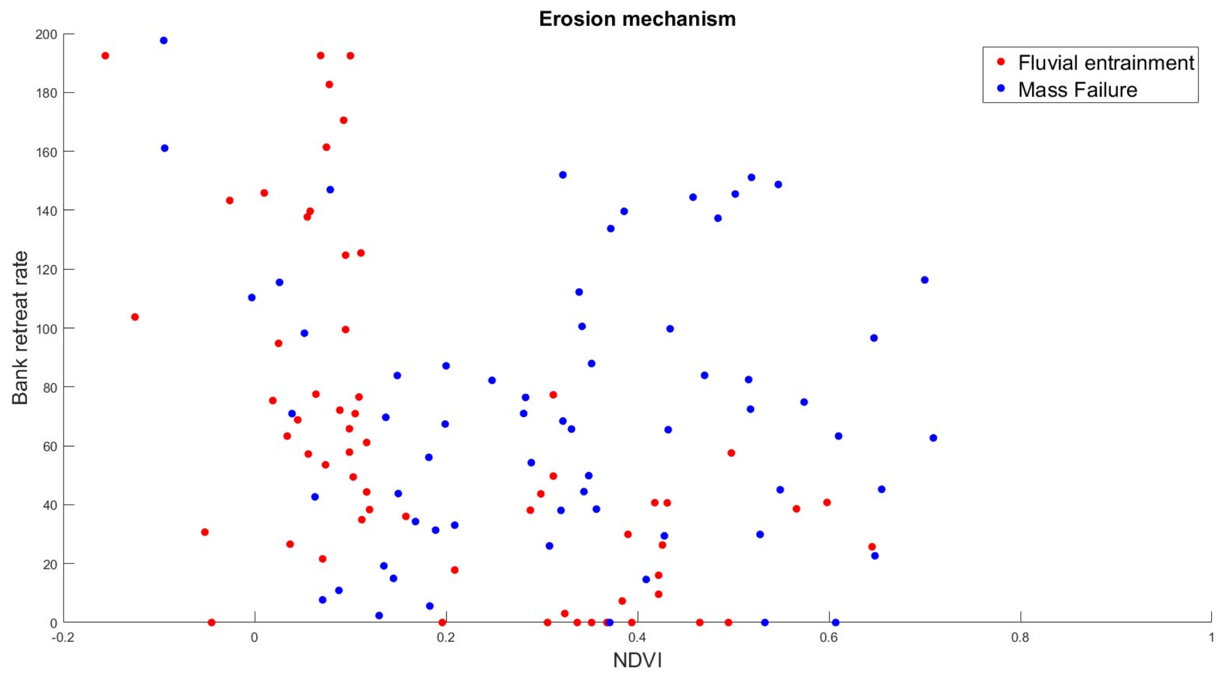

Figure 41 All bank retreat rates as function of NDVI, grouped per erosion mechanism.

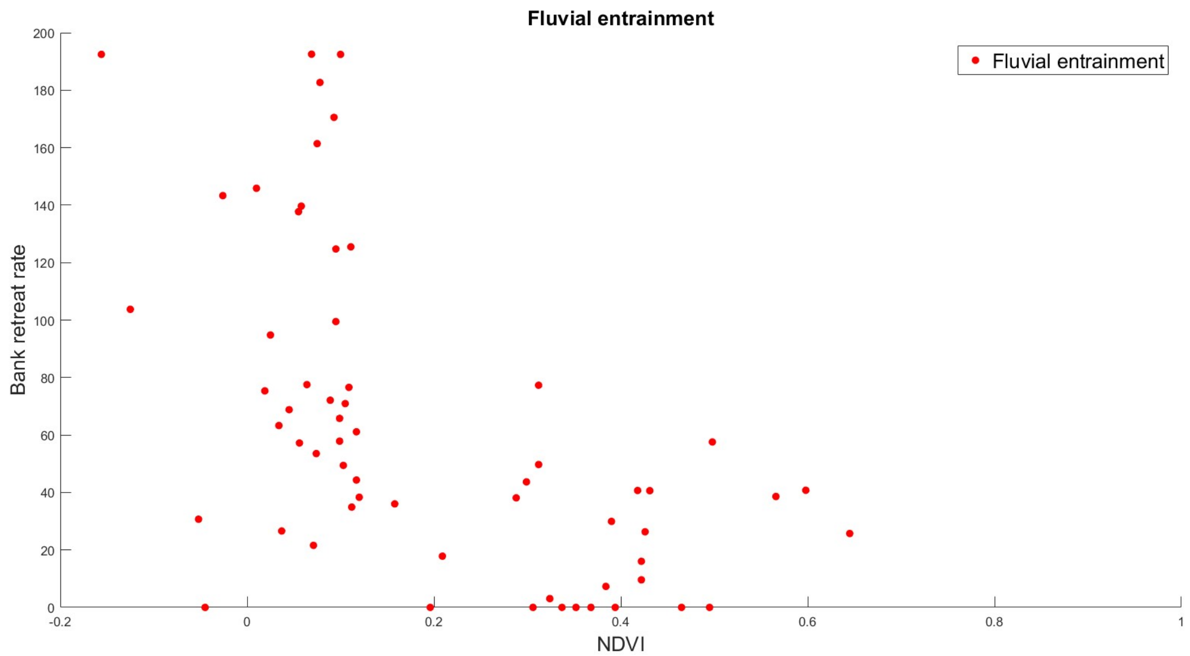

Figure 42 The bank retreat rates filtered results of the points subjected to fluvial erosion.

In Figure 43 there is made a distinction between steep, mixed and gentle (or flat) riverbanks. The gentle banks were defined as banks with a slope, and steep banks as vertical riverbanks (see chapter 1.1.2). As was already stated, there is a relation between erosion mechanism and riverbanks. Therefore similar trends are found for mixed and gentle riverbanks. As can be seen, the scatter is mainly caused by the steep riverbanks.

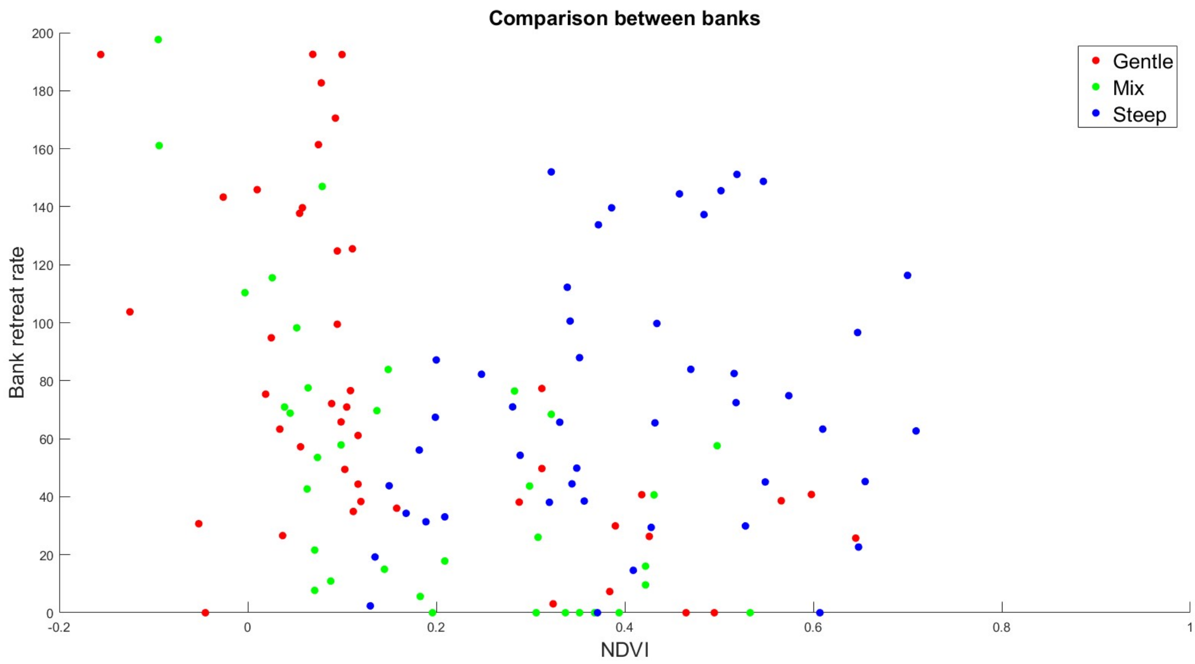

Figure 43 All bank retreat rates as function of NDVI, grouped per riverbank slope.

Finally, in Figure 44 the distinction is made between the riverbank vegetation classes from Table 15. The low classes (I and II) show a decreasing relation of bank retreat rates with increasing NDVI. The higher classes (III and IV) show an opposite response; the bank retreat rates increase with NDVI.

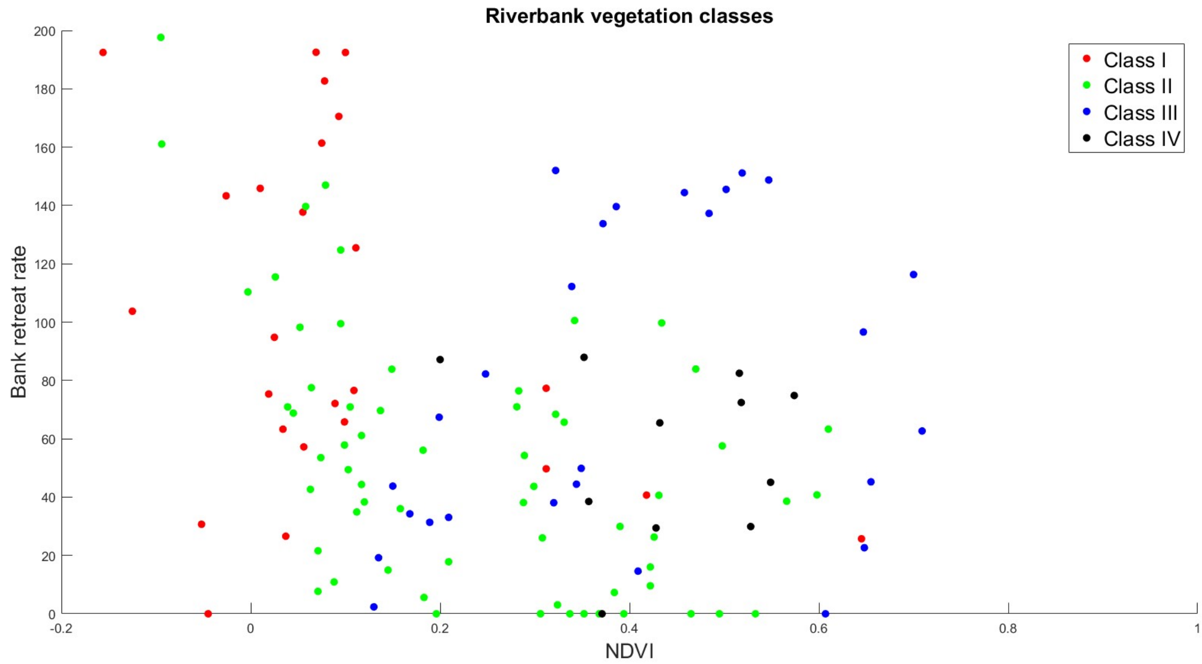

Figure 44 Results classified into riverbank vegetation classes.

V

Discussion

"It is not a bad thing finding out that you do not have all the answers. You start asking the right questions." – Erik Selvig

Figure 45 A picture of a steep riverbank in the Ayeyarwady River. The vegetation on the edge of the riverbank indicates that the riverbank is retreating rapidly and the farmer should take its crops from the land before it is lost in the river.

The results obtained from the analysis of bank retreat rates and NDVI records are discussed. The discussion is treated in the same sequence as the research is conducted, so firstly the determination of the bank retreat rates is discussed in section 5.1. The effects of vegetation on the bank retreat rates are then discussed in section 5.2. In section 5.3, the NDVI analysis is treated and in section 5.4 the relation between erosion rates and NDVI is being discussed.

5.1 Bank retreat rates from satellite images

One of the problems encountered in the determination of the (yearly) bank retreat rates is the assumption of linear lateral change, as Lawler (1993) described. The assumption that bank retreat rates are linear in time is inaccurate. Ligthart (2017) showed already that the Ayeyarwady planform changed most after a period of high water. Therefore the calculated bank retreat rates in meter per year vary from the momentary erosion rates. In this research, satellite images of two different dates (from 7 January 2014 and 11 January 2017) were used. By dividing the difference in lateral distance by a time unit, a constant bank retreat rate over the three years was obtained.

A second problem in determining bank retreat rates with satellite images is the difficulty in distinguishing bank erosion processes and fluvial entrainment from point bar propagation. As was shown in areas 2, 5, 7 and 8 (Appendix A) the flat areas were mainly deposited sediment from earlier years that were transported in subsequent years. This is not considered as bank retreat, but more as a dynamically stable riverbank dependent on sediment transport. From satellite imagery and the bank retreat analysis could be seen that the sandy areas contributed to high 'bank retreat rates', but this is better classified as high 'sediment transport rates'. During high flows, large sediment loads are transported with pulses of high intensities which causes the dynamic behaviour of the Ayeyarwady River. This sediment transport load can be reduced by the growth of vegetation on these point bars (Bennett et al., 2008), as also the results showed decreased bank retreat rates with higher NDVI values.

5.2 Effect of vegetation on erosion and bank stability

It was assumed that the degree of bank retreat was an indicator for riverbank stability. To obtain a better insight into the effects of vegetation on bank stability, nine areas of bank retreat were examined. When looking at the erosion mechanisms, especially mass failure (Lawler, 1992) is a common erosion mechanism in the Ayeyarwady River, as it was present in five of nine inspected areas. During low water levels, there is no increased resistance provided by vegetation on the riverbanks since toe erosion erodes the riverbank from below, after which mass failure occurs. It is also shown with photos that roots of vegetation do not reach the location of toe erosion. Therefore the positive effects of vegetation are overrated in reaches where riverbanks are very steep. This is also visible in Figure 41, where the blue points showed considerable scatter, following Thorne and Lewin (1979), who also found inequality in bank retreat rates of mass failure mechanisms.

The fieldwork could not provide much insight into the influence of vegetation on the Ayeyarwady riverbanks. Most important reason for this is the water level difference between seasons. The fieldwork was conducted during the dry season, i.e. low water levels, and therefore there was no contact between the flowing water and the vegetation. However, at some sites, it appeared that vegetation played a role. For example, in area 1, the height of the grass approached two meters, indicating that the grass was already present for more than a year. This means that it survived a rainy season with the accompanying high water discharges. At area 5, vegetation proved to stabilise soil, as there was a clear difference between an elevated area with vegetation on top and a bare area without vegetation at a lower elevation. However, in the Ayeyarwady River, it is difficult for vegetation to establish stability with the prevalent discharge regime, but when vegetation gets an opportunity to develop, Myanmar provides a thriving climate for vegetation to grow.

5.3 NDVI analysis

In Appendix D validation of NDVI records has shown that the NDVI records can give a good indication of the state of vegetation on the riverbanks. Photo material was compared with the NDVI records of these locations, where riverbanks with more vegetation showed higher NDVI values. The results corresponded with the classification scale of Bertoldi et al. (2011).

Similarities were the locations of maximum and minimum values in the records. Over the whole river reach, peaks showed during the dry season, around January – April. During the rainy season, from June till September, minimum values were recognisable. This is because, during high water levels, more water is present in the geometry. That means that the NDVI is lower. It is also possible that the vegetation is degraded in the rainy season. This would confirm that, besides higher flow velocities, the absence of vegetation enhances bank retreat rates. NDVI records of the rainy season could not support this statement due to cloud cover (Tang and Oki, 2006). The clouds distorted the NDVI signals significantly. Moreover, photo material of the river during the rainy season is scarce since most pictures of the Ayeyarwady River are made by tourists and are usually not made for research purposes such as riverbank stability. Besides, no additional information of the photo material (e.g. date and year) is included, which makes it difficult to recognise the hydraulic conditions. Moreover, not many tourists visit Myanmar in the rainy season. Hence, photo material could not provide an answer in the state of the vegetation on the riverbanks during the rainy season. As a rough indication, the available photo material, for example in Google Earth, can give some insight into why the NDVI values are significantly lower.

As was stated before, NDVI records are distorted by cloud cover, which, for example, can be seen in Figure 46. This figure shows the NDVI record of a retreating riverbank between January 2014 and January 2017. The NDVI values during the rainy season of 2016 were higher than in the dry season of 2016 and 2017. This implies that during the dry seasons more water is present than in the rainy season and therefore the riverbank has retreated. However, it is not possible that NDVI values rise during the rainy season when water levels are higher. In Figure 46 it can be seen that between January 2015 and January 2017 the minimum values were found during the dry season, whereas in the rainy season the values were located around zero (except for some peaks). A composite image with least cloud cover of July 2015, Figure 47, showed an abundance of clouds. The cloud cover blocks the 'view' of the Ayeyarwady River, and the clouds provide the signal that the satellites receive, which is larger than a signal of an area of water.

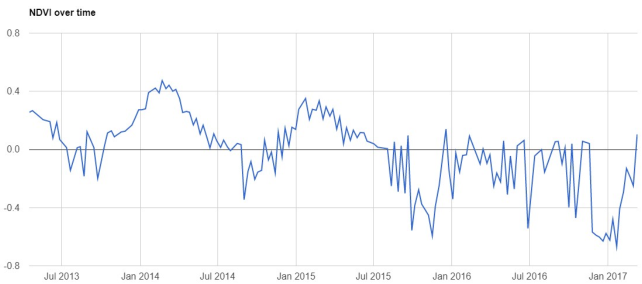

Figure 46 A (typical) NDVI record of an eroding riverbank, noticeable from the decreasing NDVI values during the dry season, and in January 2017 negative values.

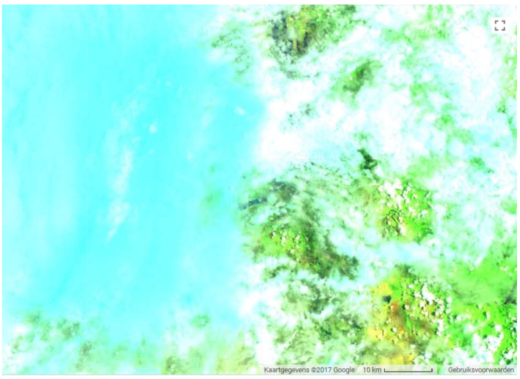

Figure 47 Composite image of the Ayeyarwady river from August 2015, indicating cloud cover during the rainy season.

The NDVI analysis showed other shortcomings, the most important one being the impossibility to distinguish different vegetation species from NDVI records solely, just as Jung et al. (2006) and Xie et al. (2008) mentioned. Different NDVI records with similar vegetation types were found on the Ayeyarwady riverbanks. Comparable NDVI records of different vegetation types were found as well. Since vegetation such as trees influences hydrodynamic and morphodynamic processes differently than grass or shrubs, a similar NDVI value does not correspond with similar stabilising effects of vegetation. This makes it difficult to relate a single NDVI value to an individual roughness coefficient since each vegetation type has its specific roughness (Baptist, 2005; Phillips and Tadayon, 2006). NDVI should, therefore, be tuned for specific applications and studies, such as a local NDVI scale for the Ayeyarwady River and another NDVI scale for the Rhine.

5.4 Bank retreat rates as a function of NDVI

The most promising results of the bank retreat analysis were found when separating the erosion mechanisms. Fluvial entrainment occurred at four of the nine inspected regions. The areas 2, 5, 7 and 8 were classified as gentle banks were fluvial entrainment was the primary erosion mechanism. The results showed that bank retreat rates decreased with increasing NDVI. The tipping point was located around an NDVI of 0.2. However, the fluvial entrainment was not considered as bank retreat. Besides, the effects of vegetation remain questionable. In the four areas, not much vegetation was observed. Furthermore, in area 8 for example, the points 8-12 showed decreased bank retreat (Figure B20), although the subsoil was invariable. This implies that the entrainment is much more dependent on location and hydraulic conditions than on a higher NDVI value. Since no vegetation was present, there is also no indication for vegetation stabilising riverbanks against fluvial entrainment, although decreased bank retreat rates were found (Figure 41 and Figure 42).

One critical note on all the results obtained is already partially mentioned, however, not fully addressed yet. The bank retreat rates are assumed constant, although it is understood that the time-averaged erosion rate differs from the momentary bank retreat rate. Bank retreat rates are probably higher during the rainy season than in the dry season. This variability is not taken into account. Moreover, NDVI depends on seasonality changes as well. Due to seasonality changes of vegetation, ageing processes or farmers that harvest their crops, vegetation (and therefore the NDVI) is not constant over a year on a specific location. The two deterministic values used for the analysis (bank retreat rate and NDVI) are as a matter of fact stochastic parameters. In this research, the NDVI on the date of 13 January 2014 is used, but the determined bank retreat rate does not occur necessarily on 13 January 2014. The actual moment of erosion and the momentary NDVI are not on the same date and on the same timescale. Bank retreat distances should be calculated over smaller time intervals, and NDVI should be updated accordingly to improve the results. When a riverbank (with or without vegetation) retreats, a 'new' NDVI value should be calculated of the remaining riverbank. Therefore in follow-up studies, this time-dependence of erosion rates and NDVI should be included.

VI

Conclusion

"I can't change the direction of the wind, but I can adjust my sails to always reach my destination." – Jimmy Dean

Figure 48 Two fishers hauling in their catch from the Ayeyarwady River. Also for them a stable river is desirable.

In this chapter, the conclusion of the research is presented. First, the sub-questions are answered, which together will lead to a concise answer to the research question. Also, a recommendation is given. In this recommendation, some suggestions for follow-up research are given. To complete the story, an advice is given to three specific stakeholders on how to use the results of this study.

The objective of this research was to investigate the effects of vegetation on riverbank stability. Relevant literature and existing knowledge about the influence of vegetation on hydrological and morphological processes have been discussed. To obtain a better understanding of the effects of vegetation, NDVI, an indicator used in remote sensing for the livelihood of vegetation, is investigated. Satellite images are used as primary source of information since up-to-date data of the Ayeyarwady River is lacking. Bank retreat rates are then compared with the NDVI to test whether NDVI can be used as vegetation indicator in river stability analyses and roughness prediction models.

What are the effects of vegetation on bank retreat rates and stability of riverbanks?

The different beneficial and detrimental effects of vegetation on riverbank stability were analysed in chapter 2. In general, the positive impact of vegetation is twofold: Firstly the increase in hydraulic resistance, causing (1) lower flow velocities, (2) diversion of flow into the main channel and (3) increased sedimentation within vegetated areas. Secondly, the presence of vegetation roots, resulting in a higher shear strength of the soil and a decrease of bank erosion. Flow deflection towards the opposite bank caused by vegetation is considered the most important negative effect since locally the bank retreat rates increase. This was also observed during the determination of the bank retreat rates to be relevant because the point bars were responsible for the bank retreat in the outer bends. The mid-channel and point bars in the Ayeyarwady River did not have much vegetation cover. Therefore, the bank retreat would also have occurred when there was no vegetation on the riverbanks and the point bars.

Regarding the specific effects of vegetation on the Ayeyarwady riverbanks, some remarks can be made. First, a large variety of vegetation types is present, which influences flow and sediment processes characteristically. Secondly, water level variability of twelve meters between the dry- and rainy season plays a crucial role in the evaluation of the net effects. The increase in hydraulic resistance provided by vegetation only plays a role when water is flowing over or through vegetation. During low water levels, steep riverbanks wear out from underneath, causing mass failure. Thirdly, roots fail to provide resistance against bank instability because the rooting depth is too small to prevent shearing of the soil. Therefore, the positive impact of the variety of vegetation on riverbank stability has not been proved during this research. Only during bank-full water levels, which are only present in August (Sloff, personal communication, 20 November 2017), vegetation can provide the beneficial effects, but have not been observed during the fieldwork.

Is the NDVI representative for the vegetation on riverbanks?

After understanding the various effects, the Normalised Difference Vegetation Index (NDVI) was analysed to validate the use of NDVI in river planform analyses. NDVI can predict the state of the vegetation on the riverbanks well. Multiple authors showed healthier vegetation to correspond with higher NDVI. Also on the Ayeyarwady riverbanks, unvegetated points showed low NDVI values, and vegetated banks showed high NDVI values, confirming that dense and healthy vegetation corresponds to higher NDVI values. It is difficult however to distinguish vegetation from the NDVI records only, supporting the statement of Xie et al. (2008). Similar NDVI values were found for different vegetation groups, e.g. trees and rice fields had comparable NDVI values, as was shown in Appendix C.

How are bank retreat rates and NDVI related?

Riverbank retreat rates were compared to NDVI records to quantify the effects of vegetation growing on riverbanks. As a measure of riverbank stability, lower bank retreat rates represent higher riverbank stability. Because of the beneficial effects of vegetation, it was expected that the retreat rates would decrease with increasing NDVI. Bank retreat was calculated with satellite images of Google Earth from 7 January 2014 and 11 January 2017.

Bank retreat rates of different locations were not comparable since different erosion mechanisms occurred. However, when areas with similar erosion mechanisms (mass failure and fluvial entrainment) were separated and the bank retreat rates of these regions compared, some trends could be identified. The areas where fluvial entrainment was the primary erosion mechanism showed a clear division. When NDVI was smaller than 0.2 maximum bank retreat rates appeared to be 200 meters per year. When NDVI was higher than 0.2 bank retreat rates of 80 meters per year were found. However, the role of vegetation was questionable since no vegetation could be observed on satellite images. Riverbank vegetation classes I and II showed similar behaviour, where classes III and IV did not show a reduction in bank retreat rates.

The significant reduction in bank retreat rates was also not found for areas where mass failure was the dominating erosion mechanism. Mass failure appeared to have considerable scatter in results. Toe erosion in combination with mass failure occurs regardless of vegetation present on the steep riverbank. A simple explanation is that NDVI does not explain the whole story behind riverbank retreat. Erosion and bank retreat rates are not only dependent on the presence of vegetation, but the hydrological impact and geological conditions also play a crucial role. In this thesis, the role of vegetation is quantified in terms of bank retreat rates, where the part of flow processes has only slightly been treated. Therefore a direct relation between decreased bank retreat rates and increasing NDVI is considered implausible.

Can NDVI be expressed as a hydraulic resistance parameter?

Different hydraulic roughness indicators have been discussed in chapter 2.2.5. Since in most research vegetation is represented by an (increase of the) roughness coefficient, the link between NDVI and roughness parameters was analysed. Various studies have tried to correlate the NDVI to physical properties of vegetation but found that NDVI cannot be used as a roughness parameter in numerical studies (Tang and Oki, 2006). However, as vegetation species can be distinguished from one another (Liu et al., 2012), hyperspectral remote sensing data become the standard (Chang, 2003) and NDVI relates with the 'greenness' of vegetation, NDVI can indicate vegetation density of a specific type. Using different sources, remote sensing provides significant information about the roughness of the subsoil, but NDVI alone is not yet able to give this. With a lot of research being done to different roughness coefficients dependent on vegetation density for different types of vegetation, it could be possible in the future to utilise NDVI as an input source for vegetation density estimations in predicting roughness coefficients (Hossain et al., 2007).

How is the Normalised Difference Vegetation Index related to the stabilising effects of vegetation on riverbanks?

An analysis of the different effects of vegetation gave no clear answer whether vegetation reduces riverbank retreat in the Ayeyarwady River. Also, the results of the bank retreat analysis showed significant scatter. The riverbanks subjected to mass failure showed no relationship, which is understandable when knowing that the riverbanks are retreating from underneath and the dense vegetation on top does not provide beneficial effects. The large scatter in the results of mass failure as primary erosion mechanism is a sign of high bank instability. Only riverbanks coping with fluvial entrainment showed reduced bank retreat rates with increasing NDVI, however, on satellite images, no vegetation was found at these regions. However, it is not possible to see which erosion mechanism takes place from the NDVI records only, and therefore riverbank stability is difficult to predict. For this research, it was possible to make some remarks about the effects of vegetation on riverbank stability because of the combined use of fieldwork and remote sensing. However, since it was noticed that various vegetation types characteristically influence hydrodynamic and morphological processes, and it was not possible to discriminate vegetation solely through NDVI records, NDVI does not seem to be an appropriate estimator for the additional effects of vegetation on riverbank stability.

Recommendation

A first recommendation is to apply this research method in other rivers. The limiting factor of this study appeared to be the high water level variability, causing large scatter in results due to the mass failure erosion mechanism. In other rivers, where water level variability does not prevail, the hypothesis can be tested better. This would also give a more precise answer whether bank retreat rates are reduced when NDVI is larger. This result was not explicitly found, because of lack of vegetation on the point bars. In line with this story, it is recommended to use the research method on smaller scales only. Nine extensive areas were examined, where it would have been better to test the use of NDVI on smaller scales, e.g. single bends or reaches of a couple of hundreds of meters. This would also improve the usability of the GEE script. The size and shape of the geometry for the determination of the NDVI can more easily be adjusted to the form of the riverbank and results will be more accurate. Another limiting factor was the cloud cover during the rainy season. Solutions to reduce cloud cover effects are given by Holben (1986), Verhoef et al. (1996), Roerink et al. (2000), Tang and Oki (2006) and Martinuzzi et al. (2007). Follow up research should, therefore, focus on cloud removal techniques for NDVI records, especially when a research area has a distinct rainy season where a lot of cloud cover is expected. Pre-processing of satellite images needs to be conducted before vegetation estimation.

A more general recommendation follows the work of Solari et al. (2015) who remarked that accretion is often not addressed in river models. As was seen in the determination of the bank retreat rates, the development of point and mid-channel bars was the driving mechanism for the bank retreat on the opposite bank. NDVI can play a role in this as well, as accreted land shows a higher NDVI value. When NDVI indicates vegetation on the point bar, it would mean that the accreted land is already stable for an extended period. This interaction between accretion and vegetation growth can be marked with the use of NDVI. Therefore the accretion of new land should be addressed more often, and the modelling of point bars in river models should be improved. This would also increase the understanding of the driving forces behind the erosion mechanisms. In this thesis, the story behind the force of the water has only slightly been treated. An estimate was made by comparing radii of curvature of river bends since sharper bends have a larger impact on the riverbanks. More information, such as hydrographs, soil data and water depths is necessary to complete the whole story.

Lastly, a real answer to the use of NDVI as a roughness predictor could not be found. In Table 11 some values for roughness coefficients were presented (Van Velzen et al., 2003). Although the vegetation types did vary, the roughness coefficients were about identical. This shows that is it difficult to represent vegetation with a single value. Properties of vegetation differ between and within vegetation groups, and even within a single plant or tree, characteristics will vary. The NDVI analysis showed no possibility to identify different vegetation types from records only, so satellite images need always to be used simultaneously. Since different vegetation types influence hydro- and morphodynamic processes in specific ways, it makes it difficult to relate a single NDVI value to a specific roughness coefficient. However, with a lot of research being done to different roughness coefficients for different types of vegetation, it could be possible to utilise NDVI as an input source for vegetation density estimations and predicting roughness coefficients (Hossain et al., 2007). For example, the relation between LAI and NDVI has frequently been investigated. According to Jalonen et al. (2013), LAI proved to be a useful indicator in estimating the strength of vegetation. This relation between LAI and NDVI can be further investigated, since LAI is also easily related to vegetation properties, such as vegetation density. Density can on its turn tell something about the roughness of the vegetation, which can be expressed in roughness coefficients that can be used in numerical models.

Last but not least a recommendation is given about how three of the most important stakeholders can use this research.

Researchers can use this research of the use of NDVI in hydraulic analyses as a stepping stone in follow-up research. The shortcomings have been described, suggestions for subsequent studies have been given already, so the focus should be on improving the use of NDVI. The importance of vegetation in natural rivers has been discussed for many decades, but the use of NDVI to describe this is new. The research of linking NDVI with roughness coefficients is probably most valuable and should, therefore, be extended.

Myanmar river engineers and the Directorate of Water Resources and Improvement of River Systems (DWIR) can apply this research to implement nature-friendly river measures. What happens nowadays is that small pieces of riverbanks get protected by embankments or cheap protection structures. That is only a temporary solution, and most importantly, the problem moves to another location. Moreover, farmers use the ‘temporary’ point bars for agriculture during low water and when the rainy season is approaching the farmers take their grown products, which leaves a vulnerable piece of land. This area erodes, is transported and causes further downstream instability due to a new point bar. River engineers and the DWIR should, therefore, map the use of the point bars and riverbanks better. The value of this free and widely available remote sensing techniques is vital for a country like Myanmar. Therefore, the researchers should share their improved knowledge with river engineers that can implement this in the Ayeyarwady River. One proposition is to plant vegetation, such as trees, bushes and grass, on point bars during low water to reduce sediment transport rates. By monitoring the developing vegetation on point bars, it is possible to stabilise river sections. NDVI can serve as an indicator which point bars develop well and grow into a stable riverbank. When river stability is maintained, the width will become more uniform, and the occurrence of point and mid-channel bars will decrease. When the flow is not diverted towards the riverbanks by the bars but deflected away by the vegetation towards the middle section of the river, the stability of the river will continuously improve.

Residents living near the Ayeyarwady River usually have no computer or internet access, for example, due to lack of money or the remote location of their houses. Therefore, distributing the findings of this research and transfer the knowledge to these people is problematic. Moreover, their understanding of the Ayeyarwady River is sufficient to deal with the dynamics of the river, as long as they can perform the daily tasks. The residents are usually not concerned with long-term planning. However, they will not be able to identify vulnerable locations where bank retreat threatens their living space. Nevertheless, from this study, it appeared that the steep riverbanks were unpredictable and very unstable. The advice for residents is to avoid building their houses near steep riverbanks, especially in outer bends of the river since the attack of the flow is largest. In dialogue with the river engineers and instances such as the DWIR residents should, therefore, be relocated to strategic locations, where at this moment people tend to move their houses based on their intuition. With the advice given by the river engineers, villages can become sustainable without the need to move, and in return, the inhabitants can maintain the nature-friendly river engineering measure, for example by letting the cattle graze the abundance of grassy vegetation. Through improved cooperation between these three stakeholders, the Ayeyarwady River is bit by bit stabilised, and a safer living environment is provided.

Bibliography

Abernethy, B., and Rutherford, I. D., 1998, Where along a river's length will vegetation most effectively stabilize streambanks?, Geomorphology, pp. 55-75.

Alavipanah, S. K., Matinfar, H. R., Rafiei Emam, A., Khodaei, K., Hadji Bagheri, R., and Yazdan Panah, A., 2010, Criteria of selecting satellite datafor studying land resources, Desert, 15, pp. 83-102.

Bakker, T., 2017, Dispersion in the Ayeyarwady river, additional thesis.

Bannari, A., Morin, D., Bonn, F., and Huete, A. R., 1995, A review of vegetation indices, Remote Sensing Reviews, 13(1), pp. 95–120.

Baptist, M. J., 2003, A flume experiment on sediment transport with flexible, submerged vegetation, Conference paper.

Baptist, M. J., 2005, Modelling floodplain biogeomorphology, doctoral thesis.

Baret, F., and Guyot, G., 1991. Potentials and limits of vegetation indices for LAI and APAR assessment, Remote Sensing of Environment, 35, pp. 161–173.

Barrios-Pina, H., Ramírez-Léon, H., Rodríguez-Cuevas, C., and Couder-Castaneda, C., 2014, Multilayer numerical modelling of flows through vegetation using a mixing-layer turbulence model, Water, 6, pp. 2084-2103.

Barsi, J. A., Lee, K., Kvaran, G., Markham, B. L., and Pedelty, J. A, 2014, The Spectral Response of the Landsat-8 Operational Land Imager, Remote Sensing, 6, pp. 10232-10251.

Bennett, S. J., Pirim, T., Barkdoll, B. D., 2002, Using simulated emergent vegetation to alter stream flow direction within a straight experimental channel, Geomorphology, 44, pp. 115-126.

Bennett, S. J., Wu, W., Alonso, C. V., and Wang, S. S. Y., 2008, Modelling fluvial response to in-stream woody vegetation: Implications for stream corridor restoration, Earth Surface Processes and Landforms, 33, pp. 890-909.

Bertoldi, W., Drake, N. A., and Gurnell, A. M., 2011, Interactions between river flows and colonizing vegetation on a braided river: exploring spatial and temporal dynamics in riparian vegetation cover using satellite data, Earth Surface Processes and Landforms, 36, pp. 1474-1486.

Bogaard, T. A., Rutten, M. M., Hut, R., 2017, Charting the Irrawaddy river with balloons and GPS trackers, Retrieved on 30 March 2017, Retrieved from *https://www.tudelft.nl/2017/tu-delft/charting-the-irrawaddy-river-with-balloons-and-gps-trackers/*

Boruah, S., Gilvear, D., Hunter, P., and Sharma, N., 2008, Quantifying channel planform and physical habitat dynamics on a large braided river using satellite data, River Research and Applications, 24(5), pp. 650-660.

Bouma, T. J., Van Duren, L. A., Temmerman, S., Claverie, T., Blanco-Garcia, A., Ysebaert, T., and Herman, P. M. J., 2007, Spatial flow and sedimentation patterns within patches of epibenthic structures: Combining field, flume and modelling experiments, Continental Shelf Research, 27, pp 1020-1045.

Camporeale, C., Perucca, E., Ridolfi, L., and Gurnell, A. M., 2013, Modelling the interactions between river morphodynamics and riparian vegetation, Reviews of Geophysics, 51, 379-414.

Cardno, C. A., 2016, Global satellite coverage improves flood mapping, Civil Engineering, Retrieved on 16 September 2017, Retrieved from *http://www.asce.org/magazine/20160105-global-satellite-coverage-improves-flood-mapping/*

Carroll, R. W. H., Warwick, J. J., James, A. I., and Miller, J. R., 2004, Modelling erosion and overbank deposition during extreme flood conditions on the Carson River, Nevada, Journal of Hydrology, 297, pp. 1-21.

Chang, C., 2003, Hyperspectral imaging, Techniques for Spectral Detection and Classification, Springer, Kluwer Academic/ Plenum Publishers, New York.

Chu, D., Lu, L., and Zhang, T., 2007, Sensitivity of Normalized Difference Vegetation Index (NDVI) to seasonal and interannual climate conditions in the Lhasa area, Tibetan plateau, China, Arctic, Antartic and Alpine Research, 39(4), pp.635-641.

Church, M., 1992, Channel morphology and typology, The rivers handbook, pp.126-143.

Climate Change Knowledge Portal, 2017, Retrieved on 6 March 2017, Retrieved from *http://sdwebx.worldbank.org/climateportal/index.cfm?page=country_historical_climate&ThisRegion=Asia&ThisCCode=MMR*

Commandeur, A., 2014, The Ayeyarwady river: A graphical introduction to Myanmar's main river, unpublished presentation.

Compositing and mosaicking, 2016, Retrieved on 6 June, 2017, Retrieved from *https://developers.google.com/earth-engine/ic_composite_mosaic*

Corenblit, D., Tabacchi, E., Steiger, J., and Gurnell, A. M., 2007, Reciprocal interactions and adjustments between fluvial landforms and vegetation dynamics in river corridors: a review of complementary approaches, Earth Surface Processes and Landforms, 34, pp. 1790-1810.

Cowan, W.L., 1956, Estimating hydraulic roughness coefficients, Agricultural Engineering, 37(7), pp. 473-475.

Crosato, A., 2008, Analysis and modelling of river meandering, doctoral thesis.

Dabney, S. M., Meyer, L. D., and McGregor, K. C., 1997, Sediment control and landscape modification with grass hedges, in Management of Landscapes Disturbed by Channel Incision, edited by Wang, S. S. Y., Langedoen, E. J., and Shields Jr., F. D., pp. 1093-1099.

Dapporta, S., Rinaldi, M., Casagli, N., and Vannocci, P., 2003, Mechanisms of riverbank failure along the Arno River, Central Italy, Earth Surface Processes and Landforms, 28, pp. 1303-1323.

Darby, S. E., and Thorne, C. R., 1996, Stability analysis for steep, eroding, cohesive riverbanks, Journal of Hydraulic Engineering, ASCE, 122, pp. 443-454.

Darby, S.E., 1999, Effect of riparian vegetation on flow resistance and flood potential, Journal of Hydraulic Engineering, 125(5).

Deltares, 2016, De big data revolutie in watermanagement, Retrieved on July 14, 2017, Retrieved from *https://www.deltares.nl/nl/blog/de-big-data-revolutie-in-water-management/*

Dietrich, W. E., and Smith, J. D., 1983, Influence of point bar on flow through curved channels, Water Resources Research, 19, pp. 1173-1192.

Dietrich, W. E., and Smith, J. D., 1984, Bed load transport in a river meander, Water Resources Research, 20, pp. 1355-1380.

Dijkstra, J. T., 2003, The influence of vegetation on scroll bar development, M.Sc. Thesis, Delft University of Technology.

Dijkstra, J. T., Uittenbogaard, R. E., and Stive, M. J. F., 2006, Modelling hydrodynamics in eelgrass (Zostera Marina) beds, Conference paper.

Donchyts, G., Baart, F., Winsemius, H., Gorelick, N., Kwadijk, J., and van de Giesen, N., 2016, Earth's surface water change over the past 30 years, *Nature Climate Change*, 6(9), pp. 810-813.

Elliot, A. H., 2000, Settling of fine sediment in a channel with emergent vegetation, Journal of Hydraulic Engineering, 126, pp. 570-577.

Fahti-Moghadam, M., Kashefipour, S. M., Ebrahimi, N. G., and Emamgholizadeh, S., Physical and numerical modelling of submerged vegetation roughness in rivers and flood plains, Journal of Hydraulic Engineering, 16(11), pp. 858-864.

Ferguson, R. I., 1987, Hydraulic and sedimentary controls of channel pattern, River Channels. Environment and Processes, pp. 129-158.

Google Earth Engine Developer's guide, 2017, Retrieved on 30 May 2017, Retrieved from *https://developers.google.com/earth-engine/*

Goward, S. N., Markham, B., Gye, D. G., Dulaney, W., and Yang, J., 1991, Normalized difference vegetation index measurements from the advanced very high resolution radiometer, Remote Sensing of Environment, 35(2-3), pp. 257-277.

Graham, S., 1999, Clouds and Radiation, Retrieved on 3 November 2017, Retrieved from *https://earthobservatory.nasa.gov/Features/Clouds/*

Gray, D. H., and Leiser, A. T., 1982, Biotechnical Slope Protection and Erosion Control, VanNostrand Reinhold, New York.

Gray, D. H., and Sotir, R. B., 1996, Biotechnical and soil bioengineering slope stabilization: A practical guide for erosion control, John Wiley and Sons Ltd, New York, United States.

Gurnell, A. M., and Petts, E. G., 2002, Island-dominated landscapes of large floodplain rivers, a European perspective, Freshwater Biology, 47, pp. 581-600.

Hickin, E. J, 1974, The development of meanders in natural river-channels, American Journal of Science, 274, pp. 414-442.

Hickin, E. J., 1984, Vegetation and river channel dynamics, The Canadian Geographer, 28, pp. 111-126.

Holben, B. N., 1986, Characteristics of maximum-value composite images from temporal AVHRR data, International Journal of Remote Sensing, 7(11), pp. 1417-1434.

Holton, J. R., 1979, Equatorial wave-mean flow interaction: A numerical study of the role of the latitudinal shear, Journal of the Atmospheric Sciences, 36, pp. 1030-1040.

Howard, A. D., 1984, Simulation model of meandering, in River Meandering, edited by Elliott, C. M., pp. 952-963, American Society of Civil Engineering, New York.

Huete, A. R., 1988, A soil adjusted vegetation index (SAVI), Remote Sensing of the Environment, 25, pp. 295-309.

Huete, A. R., 2015, Vegetation indices, Encyclopedia of Remote Sensing, Part of the series Encyclopedia of Earth Sciences Series, pp. 883-886.

Hupp, C. R. and Simon, A., 1991, Bank accretion and the development of vegetated depositional surfaces along modified alluvial channels, Geomorphology, (4), 111-124.

Hupp, C. R., 2000, Hydrology, geomorphology and vegetation of coastal plain rivers in the south-eastern USA, Hydrological processes, 14, pp. 2991-3010.

Hupp, C. R., and Osterkamp, W. R., 1996, Riparian vegetation and fluvial geomorphic processes, Geomorphology, 14, pp. 277-295.

Ikeda, S., Parker, G., Sawai, K., 1981, Bend theory of river meanders. I: Linear development, Journal of Fluid Mechanics, 112, pp. 363-377.

Jalonen. J., Järvelä, J., and Aberle, J., 2013, Leaf area index as vegetation density measure for hydraulic analyses, Journal of Hydraulic Engineering, 139(5), pp. 461-469.

Jung, M., Henkel, K., Herold, M., Churkina, G., 2006, Exploiting synergies of global land cover products for carbon cycle modeling, Remote Sensing of Environment, 101, pp. 534-553.

Justice, C. O., Townshend, J. R. G., Holben, B. N., and Tucker, C. J., 1985, Analysis of the phenology of global vegetation using meteorological satellite data, International Journal of Remote Sensing, 6(8), pp. 1271-1318.

Kirkby, M., 1995, Modelling the links between vegetation and landforms, Geomorphology, 13, pp. 319-335.

Kouwen, N., and Unny, T., 1973, Flexible roughness in open channels, Journal of the Hydraulics Division, 99(5), pp. 713-728.

Kouwen, N., Unny, T., and Hill, H.M., 1969, Flow retardance in vegetated channels, Journal of Irrigation and Drainage Division, 95(IR2), pp. 329-342.

Kummu, M., Lu, X. X., Rasphone, A., Sarkkula, J., and Koponen, J., 2008, Riverbank changes along the Mekong River: Remote sensing detection in the Vientane - Nong Khai region, Quarternary International, 186(1), pp. 100-112.

Langedoen, E. J., M.ASCE, and Simon, A., 2009, Modelling the evolution of incised streams II: Streambank erosion, Journal of Hydraulic Engineering, 135(6), pp. 476-486.

Lawler, D. M. (1995). The impact of scale on the processes of channel-side sediment supply: a conceptual model, in Effects of scale on interpretation and management of sediment and water quality: IAHS, 226, pp. 175-184.

Lawler, D. M., 1992, Process dominance in bank erosion systems, in Lowland floodplain rivers edited by Carling, P. A., and Petts, G. E., 117-59, Wiley, Chichester.

Lawler, D. M., 1993, The measurement of riverbank erosion and lateral channel change: A review, Earth Surface Processes and Landforms, 18, pp. 777–821.

Lewin, J., 1976, Initiation of bed forms and meanders in coarse-grained sediment, GSA Bulletin, 87(2), pp. 281-285.

Ligthart, D., 2017, The morphodynamic influencing processes in braided rivers: A case study on the Ayeyarwady river, master thesis.

Lillesand, T. M., Kiefer, R. W., and Chipman, J. W., 2004, Remote sensing and image interpretation, 5th edition, New York, Wiley.

Liu, H. Q., and Huete, A. R., 1995, A feedback based modification of the NDVI to minimize canopy background and atmospheric noise, IEEE Transactions on Geoscience and Remote Sensing, pp. 457-465.

Liu, D., Chen, J., Wu, G., and Duan, H., 2012, SVM-Based Remote Sensing Image Classification and Monitoring of Lijiang Chenghai, *2012 2nd International Conference on Remote Sensing, Environment and Transportation Engineering*, Nanjing, pp. 1-4.

Lokin, L. R., 2017, The influence of vegetation on flow and sediment transport mechanisms, master thesis.

Longitudestore, 2016, How to measure Latitude and Longitude, Retrieved on 14 July 2017, Retrieved from *http://longitudestore.com/how-big-is-one-gps-degree.html*

López, F., and García, M. H., 2001, Mean flow and turbulence structure of open-channel flow through non-emergent vegetation, Journal of Hydraulic Engineering, 125(5), pp. 392-402.

Lowrance, R. R., McIntyre, S., and Lance, C., 1988, Erosion and deposition in a field/ forest system estimated using Cesium-137 activity, Journal of Soil and Water Conservation, 43, pp. 195-199.

Macking, J. H., 1956, Cause of braiding by a graded river, Bulletin of the Geological Society of America, 67, pp. 1717-1718.

Martinuzzi, S., Gould, W. A., and Ramos González, O. M., 2007, Creating cloud-free Landsat ETM+ data sets in tropical landscapes: Cloud and cloud-shadow removal, Gen. Tech. Rep. IITF-32. Rio Piedras, PR: U.S. Department of Agriculture, Forest Service, International Institute of Tropical Forestry. 12 p.

Maurya, S. P., and Yadav, A. K., 2016, Evaluation of course change detection of Ramganga river using remote sensing and GIS, India, Weather and Climate Extremes, 13, pp. 68-72.

McKenney, R., Jacobson, R. B., Wertheimer, R. C., 1995, Woody vegetation and channel morphogenesis in low-gradient, gravel-bed streams in the Ozark Plateaus, Missouri and Arkansas, Geomorphology, 13, pp. 175-198.

Morison, J. R., O'Brien, M. P., Johnson, J. W., and Schaaf, S. A., 1950, The force exerted by surface waves on piles, Petroleum Transactions, American Institute of Mining Engineers, 189, pp. 149-154.

Mosselman, E., Shishikura, T., and Klaassen, G. J., 2000, Effect of bank stabilization on bend scour in anabranches of braided rivers, Physics and Chemistry of the Earth, 25, pp.699-704.

Nadler, C. T., and Schumm, S. A., 1981, Metamorphosis of South Platte and Arkansas rivers, eastern Colorado, Physical Geography, 2, pp. 95-115.

Nanson, G. C., 1980, Point bar and floodplain formation of the meandering Beatton River, Northeastern British Columbia, Canada, Sedimentology, 27, pp. 3-29.

Nanson, G. C., and Hickin, E. J., 1983, Channel migration and incision on the Beatton river, Journal of Hydraulic Engineering, ASCE, 109, pp. 327-337.

Nanson, G.C., Barbetti, M., and Taylor, G., 1995, River stabilisation due to changing climate and vegetation during the late Quaternary in Western Tasmania, Australia, Geomorphology, 13, pp. 145-158.

Nepf, H. M., 1999, Drag, turbulence and diffusion in flow through emergent vegetation, Water Resources Research, 35(2), pp. 479-489.

Nepf, H. M., and Vivoni, E. R., 2000, Flow structure in depth-limited, vegetated flow, Journal of Geophysical Research, 105, pp. 28547-28557.

Normalized Difference Vegetation Index, 2013, Retrieved on 17 October, Retrieved from *http://wiki.landscapetoolbox.org/doku.php/remote_sensing_methods:normalized_difference_vegetation_index*

O'Loughlin, C., and Ziemer, R. R., 1982, The importance of root strength and deterioration rates upon edaphic stability in steepland forests, Proceedings of I.U.F.R.O. Workshop P.1.07-00 Ecology of Subalpine Ecosystems as a Key to Management, Corvallis, Oregon State University, pp. 70-78.

Osman, A. M., and Thorne, C. R., 1988, Riverbank stability analysis. I: Theory, Journal of Hydraulic Engineering, 114.

Ottevanger, W., Blanckaert, K., and Uijttewaal, W. S. J., 2012, Processes governing the flow redistribution in sharp river bends, Geomorphology, 163, pp. 45-55.

Panda, S. S., Ames, D. P., and Panigrahi, S., 2010, Application of vegetation indices for agricultural crop yield prediction using neural network techniques, Remote Sensing, 2(3), pp. 673-696.

Partheniades, E., 1965, Erosion and deposition of cohesive soils, Journal of the Hydraulics Division, ASCE, v. 91, No. HY1, Proceedings paper 4202, pp. 105-139.

Pearson, R. L., and Millar, L. D., 1972, Remote mapping of standing crop biomass for estimation of the productivity of the short-grass Prairie, Pawnee National Grasslands, Colorado, Proceedings of the 8th International Symposium on Remote Sensing of Environment, Ann Arbor, MI, pp. 1357-1381.

Pettorelli, N., Vik, J. O., Mysterud, A., Gaillard, J. M., Tucker, C. J., and Stenseth, N. C., 2005, Using the satellite-derived NDVI to access ecological responses to environmental change, Trends in Ecology and Evolution, 20(9), pp. 503-510.

Phillips, J. V., Tadayon, S., 2006, Selection of Manning's roughness coefficient for natural and constructed vegetated and non-vegetated channels, and vegetation maintenance plan guidelines for vegetated channels in Central Arizona, U.S. Geological Scientific Investigations Report 2006-5108, 41 p.

PhysicsOpenLab, 2017, Retrieved on 23 June, 2017, retrieved from *http://physicsopenlab.org/2017/01/30/ndvi-index/*

Pinter, P. J., 1993, Solar angle independence in the relationship between absorbed PAR and remotely sensed data for alfalfa, Remote Sensing of Environment, 46, pp. 19-25.

Pinty, B., and Verstraete, M. M., 1992, GEMI: a non-linear index to monitor global vegetation from satellites, *Vegetatio*, 101(1), pp. 15-20.

Pollen-Bankhead, N., and Simon, A., 2009, Enhanced application of root-reinforcement algorithms for bank-stability modelling, Earth Surface Processes and Landforms, 34, pp. 471-480.

Pollen-Bankhead, N., and Simon, A., 2010, Hydrologic and hydraulic effects of riparian root networks on streambank stability: Is mechanical root-reinforcement the whole story?, Geomorphology, 16(3), pp. 353-362.

Qi, J., Chehbouni, A., and Huete, A. R., 1994, A modified soil adjusted vegetation index, *Remote Sensing of Environment*, 48, pp. 119-126.

Robinson, R. A. J., Bird, M. I., Nay Win Oo, Hoey, T. B., Maung Maung Aye, Higgitt, D. L., Lu, X. X., Aung Swe, Tin Tun, and Swe Lhaing Lin, 2007, The Irrawaddy river sediment flux to the Indian Ocean: The original Nineteenth century data revisited, The Journal of Geography, 115, pp. 629-640.

Roerink, G. J., and Menenti, M., 2000, Reconstructing cloudfree NDVI composites using Fourier analysis of time series, International Journal of Remote Sensing, 21(9), pp. 1911-1917.

Rominger, J. T., S.M.ASCE, Lightbody, A. F., A.M.ASCE, Nepf, H. M., A.M.ASCE, 2010, Effects of added vegetation on sand bar stability, Journal of Hydraulic Engineering, 136(12), pp. 994-1002.

Running, S. W., 1990, Estimating primary productivity by combining remote sensing with ecosystem simulation, edited by Hobbs, R. J., and Mooney, H. A., Remote sensing of biosphere functioning, Springer-Verlag, New York, pp. 65-86.

Schiereck, G. J. and Verhagen, H. J., 2012, Introduction to bed, bank and shore protection, 2nd edition.

Schumm, S. A., and Khan, H. R., 1972, Experimantal study of channel patterns, Bulletin of the geological society of America, pp. 1755-1770.

Schumm, S. A., and Lichty, R. W., 1963, Channel widening and floodplain construction along Cimarron River in Southwestern Kansas, U.S. Geological Survey Professional Paper 352D.

Schuurman, F., 2015, Bar and channel evolution in meandering and braiding rivers using physics-based modeling, Earth Sciences, 79, pp. 1-162.

Sha, Z., Bai, Y., Xie, Y., 2008, Using a hybrid fuzzy classifier (HFC) to map typical grassland vegetation in Xilinhe River Basin, Inner Mongolia, China, International Journal of Remote Sensing, 29(8), pp. 2317-2337.

Shields, A., 1936, Anwendung der Aehnlichkeitsmechanik und der Turbulenzforschung auf die Geschiebebewegung, Mitt. Preuss. Versuchsanst. Wasserbau Schiffbau, 26, 26.

Simon, A., 1999, The nature and significance of incised river channels, in Incised River Channels: Processes, Forms, Engineering and Management, edited by Darby, S. E. and Simon, A., pp. 3-18, John Wiley and Sons, London.

Simon, A., and Collison, A. J. C., 2002, Quantifying the mechanical and hydrologic effects of riparian vegetation on streambank stability, Earth Surface Processes and Landforms, 27(5), pp. 527-546.

Simon, A., Bennett, S. D., Neary, V. S., 2004, Riparian vegetation and fluvial geomorphology: Problems and opportunities, in Riparian vegetation and fluvial geormorphology, edited by Bennett, S. J., and Simon, A., Wiley, American Geophysical Union, Washington, D.C., pp. 1-10.

Smith, D. G., 1976, Effect of vegetation on lateral migration of anastomosed channels of a glacier meltwater river, GSA Bulletin, 87(6), pp. 857-860.

Solari, L., Van Oorschot, M., Belletti, B., Hendriks, D., Rinaldi, M., and Vargas Luna, A., 2015, Advances on modelling riparian vegetation-hydromorphology interactions. River Research and Applications, 32, pp. 164-178.

Su, Z., 2000, Remote sensing of land use and vegetation for mesoscale hydrological studies, International Journal of Remote Sensing, 21(2), pp. 213-233.

Sukhodolov, A. N., and Sukhodolova, T. A., 2010, Case study: Effect of submerged aquatic plants on turbulence structure in a lowland river, Journal of Hydraulic Engineering, 136(7).

Tal, M., and Paola, C., 2007, Dynamic single-thread channels maintained by the interaction of flow and vegetation, Geology, 35(4), pp. 347-350.

Tal, M., Gran, K., Murray, A. B., Paola, C., Hicks, D. M., 2004, Riparian vegetation as a primary control on channel characteristics in multi-thread rivers, in Riparian vegetation and fluvial geormorphology, edited by Bennett, S. J., and Simon, A., Wiley, pp. 1-10.

Tang, Q., and Oki, T., 2006, Daily NDVI relationship to cloud cover, Journal of Applied Meteorology and Climatology, 46(3), pp. 377-387.

Temmerman, S., Bouma, T. J., Govers, G., Wang, Z. B., De Vries, M. B., and Herman, P. M. J., 2005, Impact of vegetation on flow routing and sedimentation patterns: Three-dimensional modelling for a tidal marsh, Journal of Geophysical Research, 110, F04019.

Thorne, C. R., 1990, Effects of vegetation in riverbank erosion and stability, Vegetation and erosion, edited by Thornes, J. B., pp. 125-143, John Wiley and Sons, Chichester.

Thorne, C. R., and Lewin, J., 1979, Bank processes, bed material movement and planform development in a meandering river, in Adjustments of the fluvial system, edited by Rhodes, D. D., and Williams, G. P., Kendall/Hunt Publishing company, Dubuque, Iowa.

Tsujimoto, T., 1999, fluvial processes in streams with vegetation, Journal of Hydraulic research, 37, pp. 678-682.

Tucker, C. J., and Sellers, P. J., 1985, Satellite remote sensing of primary production, International Journal of Remote Sensing, 7(11), pp. 1395-1416.

USGS Landsat 8 Surface Reflectance, 2017, Retrieved on 16 October 2017, Retrieved from *https://explorer.earthengine.google.com/#detail/LANDSAT%2FLC08%2FC01%2FT1_SR*

Van De Wiel, M. J., and Darby, S. E., 2007, A new model to analyse the impact of woody riparian vegetation on the geotechnical stability of riverbanks, Earth Surface Processes and Landforms, 32(14), pp. 2185-2198.

Van der Velden, J., 2015, Understanding river dynamics of the Ayeyarwady river, master thesis.

Vargas Luna, A., 2016, Role of vegetation on riverbank accretion, doctoral thesis.

Vargas Luna, A., Crosato, A., Uijttewaal, W. S. J., 2012, Research on riverbank accretion, NCR days 2012 – The dutch approach: Blessing in disguise?

Verhoef, W., Menenti, M., and Azzali, S., 1996, A colour composite of NOAA-AVHRR- NDVI based on time series (1981–1992), International Journal of Remote Sensing, 17, pp. 231–235.

VPdelta, 2017, Partners voor Water: Innovaties voor slimme metingen in Myanmar, retrieved on 22 March 2017, Retrieved from *https://www.vpdelta.nl/nl/delta-story/partners-voor-water-innovaties-voor-slimme-metingen-in-myanmar*

Wu, F., Shen, H. W., M.ASCE, and Chou, Y., 1999, Variation of roughness coefficients for unsubmerged and submerged vegetation, Journal of Hydraulic Engineering, 125(9), pp. 934-942.

Wu, W., and He, Z., 2009, Effects of vegetation on flow conveyance and sediment transport capacity, International Journal of Sediment Research, 24(3), pp. 247-259.

Wu, W., Shields Jr., F. D., Bennett, S. J., and Wang, S. S. Y., 2005, A depth-averaged two-dimensional model for flow, sediment transport, and bed topography in curved channels with riparian vegetation, Water Resources Research, 41, W03015.

Wynn, T. M., Mostaghimi, S., and Alphin, E. F., 2004, The effects of vegetation on stream bank erosion, Annual meeting of the American Society of Agricultural and Biological Engineering, Paper No. 042226.

Xie, Y., Sha, Z., and Yu, M., 2008, Remote sensing imagery in vegetation mapping: a review, Journal of Plant Ecology, 1, pp. 9-23.

Zeimer, R. R., and Swanston, D. N., 1977, Root Strength Changes After Logging in Southeast Alaska, U.S.D.A. Forest Service, PNW Research Station, Portland, Oregon.

Appendices

Appendix A – Flow processes

As has been discussed in chapter 2, the flow of water is the destabilising force exerting on the riverbanks. The flow of water in a straight, open channel with a shallow rectangular cross-section can be described as a channel with infinite width. This can be described with the mass balance and the momentum balance equations. When water is considered as incompressible, the mass balance reduces to a volume balance, which is also known as the continuity equation. The continuity equation states that the volume through a cross-section does not change. This means that the discharge over a specific reach is constant. The momentum balance is a balance between inertia, forcing due to gravitation and the resistance imposed by the channel bed.

A.1 Steady, uniform flow

A flow is called steady if the velocity at any point in time does not change within the channel. If the flow is uniform, the velocity pattern is constant within a cross-section in the direction of the flow. If the current is steady and uniform, the surface slope of the water and the frictional slope of the river bed are equal, since inertia-effects are absent. The formulation for uniform flow originates from the remaining terms from the momentum balance, which are the frictional resistance force, supplied by the river bed, and the gravitational force in the streamwise direction, imposed by the slope. The most common form of this formulation is the Chézy equation, which is also known as Chézy's law for uniform flow:

$$u = C \cdot \sqrt{d \cdot i}$$

Where u is the flow velocity in the streamwise direction, C the Chézy coefficient, d is the water depth, and i is the bed slope. In steady, uniform flow the vertical velocity profile can be described as a logarithmic profile, with an average velocity at about 0.4 times the water depth from the bottom (Schiereck, 2012). The Chézy equation makes use of the Chézy coefficient, which is a smoothness coefficient rather than a roughness coefficient; the higher the value of C, the lower the roughness. In Figure A1 uniform flow is schematized. The velocity as a function of depth can be expressed in terms of the friction velocity (Holton, 1979):

$$u(z) = \frac{u_*}{\kappa} ln\left(\frac{z}{z_0}\right)$$

in which u_* is the friction velocity, κ the von Karman constant, z is the height above the bed, and z_0 the roughness height. This results in a logarithmic velocity profile over the depth.

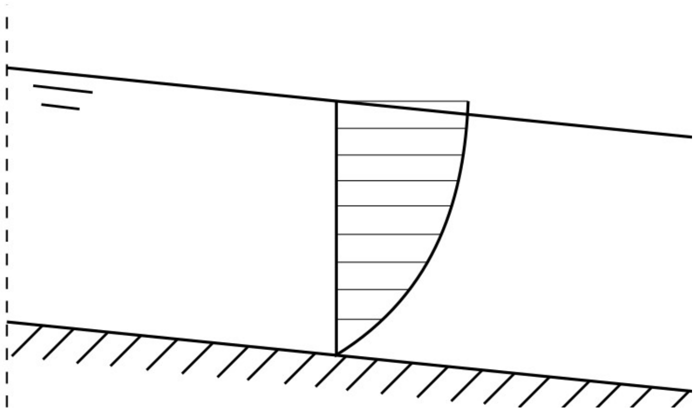

Figure A1 Uniform flow in a schematized river cross-section. Depicted is the logarithmic velocity profile, which can be described by Chézy's law.

A.2 Flow in a river channel

In practice, flow in a channel is never uniform. Variations in discharge, irregularities of the river bed, river tributaries, variable resistances or width changes are few examples that cause natural rivers to deviate from a uniform flow. River beds have different roughness characteristics, and in a straight stream, the current is therefore not uniformly distributed through the cross-section. Hence the flow is sloshing through the channel: it strikes the bank and is afterwards deflected to the opposite bank further downstream. Also, when flow lines converge (diverge) the flow velocity increases (decreases). Besides accelerations and decelerations of the flow, another situation arises, namely that the flow velocities adjust to the river bed. Chézy's law prescribes that depth-averaged velocities scale with the square of the flow depth, such that higher flow velocities tend to concentrate in the deeper parts of the cross-section (Dietrich and Smith, 1983). Finally, acceleration and deceleration cause, respectively, decrease and increase in turbulence intensity (Schiereck, 2012), which also has a significant contribution to the flow field in open channels.

When flow in a channel is being discussed, usually the primary flow is meant, which is the flow in streamwise direction. However, besides primary flow, secondary flow is present in natural rivers, often caused by objects, obstacles or irregularities where viscous forces exist. It is defined as the flow perpendicular to the streamwise, primary flow. The secondary flow is the result of a force balance between the centrifugal force and a pressure force. The secondary flow includes all variations from the primary flow field in longitudinal and transverse directions. The combined effect of secondary flow and flow concentration makes the outer bends of rivers vulnerable to erosion, whereas inner bends are imposed to sedimentation. However, it is not the spiralling motion of the flow that erodes the outer bank; the secondary flow increases the loads on the riverbank by modifying river geometry into a shallower and a deeper part (Ottevanger et al., 2012).

For the description of water in a channel, it was assumed the channel to have an infinite width, which in practice is not the case. The momentum and mass balance often need additional terms for various situations or different reaches on specific process scales. Furthermore, the presence of non-uniform, unsteady flow, turbulence, secondary flows and fluctuating discharge levels causes different flow fields and additional stresses on riverbed and banks, and therefore other erosion- and sedimentation rates when compared to the steady, uniform flow.

Appendix B – Determining bank retreat rates and NDVI of the Ayeyarwady River

In this Appendix, the bank retreat rates are determined, and it is researched whether vegetation, represented by Normalised Difference Vegetation Index (NDVI), influences it. From the Aquamonitor, nine locations within the research area are selected that showed bank retreat, which are indicated in Figure B1 and Figure B2. The locations and characteristics are summarised at the beginning of each area description. The bank retreat rates are determined with Google Earth by comparing riverbanks of different years with each other. Also, the NDVI of the different areas along the riverbank is determined, and plotted in figures. The NDVI is presented on the horizontal axis and the calculated bank retreat rates on the vertical axis. Bank retreat is assumed as positive values. In this analysis, it is tested whether a higher NDVI results in lower bank retreat rates.

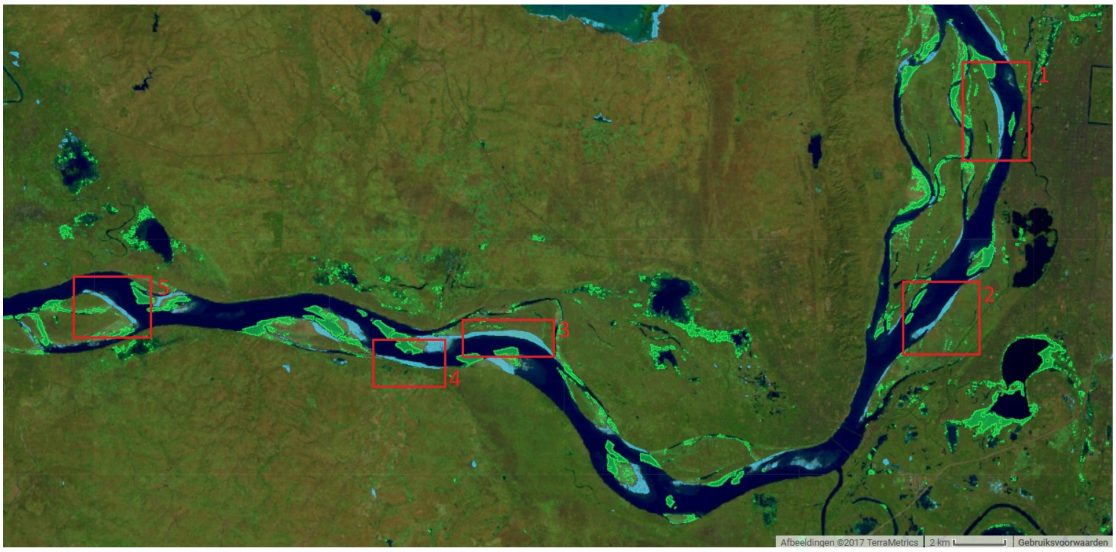

Figure B1 River reach around Mandalay (near area 1). The five research areas are highlighted in red.

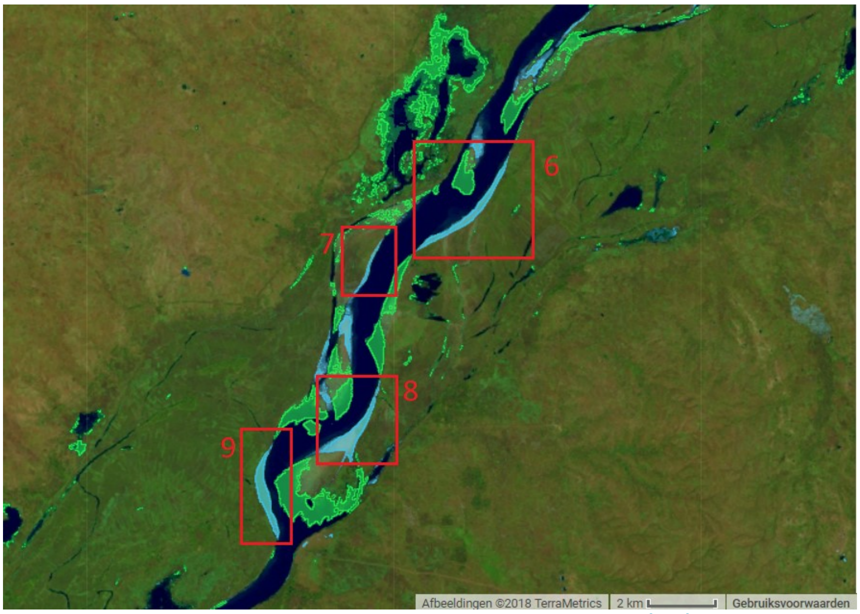

Figure B2 The Ayeyarwady river further downstream, with the other research areas (6-9).

In the next section, all different areas are discussed separately, and each riverbank is shown in Google Earth as a path. All figures date from the year 2014, so that the original riverbank is clearly visible. The blue lines represent the riverbank in 2014; the yellow lines represent the riverbank in 2017. The numbered points in the figures are the coordinates. For each different figure, an analysis is given with the most noteworthy details. In Table B1 background information about the Google Earth satellite images data is presented. Also, the number of coordinates and the date on which the NDVI is calculated are given.

Table B1 Table with information of the data of the satellite imagery, the number of coordinates per area and the date of NDVI values retrieved.

Area	Date of original riverbank	Compared with riverbank at	Number of coordinates	Date of NDVI
1	07/01/2014	11/01/2017	11	13/01/2014
2	07/01/2014	20/12/2016	17	13/01/2014
3	07/01/2014	11/01/2017	8	13/01/2014
4	07/01/2014	11/01/2017	10	13/01/2014
5	02/02/2014	11/01/2017	13	13/01/2014
6	15/02/2014	02/01/2017	19	13/01/2014
7	15/02/2014	02/01/2017	19	13/01/2014
8	15/02/2014	02/01/2017	12	13/01/2014
9	15/02/2014	22/01/2017	17	13/01/2014

Area 1

Table B2 Characteristics of area 1.

Characteristics area 1	
Location	Inner bend
Average NDVI	0.439
NDVI range (min-max)	0.2 - 0.574
Average bank retreat rate	55.7 m/yr
Erosion mechanism	Toe erosion and mass failure
Reason for bank retreat	Propagating mid-channel bar
Riverbank	Steep

Area 1 is located next to Mandalay, the start point of the fieldwork, on the opposite riverbank. Although this section is located in the inner bend, the last couple of years erosion has caused the bank to retreat, see Figure B3. The mid-channel bar (situated around points 1-4) pushes the flow towards the inner bend, causing inner bend erosion. From satellite images, it is noticed that the mid-channel bar originated in 2014 and propagated after each river flood downstream in the flow direction (towards points 9-11 in 2017). It is therefore expected, that when the bar propagates further downstream in coming years, bank retreat will also occur downstream of point 11.

Figure B3 Area 1 - Comparison riverbanks 7 January 2014 with 11 January 2017.

The steep riverbanks indicate that the primary erosion mechanism is toe erosion, after which mass failure takes place. In this thesis, steep riverbanks are defined as vertical riverbanks, such as shown in Figure B4 and Figure B5. Gentle or mild sloped banks are defined as banks with a slope, e.g. the slopes on the background on Figure 1, although these slopes are still relatively steep. The grassy vegetation does not help to prevent toe erosion at this location, however, during high water, vegetation of that size has significant impact on the diversion of flow and the stability of the riverbank. The vegetation height proves that the vegetation is present for already multiple years, indicating that it can withstand high water levels and fluvial entrainment.


Figure B4 Riverbank in area 3. Note the length of the vegetation with regard to the length of the human.


Figure B5 Grassy vegetation on this riverbank is not able to prevent toe erosion and mass failure.

When analysing the NDVI values, it shows a broad range of values (0.2-0.574), however, vegetation is quite uniform in species and space. Figure B6 shows a significant scattering of the points and the hypothesis is not confirmed here since points with high NDVI still have high bank retreat rates.

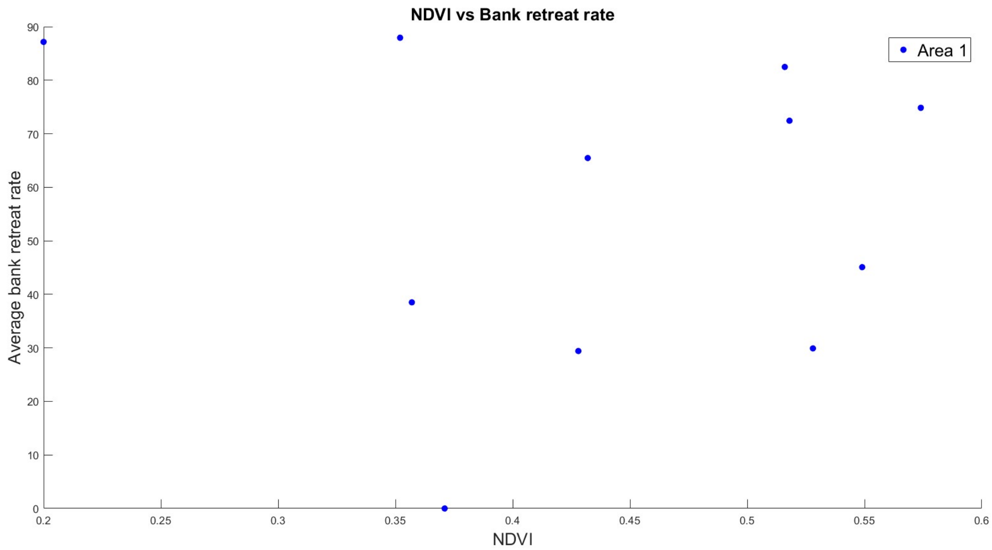

Figure B6 Bank retreat rate as a function of the NDVI for area 1.

Area 2

Table B3 Characteristics of area 2.

Characteristics area 2	
Location	Meandering river section
Average NDVI	0.270
NDVI range (min-max)	0.045 - 0.489
Average bank retreat rate	27.3 m/yr
Erosion mechanism	Fluvial entrainment
Reason for bank retreat	Sediment ‘pulsing’ through the river
Riverbank	Mainly steep

The second area shows significant riverbank retreat, especially in the lower reach of the area, where a sandy material is present, shown in Figure B7. When looking at the middle part of this section, there is no bank retreat. This is also the reason that the average bank retreat rate is lower compared to area 1. One reason for that is the presence of the point bar, that contributes to the deflection of flow away from the riverbank. The whole floodplain submerges during high water, and the bank gets attacked. However, the point bar provides some protection from the direct attack of water, especially during lower water levels. From point 12, there is a nearly uniform amount of bank retreat. It appears, especially in this section, that large amounts of sediments propagate downstream like a ‘pulse’ during high discharges. After an analysis of satellite images, it is expected that the eroded area from point 12-17 will be replenished by the propagating point bar between points 5 and 11. Therefore, this section is not subjected to bank erosion, but rather to an evolving riverbank dependent on sediment availability. Interesting is that the two rocky hills constrict the end of this river reach (downstream of point 17) and that the riverbanks do not retreat. This narrowing causes high flow velocities, and therefore large water depths (Sloff, personal communication, 20 November 2017). Because of the fixed end provided by the stable mountain ridge and the weaker soil upstream, this reach has shown very dynamic behaviour in the past. The movement was limited by the mountain ridge at the left side and the elevated embankment at the right, protecting the city.

In Figure B8 the bank retreat rates as a function of NDVI are scattered as well. The range between NDVI values is larger than in the first area, mainly because of the presence of the point bar (sandy material). Bank retreat rates are comparable between area 1 and area 2, although this section is not located in an inside bend. The average bank retreat rate over this reach is less compared to area 1, because of the stable middle section, and not because of higher NDVI values. The highest bank retreat rates are found in the top left corner of Figure B8, which are the points representing the sandy edge near points 14-17.

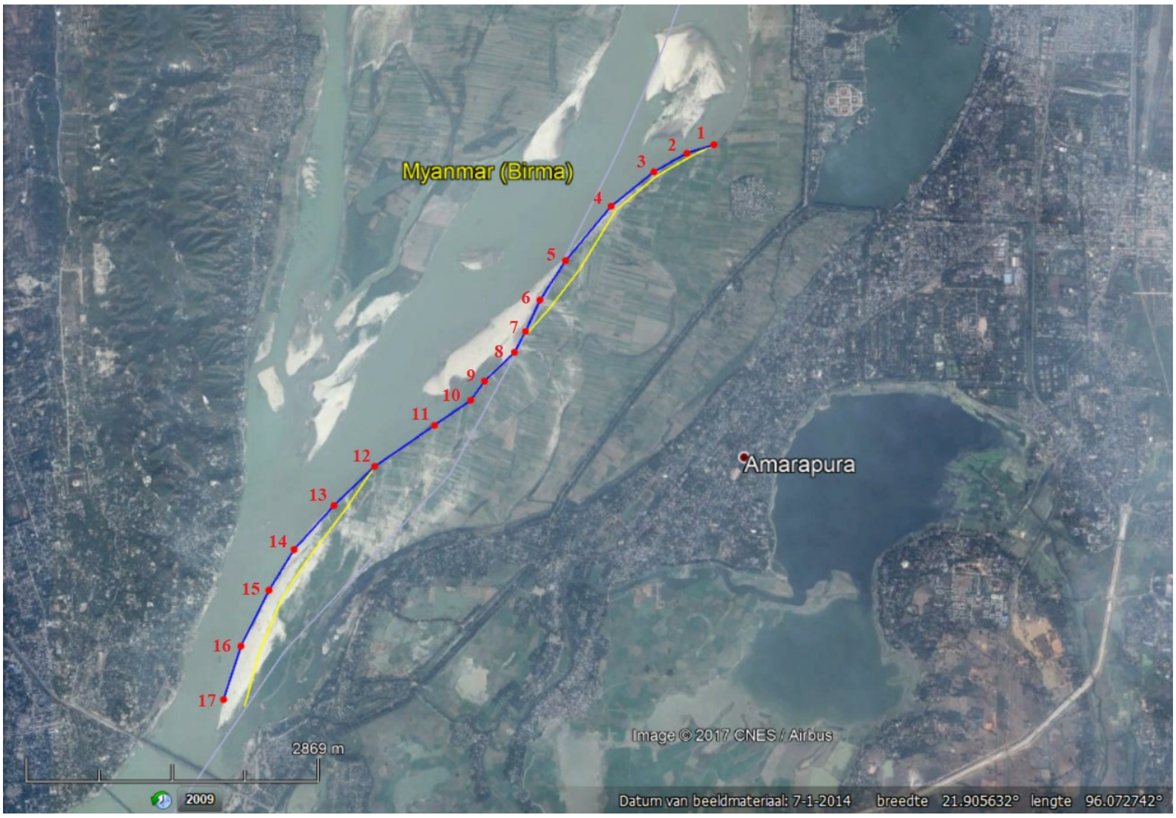

Figure B7 Area 2 - Comparison riverbanks 7 January 2014 with 20 December 2016.

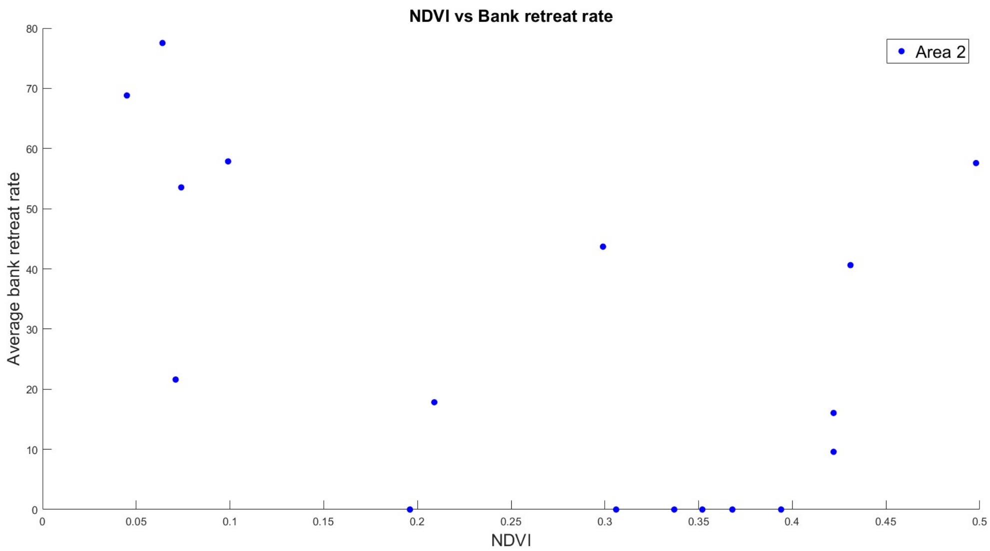

Figure B8 Bank retreat rate as a function of the NDVI for area 2.

Area 3

Table B4 Characteristics of area 3.

Characteristics area 3	
Location	Outer bend
Average NDVI	0.367
NDVI range (min-max)	0.182 - 0.610
Average bank retreat rate	74.3 m/yr
Erosion mechanism	Toe erosion and mass failure
Reason for bank retreat	Formation of inner bend point bar deflecting flow towards outer bank
Riverbank	Steep
Radius of curvature	Approx. 1000 meters

This area is characterised by continuous bank retreat, which is visible in Figure B9. The formation of the inner bend point bar caused the flow to be directed outwards. The figure shows a gradual retreat of the riverbank and is a textbook example of bank retreat in an outer bend. Area 3, 4, 6, 7, 8 and 9 are all located in an outer bend. To compare the different bank retreat rates between the areas, the radii of curvature are investigated as well, together with the development of the point bars causing flow deflection. The radius of curvature of this bend is approximately 1000 meters. This radius has increased to 1300 meters in 2017.

From the satellite image (Figure B9), it can be seen that the subsoil shows similar features, however, the NDVI records vary within a wide range (0.812-0.610). This is visible in Figure B10. The points seem to be contradictory from the hypothesis. It seems that with increasing NDVI, bank retreat rates also increase, except for point 8 (NDVI = 0.610). The average NDVI is large when compared to all other areas, however, bank retreat rates are also relatively large. The large bend radius can be the reason for that.

Figure B9 Area 3 - Comparison riverbanks 7 January 2014 with 11 January 2017.

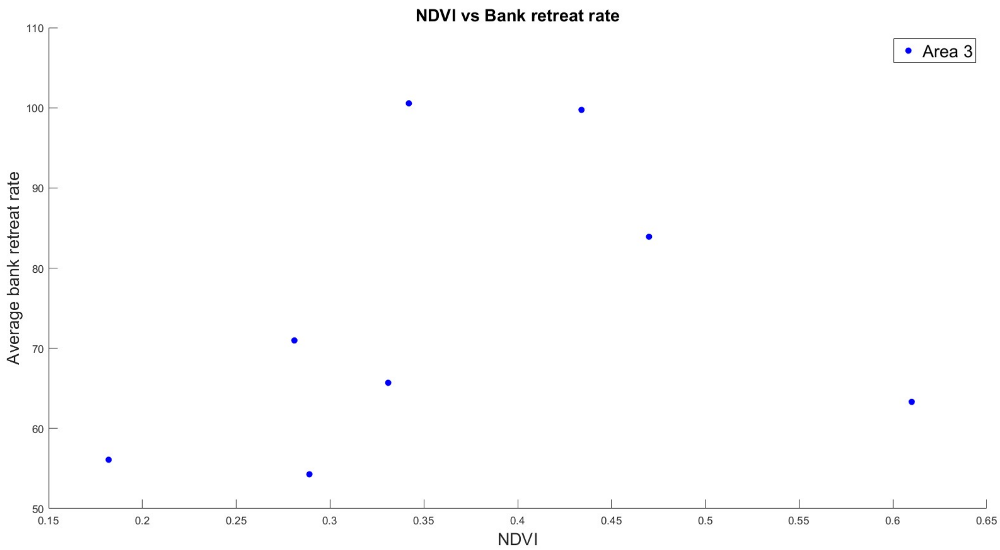

Figure B10 Bank retreat rate as a function of the NDVI for area 3.

Area 4

Table B5 Characteristics of area 4.

Characteristics area 4	
Location	Outer bend
Average NDVI	0.245
NDVI range (min-max)	0.130 - 0.409
Average bank retreat rate	33.5 m/yr
Erosion mechanism	Toe erosion and mass failure
Reason for bank retreat	Mid-channel bar deflecting flow towards outer bank
Riverbank	Steep
Radius of curvature	Approx. 550 meters

Although not explicitly visible in Figure B11 this area is located in the opposing outer bend following area 3. The erosion mechanisms are similar, and both areas have steep riverbanks. However, the average NDVI values differ 10%, and bank retreat rates are twice as large in area 3 compared to area 4. The NDVI values, as well as the bank retreat rates, are lower in area 4, therefore not supporting the hypothesis. The reason could be that area 3 is located in a sharper bend, indicating higher hydraulic loads due to curvature effects. Especially when the radii of the two curves are compared, this seems to be the cause. This radius is only 550 meter, which is approximately half of the radius in area 3. Finally, when the maximum bank retreat rates between the two areas are compared, it is noticed that these are located in the narrowest part (both points 5 in Figure B9 and Figure B11). It is obvious that bank retreat rates are not only dependent on NDVI, but also on location and the surrounding conditions.

Figure B11 Area 4 - Comparison riverbanks 7 January 2014 with 11 January 2017.

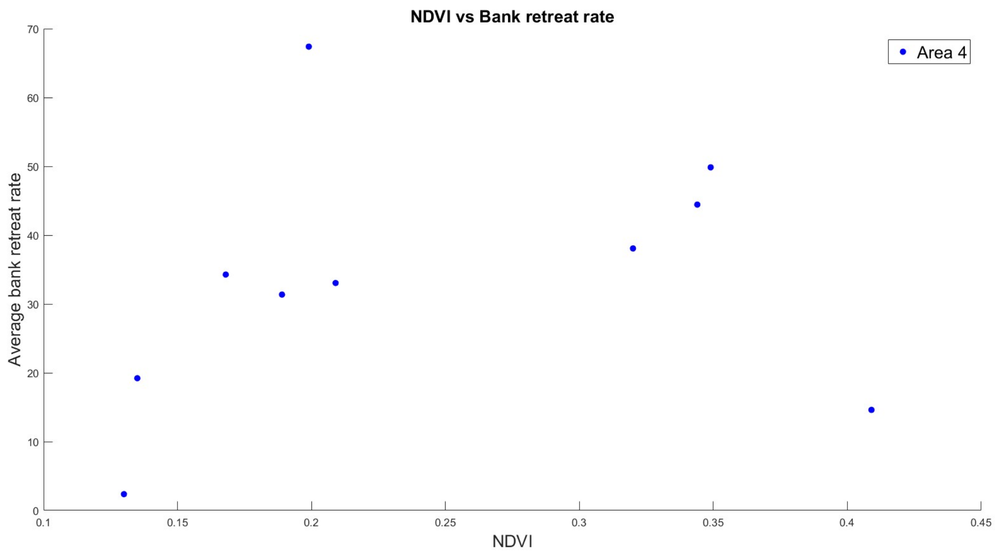

Figure B12 Bank retreat rate as a function of the NDVI for area 4.

Also, Figure B12 does not support the hypothesis, where an increasing trend is observable. This was also the case in Figure B10, so it seems that similar conditions show the same behaviour.

Area 5

Table B6 Characteristics of area 5.

Characteristics area 5	
Location	Head of a large bar
Average NDVI	0.018
NDVI range (min-max)	-0.156 - 0.111
Average bank retreat rate	100.2 m/yr
Erosion mechanism	Fluvial entrainment
Reason for bank retreat	Sediment ‘pulsing’ through the river
Riverbank	Flat area

Area 5 is subjected to a large amount of bank retreat. However, this bank retreat is mostly caused by sediment deposits against the head of a bar in 2014, which in the subsequent three years were transported further downstream. In Figure B13, it is shown that this head of the bar contains no vegetation at all, proving that it is recently deposited. From the low (negative) NDVI values can be observed that this part of the bar is often flooded, and the large bank retreat rates (order 100 meters per year) show that the material is easily being transported by fluvial entrainment.

Figure B13 Area 5 – Comparison riverbanks 2 February 2014 with 11 January 2017.

However, the riverbank showed some striking characteristics observed during the fieldwork, shown in Figure B14. There are two distinct regions discernable, namely the flat, lower, unvegetated part and a higher, vegetated part. It is expected that the grassy cover provided the subsoil additional strength and therefore remained more elevated, similar to area 1. This could raise the question whether the grassy cover that used to be on the lower part is washed away during a flood, or whether this sandy subsoil is just the result of sedimentation and gets transported in subsequent floods. The exposed part of this area is apparently eroded to a lower level during high flow velocities that the vegetated area could endure, resulting in the pattern in Figure B14.

Figure B14 Two different elevations in the Ayeyarwady river; a higher vegetated area and a lower unvegetated area.

When Figure B15 is considered, it shows relatively low scatter. The range of the NDVI is minimal, which is to be expected with the sandy cover. Therefore, the results in the graph cannot be ascribed to the effect of vegetation since it is absent.

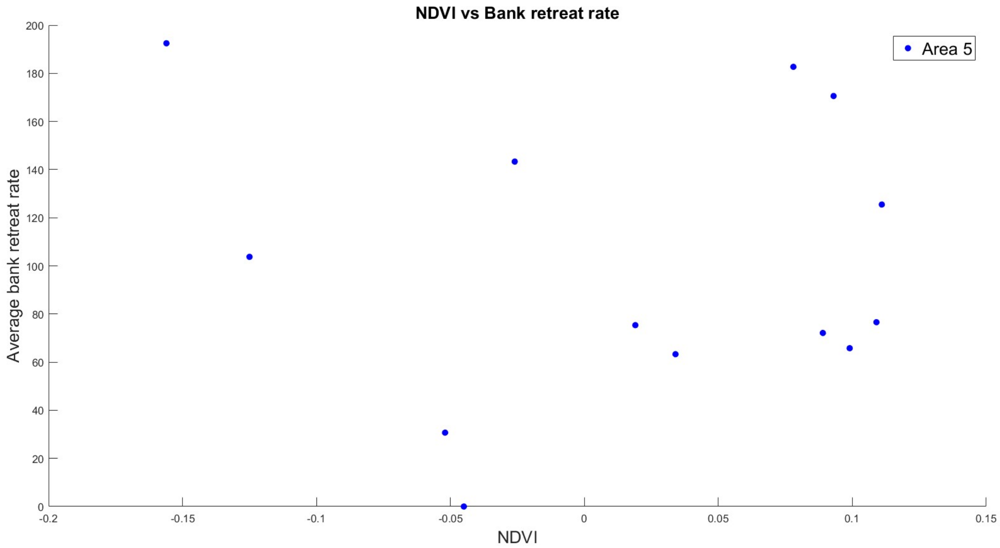

Figure B15 Bank retreat rate as a function of the NDVI for area 5.

Area 6

Table B7 Characteristics of area 6.

Characteristics area 6	
Location	Outer bend
Average NDVI	0.125
NDVI range (min-max)	-0.095 - 0.533
Average bank retreat rate	68.3 m/yr
Erosion mechanism	Toe erosion and mass failure
Reason for bank retreat	Point bar deflecting flow towards outer bank
Riverbank	Combination steep banks and flat area
Radius of curvature	Approx. 550 meters

Area 6 is a small meandering section of the Ayeyarwady River, showing point bar growth and outer bend erosion, shown in Figure B16. The radius of curvature was approximately 550 meter in 2014. The points 1-5 are protected from bank retreat by the northern point bar. However, on the opposite (left) bank, another point bar is present. This example shows very well how the point bar is responsible for pushing the flow towards the right riverbank. From point 5 significant bank retreat is present. The amount of bank retreat increases with the influence from the point bar, and after the bank retreat reaches a maximum (point 14), the bar push effect gradually decreases and bank retreat rates decline. This shows how the surrounding circumstances are responsible for the amount of bank retreat. Also, in this example, a distinction can be made between vegetated areas (5-12) and (17-19) and a flat, bare, sandy area (13-16).

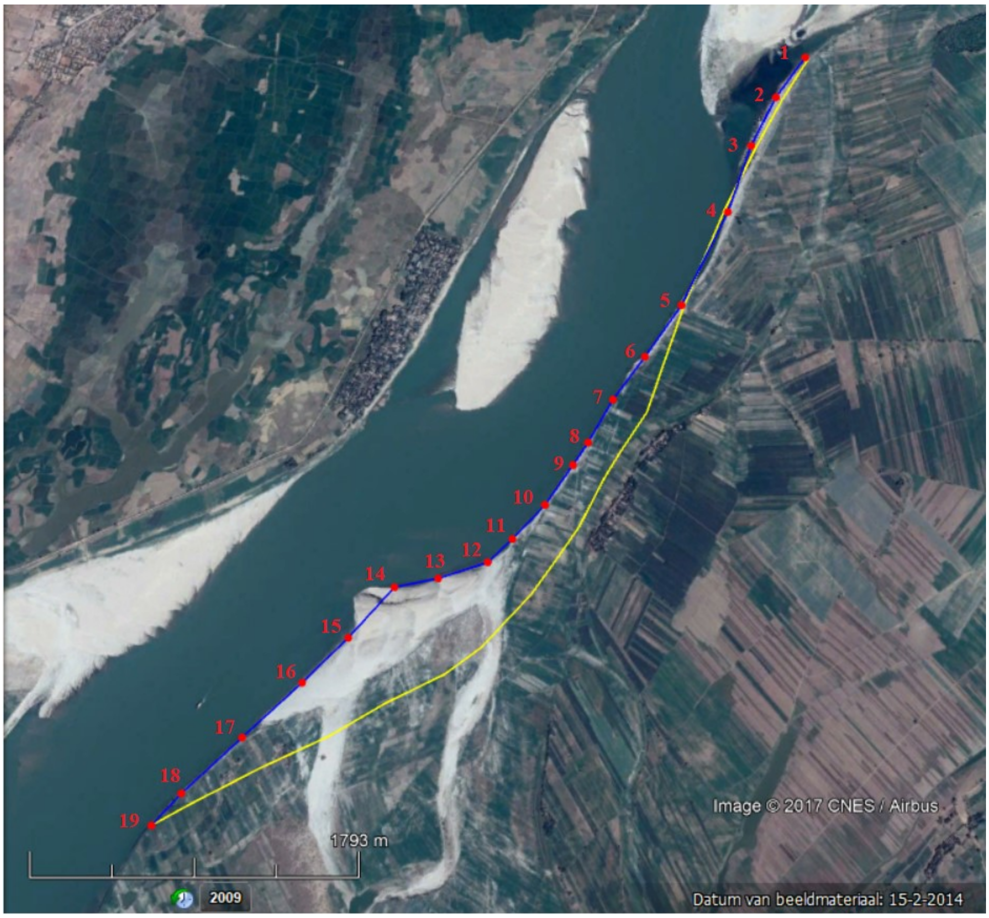

Figure B16 Area 6 – Comparison riverbanks of 15 February 2014 with 2 January 2017.

In Figure B17 there are a lot of points with an NDVI lower than 0.2. The range in bank retreat rates between these points is large. However, there seems to be a declining bank retreat rate with increasing NDVI. There are unfortunately too few points with high NDVI to fully support this statement. It is interesting to see that the bank retreat rates of the sandy part are much larger than the two vegetated parts. However, this could also be the result of the 'pulsing mode' of the river, causing the point bars to propagate downstream.

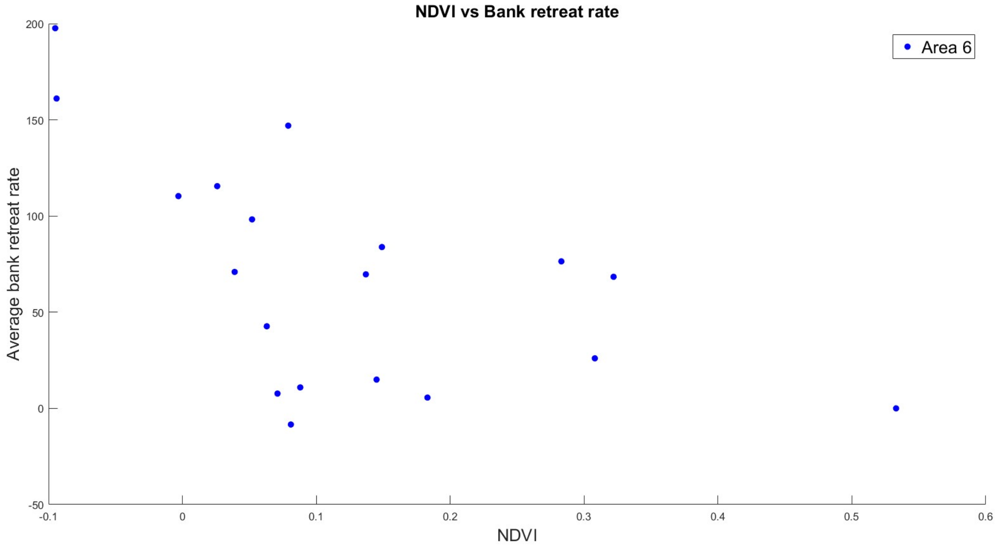

Figure B17 Bank retreat rate as a function of the NDVI for area 6.

Area 7

Table B8 Characteristics of area 7.

Characteristics area 7	
Location	Outer bend, flood plain
Average NDVI	0.264
NDVI range (min-max)	0.058 - 0.533
Average bank retreat rate	46.5 m/yr
Erosion mechanism	Fluvial entrainment
Reason for bank retreat	Outer bend erosion
Riverbank	Mostly gentle
Radius of curvature	Approx. 800 meters

Area 7 is the subsequent bank on the opposing site of area 6 and shown in Figure B18. This area located in the outer bend is a floodplain, so a large part of this area is flooded with high water. This floodplain lends itself to the comparison of a vegetated and unvegetated bank section within one reach. The first (points 3-8) and the last part (points 14-19) are unvegetated sections. In the middle segment (9-13) vegetation is present. The radius of curvature is approximately 800 meters, so it is a sharper bend than in area 6.

Figure B18 Area 7 - Comparison riverbanks of 15 February 2014 with 2 January 2017.

In Figure B19 the hypothesis seems to be correct, where four points (1, 2, 3 and 8) with a high NDVI show no bank retreat. The other locations with vegetation show similar bank retreat rates, which are lower than the unvegetated points. High bank retreat rates are observed with a low NDVI. The ten points with an NDVI smaller than 0.2 are the unvegetated numbers. This is in correspondence with area 6. Although the NDVI is constant, there is large variability in bank retreat rates. This means that not only vegetation, in the form of higher NDVI values, plays a role, but the location of flow attack is just as important. It is also possible that points 14-19 erode because of the opposite point bar that is deflecting the flow towards the outer bend, creating a similar situation as in areas 1, 3, 4 and 6.

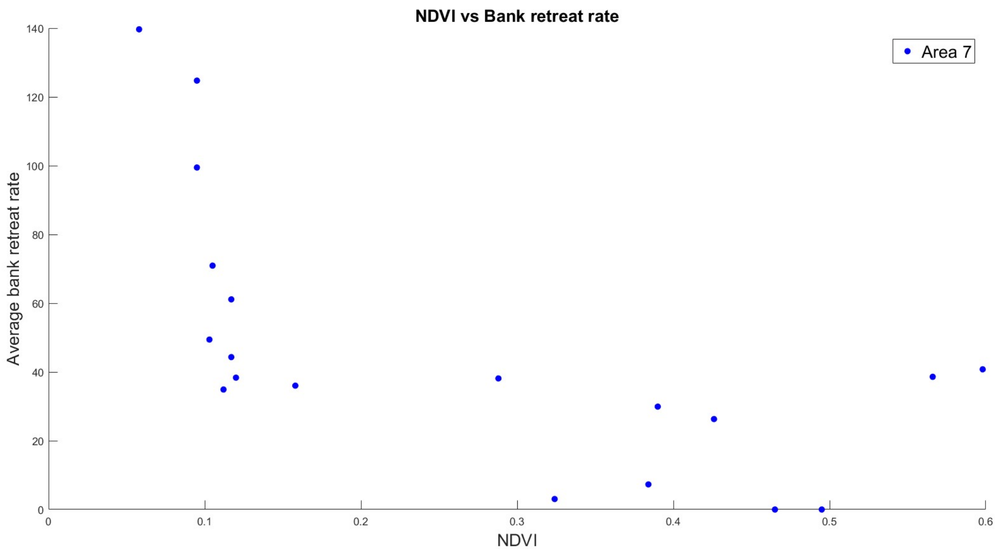

Figure B19 Bank retreat rate as a function of the NDVI for area 7.

Area 8

Table B9 Characteristics of area 8.

Characteristics area 8	
Location	Outer bend
Average NDVI	0.176
NDVI range (min-max)	0.010 - 0.645
Average bank retreat rate	100.2 m/yr
Erosion mechanism	Fluvial entrainment
Reason for bank retreat	Outer bend erosion
Riverbank	Flat area
Radius of curvature	Approx. 900 meters

In Figure B20 it is visible that also in this area the bank retreat is mainly determined by the opposite point bar, which deflects the flow towards the outer riverbank. This river bend is quite sharp, which can be the reason for the large bank retreat rate. Similar to area 3 and area 6, the maximum bank retreat can be found in the centre of the river bend. It is no coincidence that the material is sandy. Similar as in locations 2, 5, 6 and 7 the sediment is settled at a wider reach after being transported through the river. During subsequent floods, the sediment is transported further. This is, as stated before, not considered as bank retreat, but as the pulsing mode of the river sediment transport.

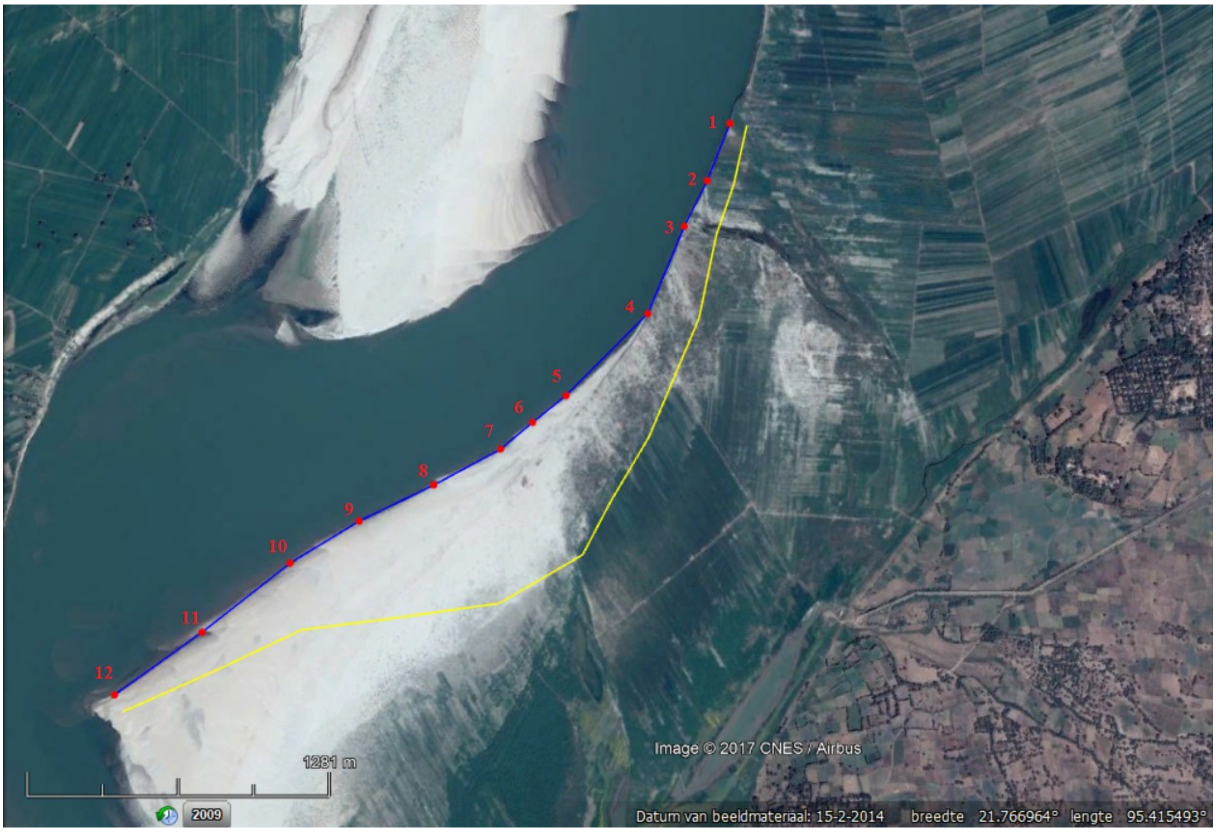

Figure B20 Area 8 - Comparison riverbanks of 15 February 2014 with 2 January 2017.

Figure B21 shows a similar trend as Figure B17 and Figure B19. However, the reduction of NDVI cannot be ascribed to vegetation, since it is not present (Figure B20).

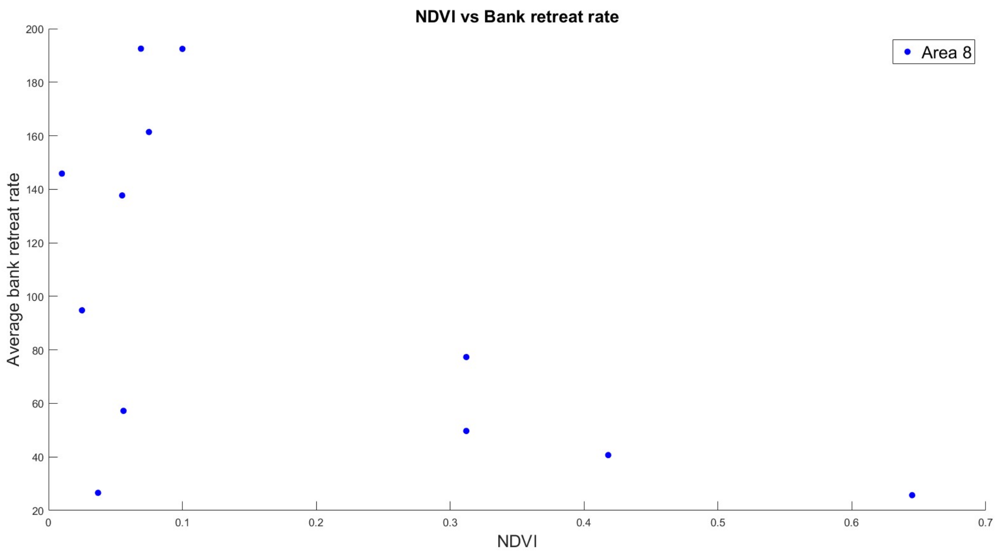

Figure B21 Bank retreat rate as a function of the NDVI for area 8.

Area 9

Table B10 Characteristics of area 9.

Characteristics area 9	
Location	Outer bend
Average NDVI	0.488
NDVI range (min-max)	0.150 - 0.709
Average bank retreat rate	102.0 m/yr
Erosion mechanism	Toe erosion and mass failure
Reason for bank retreat	Formation of inner bend point bar deflecting flow towards outer bank
Riverbank	Steep banks
Radius of curvature	Approx. 850 meters

In area 9 there is some significant bank retreat in the outer bend, Figure B22. The bank retreat rates between points 5 and 15 are contributing to the largest average bank retreat rate in this analysis. A large portion of the riverbank is eroded away as a result of the expanding point bar on the other side of the river. This point bar deflects the flow towards the bank, pressuring the opposite riverbank. Note also the small village in the lower left corner of Figure B22, that starts to experience hindrance because of the riverbank bank retreat. In a couple of years, it is necessary to move their houses.

Figure B22 Area 9 - Comparison riverbanks of 15 February 2014 with 2 January 2017.

Figure B23 and Figure B24 show the conditions of the riverbank in area 9. It is quite unusual that with so much vegetation present, the riverbank is susceptible to bank retreat. Next to the numerous trees, also smaller vegetation is present and it was expected that this combination would provide sufficient strength to prevent erosion. Apparently the force of the flow of water is too strong for the riverbank to remain stable. A contributing factor is the sharp bend.

Figure B23 Large amount of vegetation does not stop bank retreat of the riverbank.

Figure B24 The vegetation on top does not reach the toe of the bank, causing toe erosion to erode the riverbank.

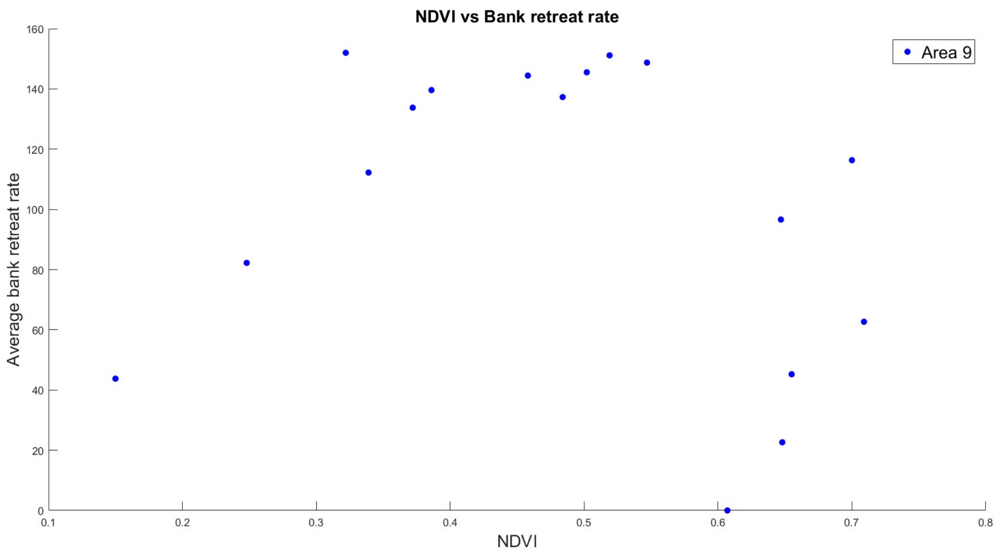

Figure B25 Bank retreat rate as a function of the NDVI for area 9.

The points in this area have the highest average NDVI, highest average bank retreat rate, as well as the largest difference between the maximum and minimum NDVI values. Hence, in comparison with the other areas, it seems that more vegetation results in higher bank retreat rates.

All the different points together are plotted in Figure B26. This graph does not show any support for the hypothesis. However, a couple of criteria is selected to refine the data found. These graphs are presented in chapter 4 ‘Results’. A distinction is made between the radii of curvature, erosion mechanisms, locations and steep and mildly sloped riverbanks.

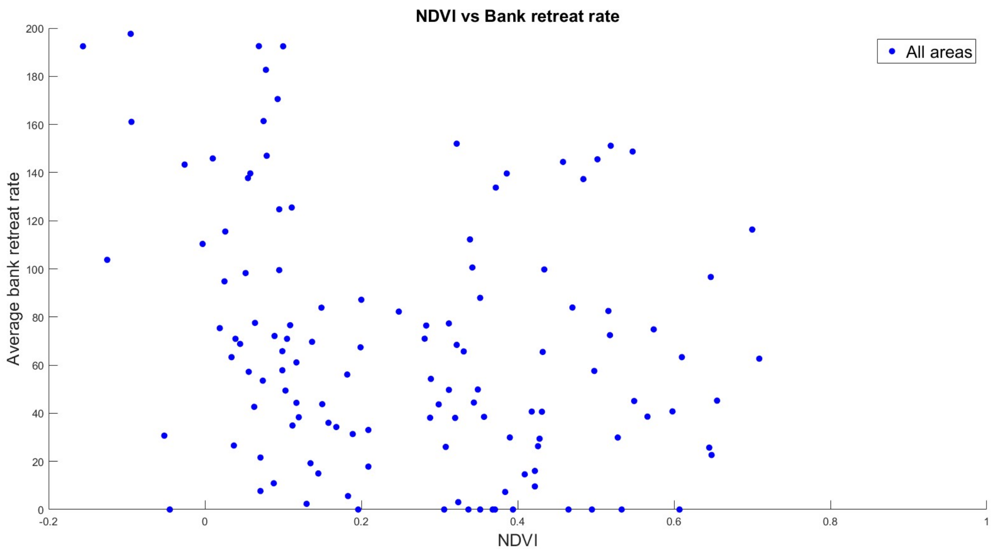

Figure B26 Result of the bank retreat of all areas together.

Appendix C – Google Earth Engine script

```
varl8=ee.ImageCollection("LANDSAT/LC8_SR"),
geometry=/* color: #d60000 */ee.Geometry.Polygon(
        [[[95.490121817165, 21.869493867247968],
          [95.4901278485097, 21.86877478995805],
          [95.49098527611659, 21.868784141285733],
          [95.49098727568025, 21.869503830506716],
          [95.49055454640825, 21.869493874517516]]]);

// Map a function over the Landsat 8 TOA collection to add an NDVI band.
var withNDVI = l8.map(function(image) {
var ndvi = image.normalizedDifference(['B5', 'B4']).rename('NDVI');
return image.addBands(ndvi);
});

// center map to study area
Map.setCenter(95.490293,21.869281,15)//location bank
print(Map.getCenter())
var point = ee.Geometry.Point([95.490293,21.869281]);
Map.addLayer(point);

var bounds = geometry

// Create a chart.
var chart = ui.Chart.image.series({
  imageCollection: withNDVI.select('NDVI'),
  region: bounds,
  reducer: ee.Reducer.mean(),
  scale: 30
}).setOptions({title: 'NDVI over time'});
// Display the chart in the console.
print(chart);
```

This script can also be retrieved via the following link:
https://code.earthengine.google.com/8e4744850e05c4def7fb0a223c90f4f9

Appendix D – NDVI validation with photo material

In this Appendix, different riverbanks are compared with each other to validate Normalised Difference Vegetation Index (NDVI) records. The photo material collected during the fieldwork acts as a benchmark. In the following figures the riverbank is displayed on the left side, where on the right side the NDVI record is presented, retrieved with the Google Earth Engine (GEE) script from Appendix C. In the NDVI graph, the date is displayed on the horizontal axis, on the vertical axis the NDVI is presented. The pictures are made in the week of the fieldwork period between 30 January and 3 February 2017. Therefore, the photo is compared with the NDVI value around 1 February 2017. In this analysis the following hypothesis is tested:

'Dense and healthy vegetation corresponds with higher NDVI values.'

As already was shown in the erosion rate analysis, the bank in area 1 existed mainly of old vegetation. A lot of roots were present, especially between the top of the riverbank and the toe region The first riverbank is covered with primarily old vegetation and thick roots, see Figure D1. From the NDVI record, it can be seen that the average is around 0.3. The maximum value is located around 0.43. The value of the NDVI at 1 February 2017 is also 0.3, which describes the state of the riverbank well. When comparing the different February months with each other, 2015, 2016 and 2017 have all an NDVI value of 0.3, indicating that the vegetation remains constant during similar seasonal conditions. The peaks are all located in the dry season. There could be three reasons for the lower values in the rainy season. Firstly, the vegetation could have perished, therefore reflect less near-infrared (NIR). Secondly, the water level is higher, therefore, a larger surface area of water is included in the calculation of the NDVI. Since water reflects less NIR, the NDVI is lower. Thirdly, during the rainy season, a lot of clouds are present, and apparently, the signal gets distorted, resulting in a disturbed record.

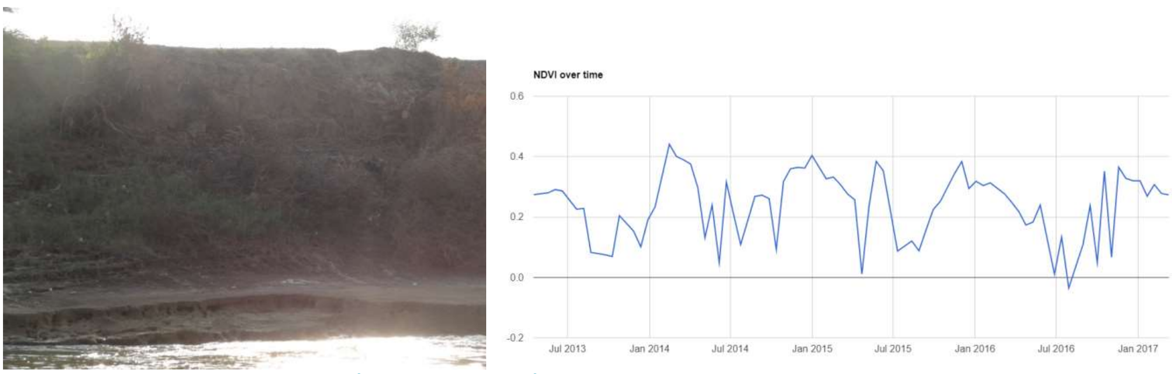

Figure D1 Riverbank at coordinates (21.8533; 95.9113), NDVI in February 2017 approximately 0.3.

When comparing the riverbank from Figure D1 with another riverbank with more livelier vegetation, the NDVI value increases, shown in Figure D2. Maximum values of 0.62 are found. Also, the average is larger, namely around 0.4. Furthermore, the peaks are around the dry season, the lower values are located in the rainy season. In both Figure D1 and Figure D2, the values are varying very much in the rainy season, resulting in a variable record. Whereas in the dry season the record is more constant, in the dry season the records show a lot of peak values that change rapidly from high to low.

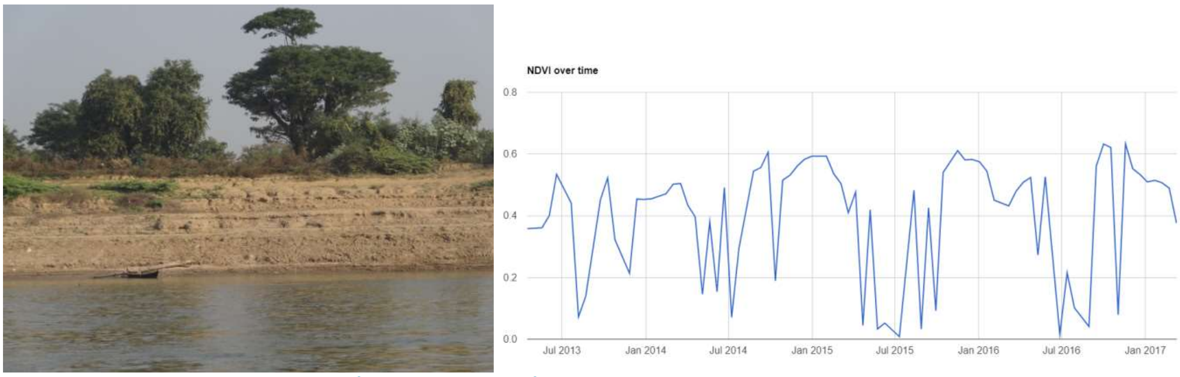

Figure D2 Riverbank at coordinates (21.9322; 95.7136) NDVI in February 2017 approximately 0.5.

At another location, presented in Figure D3, somewhat more upstream of the previous riverbank, the riverbank is not as steep as the other two riverbanks. The vegetation is smaller; There are no trees and the plants are mainly grass and shrubs. However, it shows much greener. The NDVI record contrasts significantly with the other two. There are smaller peaks and the troughs are more prolonged. It can be seen that the maximum values are still located in February. The lower parts between the months June until November are more constant. Since this bank is gentle in comparison with the previous two riverbanks, the water level difference causes high water to cover a more significant part of the riverbank. So during the rainy season and the falling stage of the flood wave, a large percentage of water cover is included in the NDVI calculation. This record shows that the increased water level is the main reason for the decreased NDVI values. The maximum value of this riverbank is around 0.6, which is similar to the previous riverbank. However, the riverbanks are dissimilar in vegetation species.

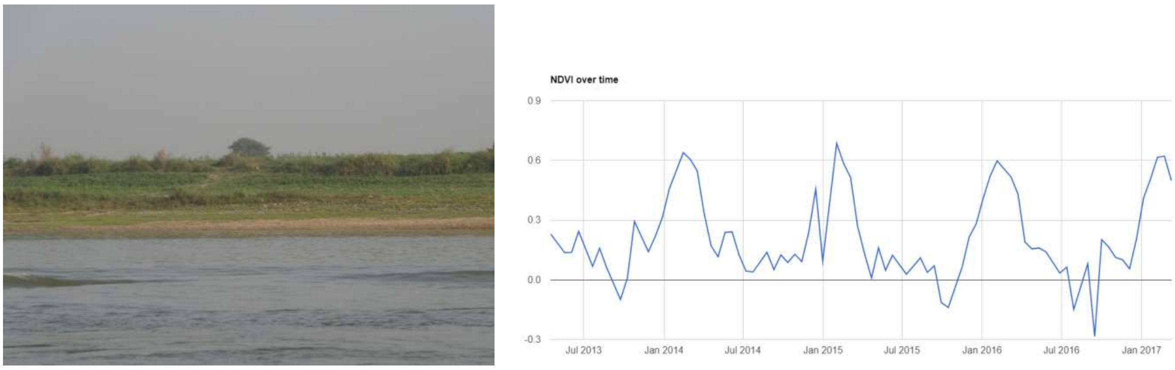

Figure D3 Riverbank at coordinates (21.9229; 95.8031), NDVI in February 2017 approximately 0.6.

Similar results are found at the opposite riverbank, where the difference between the top of the riverbank and the water level is not so large as well. This bank is also more mild instead of a steep riverbank. The NDVI records of Figure D3 and Figure D4 are comparable. It is more interesting to notice that at both locations there is grassy vegetation with occasionally some shrubs. In Figure D4, however, also trees are visible, which cannot be deduced from the NDVI record. The peaks are again in February and the value on 1 February 2017 is 0.57.

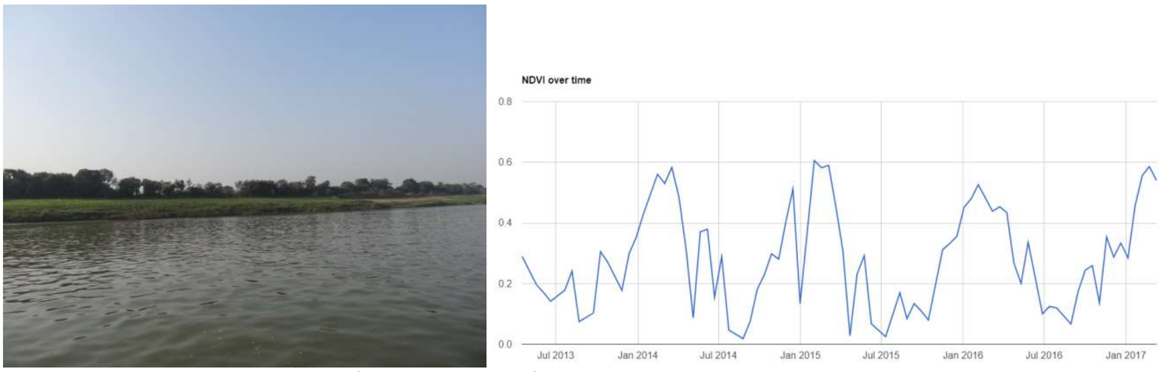

Figure D4 Riverbank at coordinates (21.9122; 95.7569), NDVI in January 2017 approximately 0.57.

In Figure D5 a combination of all the previously analysed riverbanks is shown. The bank is steep, however with a significant amount of vegetation on top. The density of trees is large, which is also visible on the NDVI record, where maximum values approach 0.84. The NDVI value of 1 February 2017 is 0.3, which is a rather small value for this kind of vegetation when comparing with the other riverbanks. The possibility of riverbank overflow is lower than the gentle riverbanks, however, is still likely to happen because of the troughs in de NDVI record. During the rainy season, the NDVI values are low, sometimes negative. Also in this record is visible that in the rainy season the values of NDVI are varying much more than in the dry season.

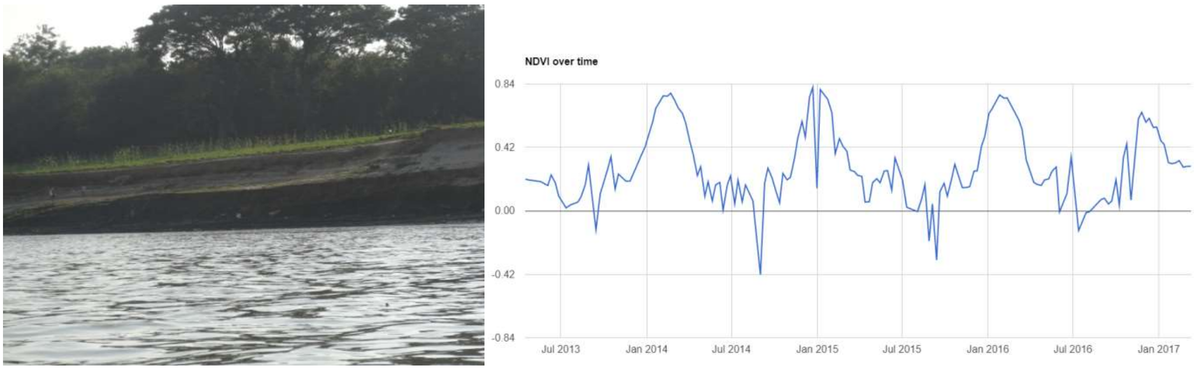

Figure D5 Riverbank at coordinates (21.7559; 95.4134), NDVI in January 2017 approximately 0.4.

The previous examples have shown that the NDVI records correspond well with the vegetation on the bank. Determining the NDVI at a random location on a riverbank at an arbitrary moment can easily be done with the GEE script of Appendix B. The method provides a first estimation of the state of vegetation on riverbanks. However, there are a couple of issues that need to be taken into account when working with the GEE script and interpreting the results.

Firstly, the positioning of the geometry, the area over which the NDVI is to be calculated, around the coordinate of consideration was chosen to be placed manually throughout the whole research (not just for this validation). The reason for this is that when a fixed placement around the coordinate is chosen, it does not always cover the riverbank accurately. Figure D6, Figure D7 and Figure D8 show how the geometry placement (red square) is determinative for the NDVI record. For example, when a fixed position, like in Figure D7, was chosen, there is no control over the area over which the NDVI is to be calculated. About 30% of river water is added in the calculation, resulting in a lower 'cell-averaged' NDVI value. NDVI records such as presented in Figure D1 - Figure D5 will then be significantly lower when a fixed placement around a coordinate is chosen. Moreover, when a riverbank section is curved, for example in a bend, within that section, there is a deviation in amount of water included in the calculation. This causes an (unknown) error.

Secondly, the size of the geometry plays a role. During this research, a fixed dimension of the geometry of approximately 40 by 40 meter is used. An adverse effect of the large size of the geometry is that it takes the average NDVI over the whole area, including the piece of land 'behind' the riverbank. For example, when comparing Figure D8 with Figure D9, the trees contribute to larger NDVI maxima. The larger the geometry, the more surrounding vegetation (or other soil material) is included in calculating the average NDVI. Moreover, the size of the geometry exceeds the dimension of single vegetation elements. When the vegetation within the geometry is uniform, this causes no problems. When there is a variety of vegetation, the NDVI graph is difficult to interpret. Another remark that can be made is that in Figure D8 the fact that the riverbank overflows is not visible from the NDVI record, however, the negative values in Figure D9 around August suggest that the section within the geometry overflows. This shows that on a smaller scale, the research method is accurate, but on a more extensive reach (several kilometres) may be time-consuming. Therefore it is recommended to apply this research method to determine NDVI values only on small scales (single bends, reaches of a couple of hundreds of meters, bars or islands) so that the geometry size/shape easily can be adjusted to the form of the riverbank.

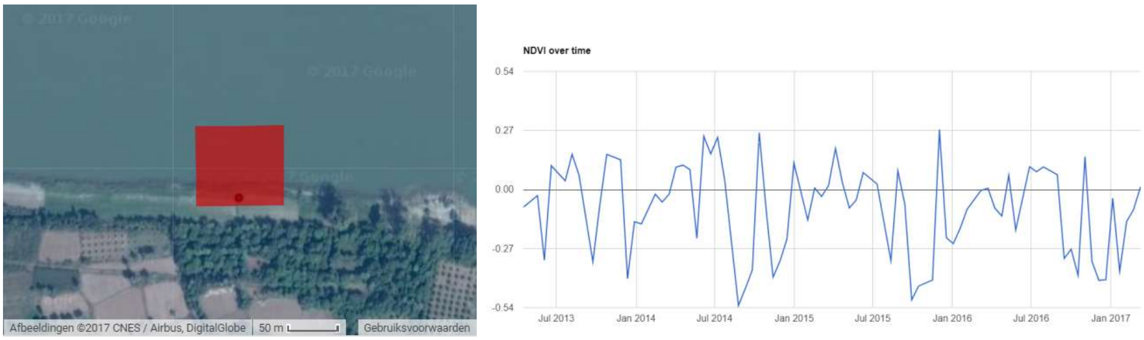

Figure D6 This series of figures show how the placement of the geometry is essential for the correct NDVI. In the geometry, a large part of water contributes to a low NDVI. Riverbank at coordinates (95.7574; 21.9122).

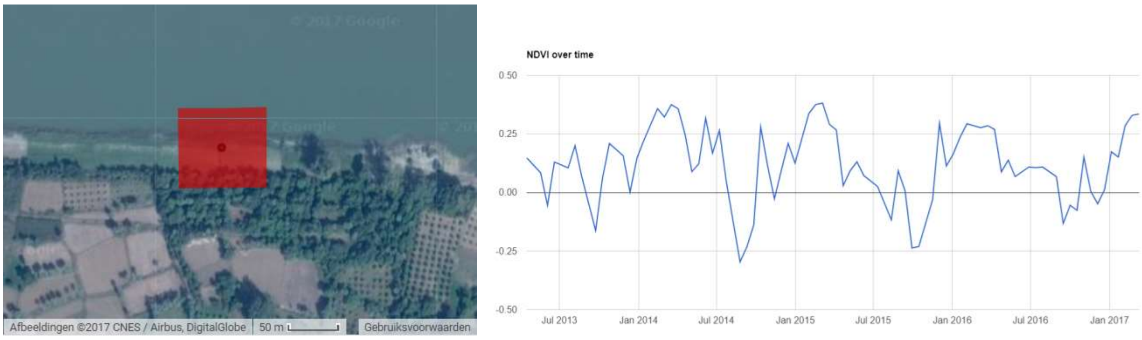

Figure D7 A smaller part of water is present and is taken into account in the NDVI calculation, resulting in higher NDVI values compared to Figure D6.

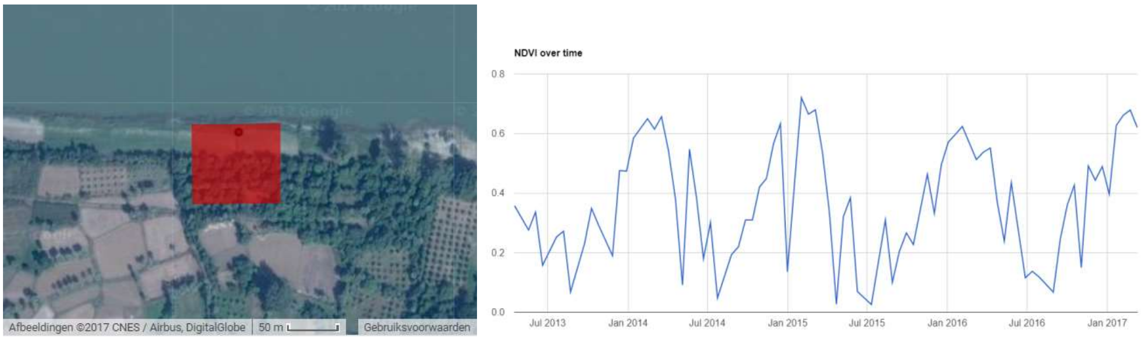

Figure D8 No water is present in the calculation of the NDVI. The NDVI values raise. Trees are introduced as well, which are not in direct contact with water, resulting in an overestimation of the NDVI.

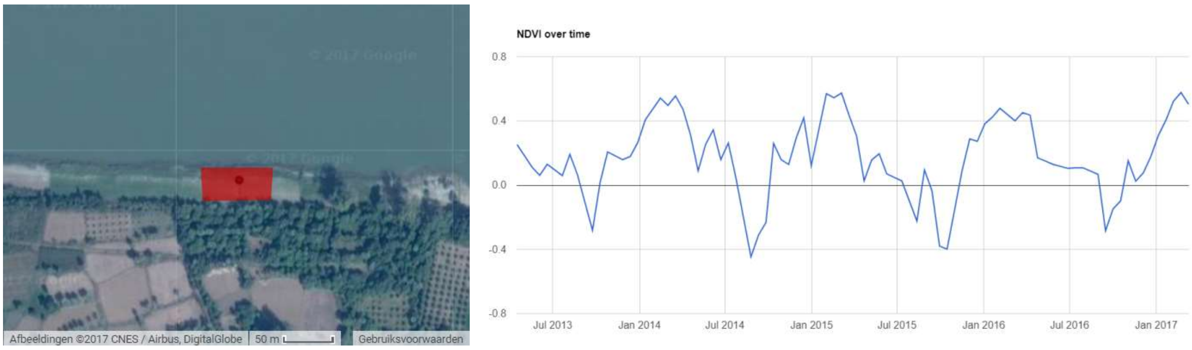

Figure D9 The influence of a different size of the geometry. In comparison with the figures above there is no influence of the trees, significantly reducing maximum NDVI values. The lower values are due to the overflowed riverbank during the rainy season.